

UNIVERSITI TEKNOLOGI MALAYSIA

DECLARATION OF THESIS / UNDERGRADUATE PROJECT PAPER AND COPYRIGHT

Author's full name : DAYANGKU NOORFAZIDAH BINTI AWANG SH'RI

Date of birth : 21 MAY 1983

Title : EFFECT OF SURFACE PRETREATMENTS ON THE DEPOSITION OF POLYCRYSTALLINE DIAMOND ON SILICON NITRIDE SUBSTRATE USING HOT FILAMENT CHEMICAL VAPOUR DEPOSITION

Academic Session: 2008/2009

I declare that this thesis is classified as

- CONFIDENTIAL** (Contains confidential information under the Official Secret Act 1972)*
- RESTRICTED** (Contains restricted information as specified by the organization where research was done)*
- OPEN ACCESS** I agree that my thesis to be published as online open access (full text)

I acknowledged that Universiti Teknologi Malaysia reserves the right as follows:

1. The thesis is the property of Universiti Teknologi Malaysia.
2. The Library of Universiti Teknologi Malaysia has the right to make copies for the purpose of research only.
3. The Library has the right to make copies of the thesis for academic exchange.

Certified by :



SIGNATURE

SIGNATURE OF SUPERVISOR

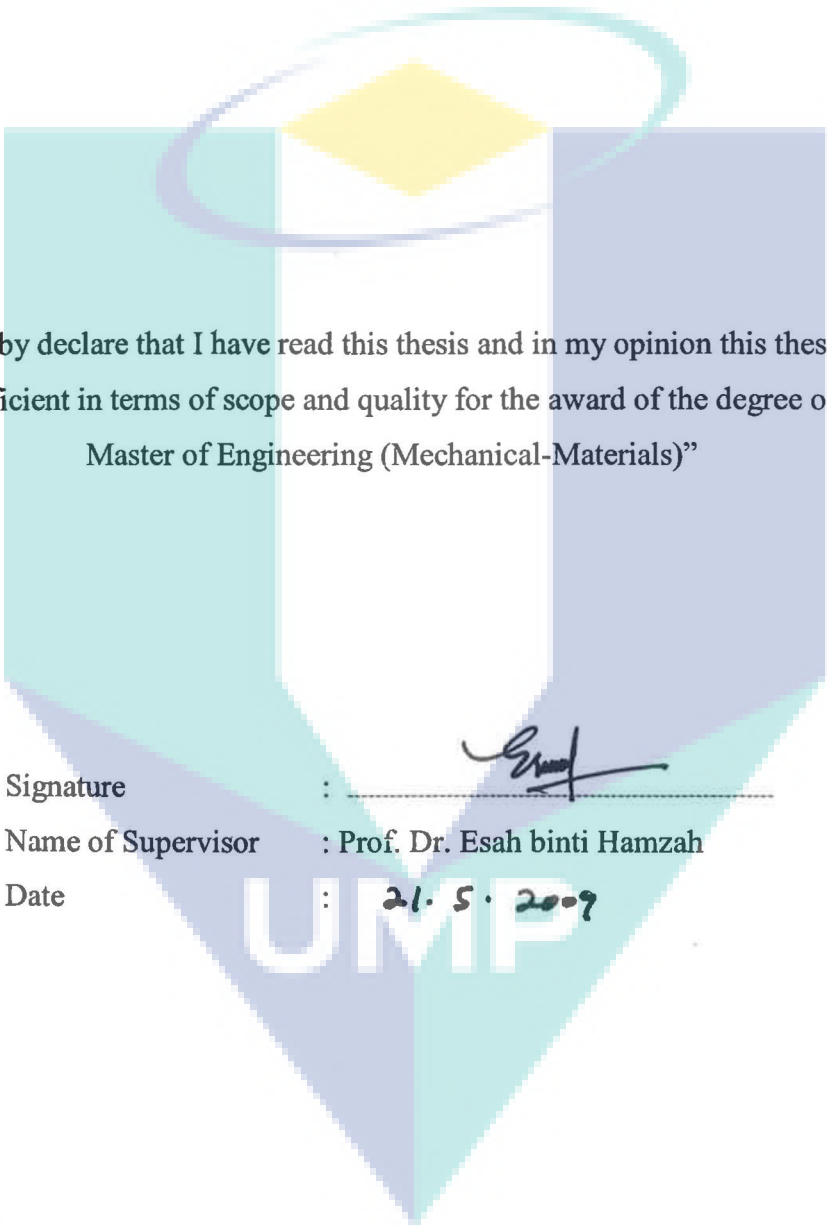
830521-13-5430
(NEW IC NO. /PASSPORT NO.)

PROF. DR. ESAH BINTI HAMZAH
NAME OF SUPERVISOR

Date : 21 MEI 2009

Date : 21 MEI 2009

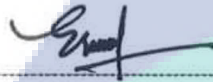
NOTES : * If the thesis is CONFIDENTIAL or RESTRICTED, please attach with the letter from the organization with period and reasons for confidentiality or restriction.



“I hereby declare that I have read this thesis and in my opinion this thesis is sufficient in terms of scope and quality for the award of the degree of Master of Engineering (Mechanical-Materials)”

Signature

:



Name of Supervisor

:

Prof. Dr. Esah binti Hamzah

Date

:

21.5.2009

**EFFECT OF SURFACE PRETREATMENTS ON THE DEPOSITION OF
POLYCRYSTALLINE DIAMOND ON SILICON NITRIDE SUBSTRATES
USING HOT FILAMENT CHEMICAL VAPOR DEPOSITION METHOD**



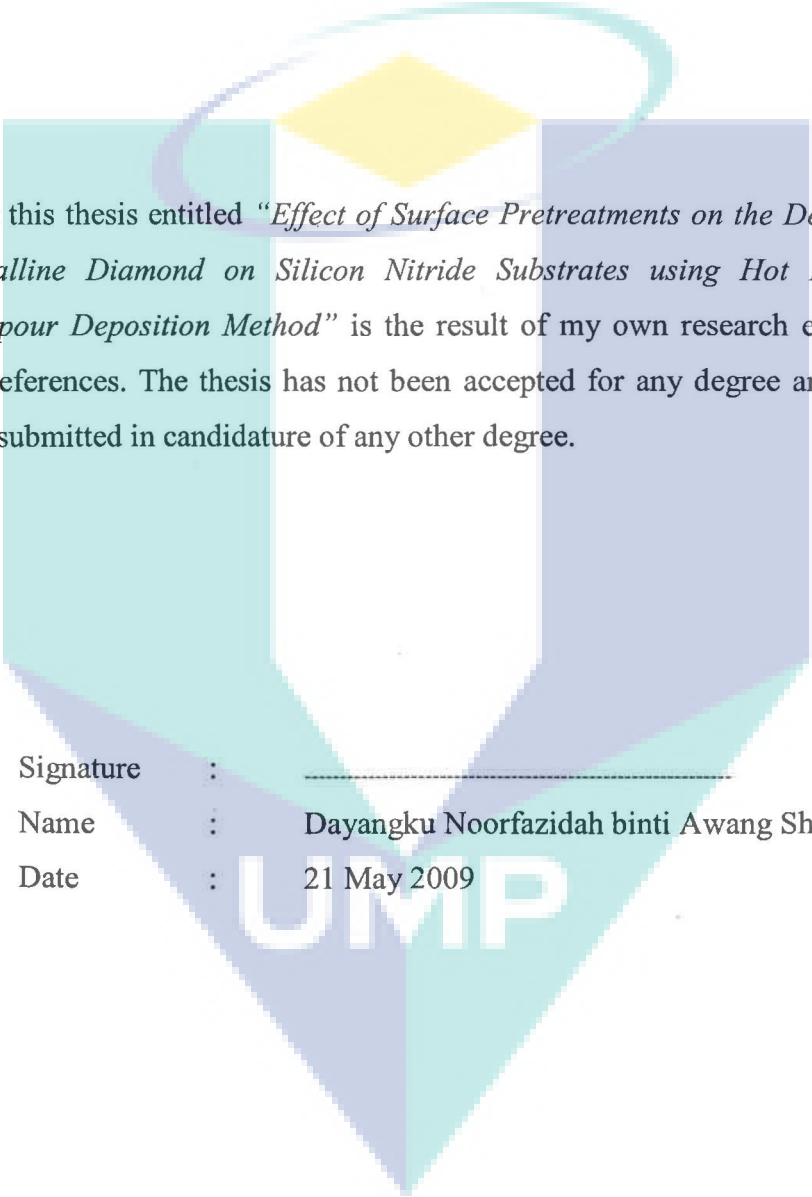
DAYANGKU NOORFAZIDAH BINTI AWANG SH'RI

A project report submitted in partial fulfilment of the
requirements for the award of the degree of
Master of Engineering (Mechanical-Materials)

UMP

Faculty of Mechanical Engineering
Universiti Teknologi Malaysia

MAY 2009

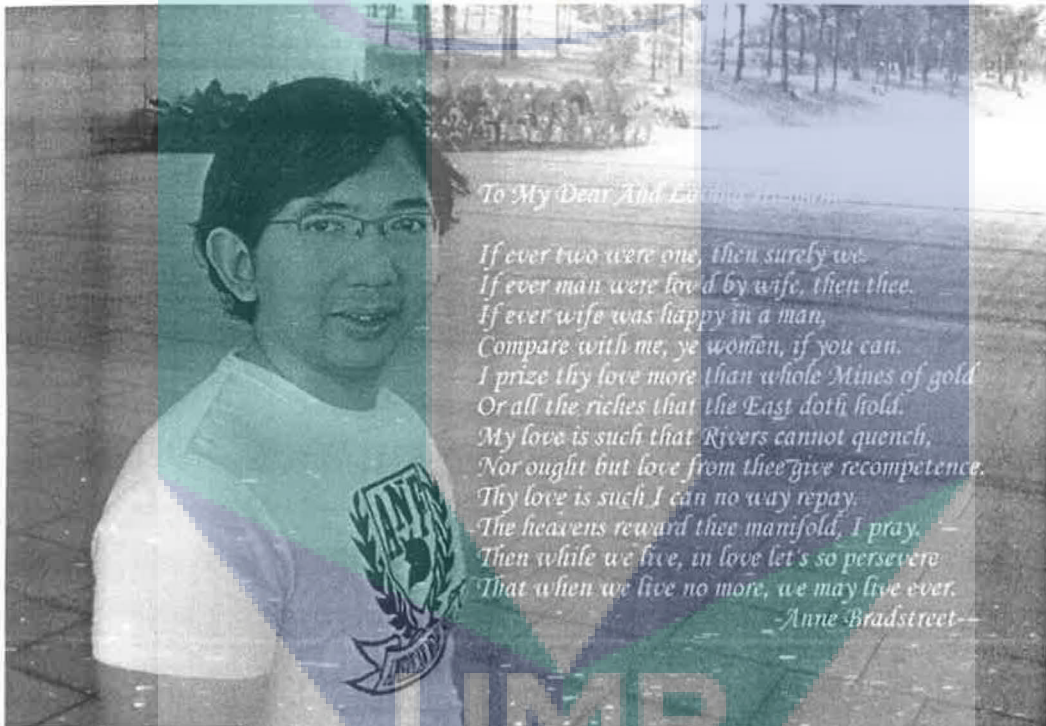


I declare that this thesis entitled "*Effect of Surface Pretreatments on the Deposition of Polycrystalline Diamond on Silicon Nitride Substrates using Hot Filament Chemical Vapour Deposition Method*" is the result of my own research except as cited in the references. The thesis has not been accepted for any degree and is not concurrently submitted in candidature of any other degree.

Signature : _____
Name : Dayangku Noorfazidah binti Awang Sh'ri
Date : 21 May 2009

*To my beloved late husband, Allahyarham Heimy Syariffyza bin Abdul Samat,
whose unconditional love and unfaltering support motivates me to always give my
best, persevere and kept me going through.*

Al-Fatihah.



ACKNOWLEDGEMENTS

All praise to Allah s.w.t who taught the mankind what they did not know. My prayers for my beloved parents, Hj Awang Sh'ri and Hajah Aishah Abdullah who gave countless sacrifice and did every effort in order to nurture me and provided the highest moral values.

I am extremely grateful to Professor Dr. Esah Hamzah for her kindly but rigorous insight gave me the motivation to finish this thesis.

I am also thankful to all technicians in Material and Manufacturing Laboratory for providing the technical support needed to complete this work. I feel obliged to express my gratitude towards my course mates for supporting me to complete this study. I also would like to thanks everyone that contributes directly and indirectly toward the completion of this study.

Finally, a particular debt of gratitude is due to my beloved late husband, Allahyarham Heimy Syariffyza bin Abdul Samat, who helped me at every step of this work. He always exhibited an extreme degree of love, understanding, sacrifice, compassion and encouragement for me; otherwise I would never been able to complete this thesis. His presence in my life will sadly be missed but he will always be remembered in my prayer.

ABSTRACT

The deposition of diamond films on a silicon nitride (Si_3N_4) substrate is an attractive technique for industrial applications because of the excellent properties of diamond. Diamond possesses remarkable physical and mechanical properties such as chemical resistant, extreme hardness and highly wears resistant. Pretreatment of substrate is very important prior to diamond deposition to promote nucleation and adhesion between coating and substrate. Polycrystalline diamonds films have been deposited on silicon nitride substrate by Hot Filament Chemical Vapor Deposition (HF-CVD) method. The Si_3N_4 substrates have been subjected to various pretreatment methods prior to diamond deposition namely chemical etching and mechanical abrasion. The structure and morphology of diamond coating have been studied using X-ray Diffraction (XRD) and Scanning Electron Microscopy (SEM) while diamond film quality has been characterized using Raman spectroscopy. The adhesion of diamond films has been determined qualitatively by using Vickers hardness tester. It was found that the diamond films formed on chemical pretreated substrates has cauliflower morphology and low adhesive strength but also have low surface roughness. Substrates that pretreated with sand blasting have yield diamond film with well-faceted morphology with high crystallinity and better adhesion. However, the surface roughness of the diamond film deposited on substrates pretreated with blasting are also higher.

ABSTRAK

Endapan filem intan diatas substrat silikon nitrid (Si_3N_4) merupakan satu teknik yang menarik kepada applikasi industri kerana sifat intan yang cemerlang. Intan memiliki sifat fizikal dan mekanikal yang menakjubkan seperti kalis bahan kimia, kekerasan yang tinggi dan sangat kalis haus. Pra-penyediaan substrat sebelum endapan intan adalah sangat penting untuk menggalakkan pertumbuhan nuklei dan meningkatkan rekatan diantara salutan dan substrat. Filem intan polihablur telah diendapkan diatas substrat silikon nitrid menggunakan kaedah endapan wap kimia filamen panas. Substrat Si_3N_4 telah melalui pelbagai kaedah pra-penyediaan sebelum endapan intan seperti punaran kimia dan lelasan mekanikal. Struktur dan bentuk salutan intan yang terhasil telah dikaji menggunakan pembelauan sinar X-ray (XRD) dan mikroskop electron imbasan (SEM) manakala kualiti filem intan telah dikaji menggunakan spektroskopi Raman. Rekatan filem intan telah dikaji secara kualitatif menggunakan ujian kekerasan Vickers. Hasil kajian menunjukkan filem intan yang terbentuk di atas substrate yang melalui pra-penyediaan kimia mempunyai morfologi *cauliflower* dan kekuatan rekatan yang rendah tetapi mempunyai kekasaran permukaan yang rendah. Substrat yang dibagas dengan pasir menghasilkan filem intan yang mempunyai segi permata dengan kehabluran yang tinggi dan kerekatan yang lebih bagus. Akan tetapi, kekerasan permukaan filem intan yang diendap diatas substrat yang dibagas dengan pasir juga lebih tinggi.

TABLE OF CONTENTS

CHAPTER	TITLE	PAGE
	DECLARATION	ii
	DEDICATION	iii
	ACKNOWLEDGEMENTS	iv
	ABSTRACT	v
	ABSTRAK	vi
	TABLE OF CONTENTS	vii
	LIST OF TABLES	xi
	LIST OF FIGURES	xii
	LIST OF APPENDICES	xvii
1	INTRODUCTION	1
	1.1 Background of the research	1
	1.2 Problem Statement	2
	1.3 Objectives and Scopes of Study	3
	1.4 Significance of the Study	4

2	LITERATURE REVIEW - ELECTRONIC PACKAGING	4
2	LITERATURE REVIEW	4
2.1	Introduction	4
2.2	An Overview on Cutting Tools	4
2.2.1	Cutting Tool Materials	5
2.2.1.1	High Speed Steel	5
2.2.1.2	Carbide	
2.2.1.3	Alumina based ceramic tools	6
2.2.1.4	Cubic Boron Nitride	7
2.2.1.5	Silicon Nitride based ceramic	7
2.2.2.2	Diamond coatings	8
2.3	Overview of Diamond as Coating Material	8
2.3.1	Structures and properties of diamond	8
2.3.2	Deposition Mechanism of Polycrystalline CVD diamond	13
2.3.2.1	Nucleation and Growth of CVD diamond	15
2.3.3	Polycrystalline diamond deposition of various substrates	20
2.3.3.1	Deposition on cemented tungsten carbide	20
2.3.3.2	Deposition on silicon nitride	21
2.3.4	Surface pretreatment	22
2.4	Deposition technique of polycrystalline diamond	25
2.4.1	Introduction	25
2.4.2	Operating principle of CVD	25
2.4.3	CVD diamond deposition techniques	26
2.4.3.2	Arc-Discharge	26
2.4.3.3	Microwave plasma-assisted CVD	27
2.4.3.1	Hot Filament CVD	28
2.5	Conclusion	32
3	RESEARCH METHODOLOGY	33
3.1	Introduction	33
3.2	Sample preparation and Pretreatment	34
3.2.1	Substrates Material	34

3.2.2	Substrate Pretreatments	36
3.2.3	Surface Roughness	39
3.3	Polycrystalline Diamond Deposition by Hot Filament Chemical Vapor Deposition Technique	40
3.4	Microstructural Characterization	42
3.4.1	Surface Morphology and Thickness by Scanning Electron Microscopy	42
3.4.2	Surface Topography and Surface Roughness by Atomic Force Microscopy	43
3.4.3	X Ray Diffraction	43
3.4.4	Diamond Quality and Residual Stress by Raman Spectroscopy	45
3.5	Adhesion properties by Vickers hardness tester	46
4	RESULTS AND DISCUSSION	48
4.1	Materials	48
4.1.1	Composition and Phase Analysis	48
4.1.2	Hardness Analysis	50
4.2	Pretreatment Analysis	50
4.2.1	Effect of pretreatment on surface roughness and morphology	50
4.2.1.1	Substrates morphology after pretreatment	50
4.2.1.2	Effect of seeding on diamond nucleation	57
4.3	Effect of chemical etching	61
4.3.1	Introduction	61
4.3.2	Effect of etching time on the morphology of the diamond film	61
4.3.3	Surface topography and surface roughness by atomic force microscopy (AFM)	65
4.3.4	Phase analysis using X-ray diffraction	71
4.3.5	Diamond quality analysis using Raman spectra	74
4.4	Effect of Mechanical pretreatment	80
4.4.1	Introduction	80

4.4.2	Effect of etching time on the morphology of the diamond film	80
4.4.3	Surface topography and surface roughness by atomic force microscopy (AFM)	81
4.4.4	Phase analysis and quality of diamond using X-ray diffraction	82
4.5	Adhesion analysis of diamond film deposited on various pretreated substrates.	85
4.5.1	Introduction	85
4.5.2	Adhesion behavior due to different indentation loads	85
4.5.3	Determination of adhesive strength	91
4.5.3.1	Adhesive strength determination based on radial crack	91
4.5.3.2	Adhesive strength determination based on delamination radius	94
4.5.4	Surface roughness with adhesion	96
4.5.5	Adhesive strength relate with sp^2/sp^3 ratio	98
5	CONCLUSIONS AND RECOMMENDATIONS	99
5.1	Conclusions	100
5.2	Recommendations for Future Works	100
	REFERENCES	101
	APPENDICES	107

LIST OF TABLES

TABLE NO.	TITLE	PAGE
Table 2.1	General properties of common cutting tool materials [4]	6
Table 2.2	Comparison between typical properties of various categories of diamond [6, 10, 11]	14
Table 2.3	Surface pretreatment for silicon nitride substrate	25
Table 2.4	Characteristics of Diamond Deposition Processes [11]	27
Table 2.5	Deposition parameter of HFCVD on Si ₃ N ₄ and WC-Co substrate	31
Table 3.1	Chemical Treatment of Si ₃ N ₄ substrates	37
Table 3.2	As-received and mechanically treated sample	38
Table 3.3	Seeding process for pretreated substrates	38
Table 3.4	HFCVD deposition parameter	40
Table 4. 1	Summary of SEM and AFM evaluation for diamond film deposited on substrates pretreated with chemical etching	70
Table 4.2	Summary of XRD and Raman Spectroscopy characterization on diamond deposited on substrates pretreated with chemical etching	79
Table 4. 3	Summary of SEM and AFM evaluation for diamond film deposited on as received and substrates pretreated with mechanical etching	83
Table 4. 4	Summary of XRD and Raman Spectroscopy characterization on diamond deposited on as received and substrates pretreated with mechanical etching	84
Table 4.5	Delamination radius of various samples under various indentation load	95

LIST OF FIGURES

FIGURE NO.	TITLE	PAGE
Figure 2.1	Schematic diagram of crystal structure of hexagonal graphite	11
Figure 2.2:	Schematic diagrams of two basic crystal structures of diamond: hexagonal lonsdaleite and cubic diamond	11
Figure 2.3	Schematic of unit cell of cubic diamond	12
Figure 2.4:	Schematic of the simple crystals shape of diamonds	13
Figure 2.5	Idiomorphic crystal shapes of diamond for different values of the growth parameter, α .	13
Figure 2.6	Generalized schematic of the physical and chemical process occurring in CVD diamond reactor	16
Figure 2.7	Simplified form of the Bachmann triangle C-H-O composition diagram in which below CO tie-line, no film growth will occur. Above the CO tie-line, non-diamond carbon is deposited except in a narrow window close to the tie-line which produces polycrystalline diamond films	17
Figure 2.8	Free energy diagram of three dimensional crystal formation (ΔG_{3D}) at constant supersaturation ($\Delta\mu$) as a function of the number of its particle, n. [13]	18
Figure 2.9:	Schematic of the reaction process occurring at the diamond surface leading to stepwise addition of CH_3 species and diamond growth	20
Figure 2.10	Growth process of a diamond film on a non-diamond substrates: (a) nucleation of individual crystallites (b-c) termination of nucleation, and growth of individual crystallite (d) faceting and coalescence of individual crystallites and formation of continuous film (e-f) some	

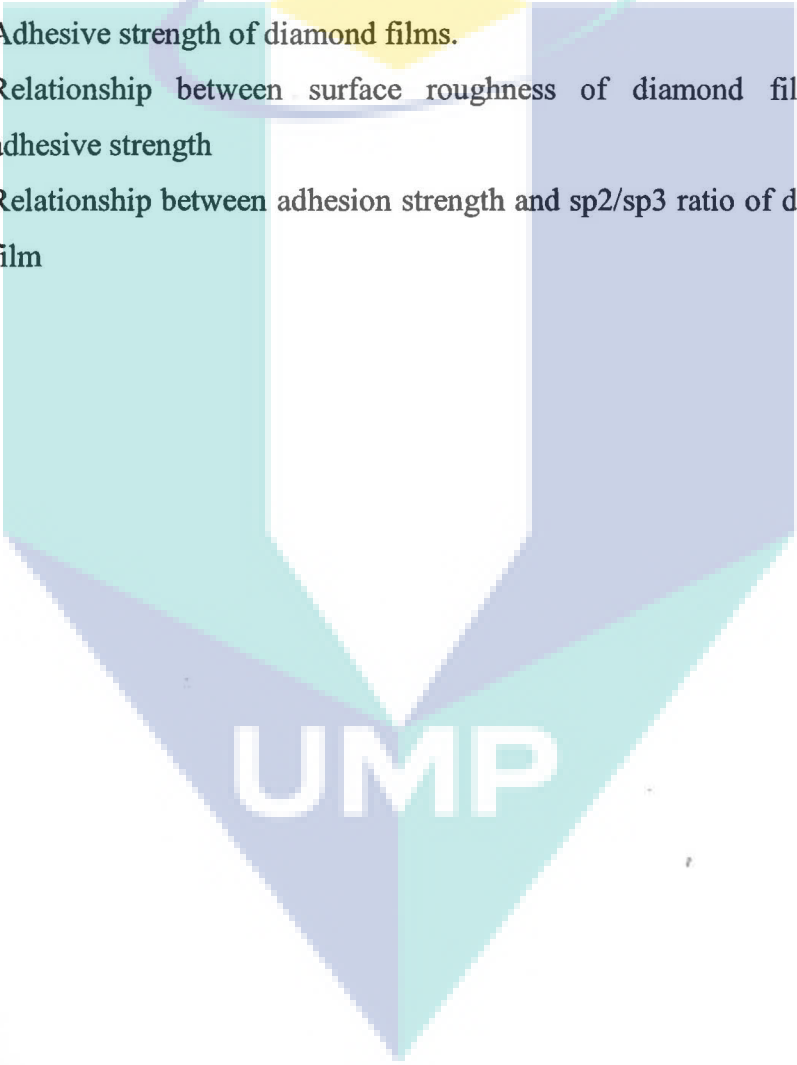
crystals grow faster and swallow their neighbours during growth of continuous film [6]. 21

- Figure 2.11 Schematic of arc-discharge apparatus for the deposition of diamond 28
- Figure 2.12 Schematic of microwave-plasma deposition 29
- Figure 2.13 Hot Filament Apparatus for deposition of diamond 30
- Figure 2.14 Schematic diagram showing the mechanisms of diamond nucleation enhancement on biases substrate. (a) Negative biasing: carbon containing cations are accelerated toward the substrate surface. (b) Positive biasing: electrons are accelerated toward the substrate surface and bombard carbon-containing molecules adsorbed on the surfaces [6]. 32
- Figure 3.1 Experimental Flow Chart 35
- Figure 3.2 Ultrasonic cleaner used to clean the sample 36
- Figure 3.3 Schematic of a profilometer used to determine the surface roughness of the materials 39
- Figure 3.4 Hot filament chemical vapor deposition (a) actual equipment and (b) schematic drawing of HFCVD equipment. 41
- Figure 3.5 HFCVD chamber configuration showing (a) front view and (b) side view. 41
- Figure 3.6 Scanning Electron Microscopy used to investigate the morphology of deposited polycrystalline diamond 42
- Figure 3.7 Atomic Force Microscopy used for topography and surface roughness analysis 43
- Figure 3.8 Bragg's Law explaining the diffraction of crystals 44
- Figure 3.9 X-Ray Diffractometer (XRD) used to determine composition and phase analysis of the coating 44
- Figure 3.10 Raman Spectroscopy Equipment 46
- Figure 3.11 Vickers Hardness Tester indenter (a) actual equipment and (b) schematic of hardness measurement 47
- Figure 4.1 (a) As-received Si_3N_4 substrates and (b) optical micrograph of Si_3N_4 (x200) 48
- Figure 4.2 EDX spectrum of Si_3N_4 49
- Figure 4.3 XRD spectrum of as-received Si_3N_4 49
- Figure 4.4 Vickers indentation on Si_3N_4 50

Figure 4.5	FE-SEM micrograph of substrates surface due to (a) acid etching, (b) strong acid etching and (c) basic etching.	52
Figure 4.6	AFM image analysis showing (a) top view and (b) 3-dimensional view of substrates undergoes strong acid etching for 20 minutes.	52
Figure 4.7	Mechanism of wet chemical etching	53
Figure 4.8	AFM images of surface topography of Si ₃ N ₄ substrate pretreated by sand blasting.	54
Figure 4.9	Schematic diagram of blasting mechanism	55
Figure 4.10	AFM images of surface topography of Si ₃ N ₄ substrate pretreated by grinding process	55
Figure 4.11	Schematic diagram of grinding mechanism	56
Figure 4.12	Surface roughness (Ra) before and after surface pretreatment	57
Figure 4.13	Diamond nucleation on substrates pretreated with (a) acid etching (b) strong acid etching and (c) basic etching	58
Figure 4.14	Diamond nucleation on non-seeded, (a) as-received (b) pretreated by blasting and (c) pretreated by grinding substrates.	59
Figure 4.15	Schematic diagram of mechanisms for diamond nucleation enhancement of scratched substrates [7]	60
Figure 4.16	SEM micrograph of Vickers indentation on Si ₃ N ₄ substrates pretreated by grinding on (a) seeded and (b) unseeded sample.	60
Figure 4.17	SEM showing diamond film deposited on substrate pretreated with acid etching for (a) 10 (b) 20 and (c) 30 minutes.	62
Figure 4.18	SEM showing diamond film deposited on substrate pretreated with strong acid etching for (a) 10 (b) 20 and (c) 30 minutes.	63
Figure 4.19	SEM showing diamond film deposited on substrate pretreated with basic etching for (a) 10 (b) 20 and (c) 30 minutes.	63
Figure 4.20	Schematic of ballas-like particle growth suggesting preferential <110> orientation during NCD film deposition [10].	64
Figure 4.21	AFM 3D topography of diamond film deposited on acid etched substrates for (a) 10 (b) 20 and (c) 30 minutes.	65
Figure 4.22	AFM 3D topography of diamond film deposited on strong acid etched substrates for (a) 10 (b) 20 and (c) 30 minutes.	66
Figure 4.23	AFM 3D topography of diamond film deposited on basic etched substrates for (a) 10 (b) 20 and (c) 30 minutes.	67

Figure 4.24	AFM profile of diamond film deposited on acid etched substrates showing (a) highly faceted crystalline morphology and (b) cauliflower morphology	68
Figure 4.25	X-ray diffraction pattern of diamond film deposited on acid etched substrates for (a) 10 (b) 20 and (c) 30 minutes	72
Figure 4.26	X-ray diffraction pattern of diamond film deposited on strong acid etched substrates for (a) 10 (b) 20 and (c) 30 minutes	73
Figure 4.27	X-ray diffraction pattern of diamond film deposited on basic etched substrates for (a) 10 (b) 20 and (c) 30 minutes	73
Figure 4.28	Raman spectra comparison between substrates pretreated in acid etching for (a) 10 (b) 20 and (c) 30 minutes.	75
Figure 4.29	Raman spectra comparison between substrates pretreated in strong acid etching for (a) 10 (b) 20 and (c) 30 minutes.	76
Figure 4.30	Raman spectra comparison between substrates pretreated in basic etching for (a) 10 (b) 20 and (c) 30 minutes.	76
Figure 4.31	Fe-SEM micrograph of diamond film deposited on (a) as-received (b) pretreated by blasting and (c) pretreated by grinding substrates.	80
Figure 4.32	3D topography of diamond film deposited on (a) as-received (b) pretreated by blasting and (c) pretreated by grinding substrates.	81
Figure 4.33	XRD peaks comparison of diamond film deposited on as-received, pretreated by blasting and pretreated by grinding substrates.	82
Figure 4.34	Raman spectra of diamond film deposited on as-received, pretreated by blasting and pretreated by grinding substrates.	82
Figure 4.35	Vickers indent on the diamond film at load 5kgf, 10kgf and 30kgf, respectively on sample treated with acid etching for 20 minutes.	86
Figure 4.36	SEM images of Vickers indent on acid etched pretreated samples	87
Figure 4.37	SEM images of Vickers indent on strong acid etched pretreated samples	88
Figure 4.38	SEM images of Vickers indent on basic etched pretreated samples	89
Figure 4.39	SEM images of Vickers indent on as-received and mechanically pretreated substrates	90
Figure 4.40	Indentation load versus crack length curves for diamond films with different surface pretreatment	92

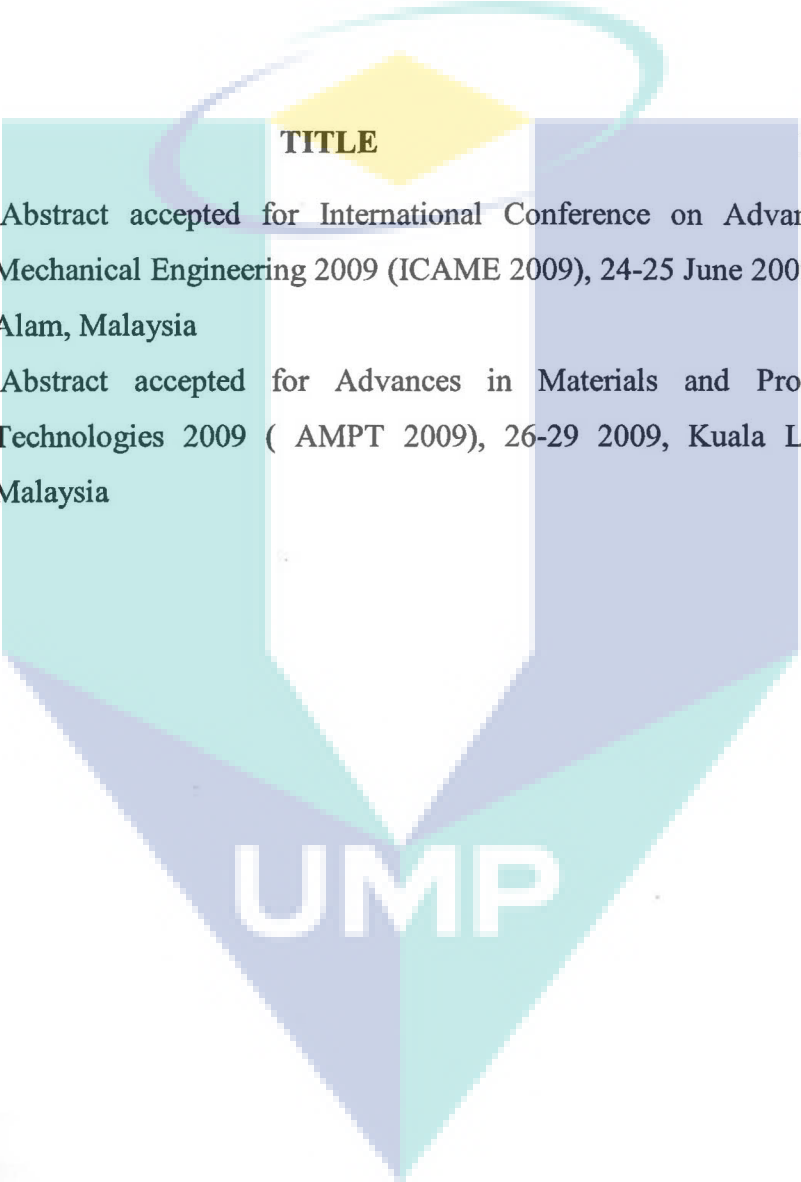
Figure 4.41	Adhesive strength of diamond film deposited on various surface pretreated substrates	92
Figure 4.42	Crack response of diamond deposited on (a) basic etched and (b) pretreatment by blasting to Vickers indentation	93
Figure 4.43	Typical crack response of diamond film due to Vickers indentation observed under optical microscopy.	94
Figure 4.44	Plot of delamination radius versus load for strong acid pretreated substrates	95
Figure 4.45	Adhesive strength of diamond films.	96
Figure 4.46	Relationship between surface roughness of diamond film and adhesive strength	97
Figure 4.47	Relationship between adhesion strength and sp^2/sp^3 ratio of diamond film	98

The logo for UMP (University of Malaya) is a large, downward-pointing arrow shape. It is composed of four colored triangular sections: two light blue sections on the left and right, and two light green sections at the bottom. The letters 'UMP' are written in white, bold, sans-serif font across the center of the arrow.

UMP

LIST OF APPENDICES

FIGURE NO.	TITLE	PAGE
A1	Abstract accepted for International Conference on Advances in Mechanical Engineering 2009 (ICAME 2009), 24-25 June 2009, Shah Alam, Malaysia	108
A1	Abstract accepted for Advances in Materials and Processing Technologies 2009 (AMPT 2009), 26-29 2009, Kuala Lumpur, Malaysia	109

The logo of Universiti Malaysia Perlis (UMP) is a large, downward-pointing arrow shape. It is composed of four triangular sections meeting at a central point. The top-left and bottom-right sections are light blue, while the top-right and bottom-left sections are light green. The letters 'UMP' are printed in white, bold, sans-serif font across the center of the arrow.

UMP

CHAPTER 1

INTRODUCTION

1.1 Background of the research

Apart from their appeal as highly treasured gemstones, diamond possesses a remarkable physical properties such as extreme hardness, high thermal conductivities, excellent infrared transparency and remarkable semiconductor properties making diamond one of technologically valuable materials. However, it has proved very difficult to exploit these properties, due to the cost and scarcity of large natural diamond.

Many attempts have been made to synthesize diamond artificially using graphite as starting material. This proved very difficult, mainly because at room temperature and atmospheric pressure, graphite is the thermodynamically stable allotrope of carbon. Although the standard enthalpies of diamond and graphite are differ only by 2.9 kJ mol^{-1} , a large activation barrier separates the two phases preventing interconversion between them at room temperature [1]. To overcome these problem, high pressure high temperature (HPHT) growth techniques has been introduced by General Electric to produce industrial diamond. However, the drawback of HPHT method is that it still

produces diamond in form of single crystal thus limiting the range of application it can be used.

This leads to the idea of producing diamond from gas phase at much lower pressure in which carbon atoms could be added one-at-a-time to an initial template, in such a way tetrahedrally bonded carbon network forms. It can be achieved by using chemical vapor deposition (CVD) method. CVD involves a gas phase chemical reaction occurring above solid surfaces, which causes deposition onto that surface. All CVD techniques for producing diamond film require a mean of activating gas-phase carbon-containing precursor molecules[2]. This gas phase activation is achieved typically by using one of these three basic methods:

- External heating (as in hot filament CVD)
- Plasma activation (as in Plasma assisted CVD)
- A combination of thermal and chemical activation (as in flame CVD)

The applications for which CVD diamond films can be used are closely related to the various extreme physical properties they exhibit. The extreme hardness and high wear resistance of the diamond makes it an ideal candidate for use as coating material in cutting tool.

1.2 Problem Statement

Diamond coating have a great application as wear resistant layers on tools. Such diamond-coated hard metal and ceramic inserts are used successfully in machining fiber-reinforced plastic, graphites and aluminium alloys. However, in order for CVD diamond to be used as coating for tools and wear parts, it has been shown that two problem must

be overcome first. The problems are the diffusion of atoms from the substrate to the diamond and diffusion of carbon atoms to the substrate, and also the adhesion and residual stress in interlayer of diamond coating [3]. Poor adhesion can be caused by many factors such as mismatch of coefficient of thermal expansion (CTE) between diamond and substrate, residual stress, impurities and others.

1.3 Objectives and Scopes of Study

The objectives of this study are to study the effect of substrate surface treatment on morphology, coating adhesion, surface roughness and residual stress of polycrystalline diamond coated on silicon nitride. Surface treatment of the substrate is very important in order to produce high quality diamond coating with high adhesion strength.

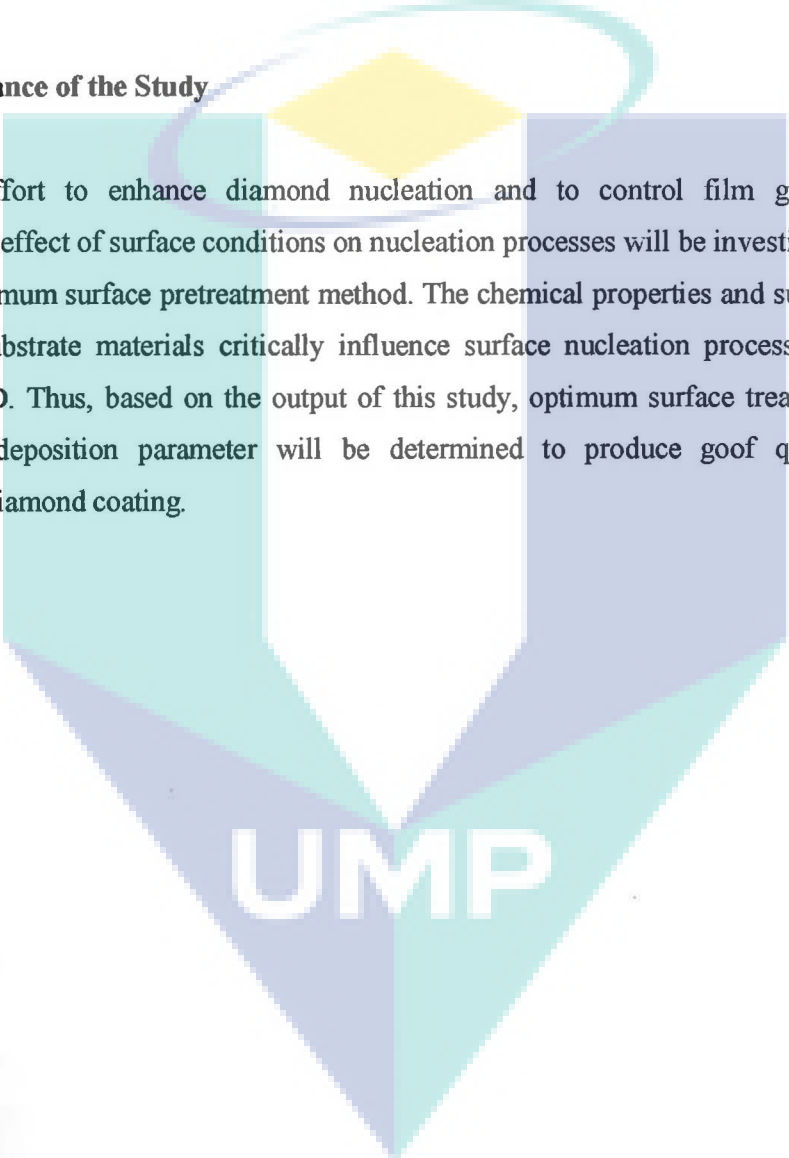
The scope of the research includes:

- a) Polycrystalline diamond deposited on silicon nitride substrate using Hot Filament Chemical Vapor Deposition machine using 99% CH_4 gas as precursor.
- b) Prior to diamond deposition, the substrate undergoes various surface pretreatment processes as following:
 - i. The surface was blasted with SiC 180 for 30 sec (mechanical pretreatment)
 - ii. The surface was grinded with 180 grit for 5 minutes followed by 600 grit for 5 minutes (mechanical pretreatment)
 - iii. The surface was etched with various chemical reagents (chemical etchings)

c) Characterization on microstructure, morphologies and mechanical properties using scanning electron microscopy, atomic force microscopy, Raman Spectroscopy, X-ray diffraction and Vickers hardness indenter

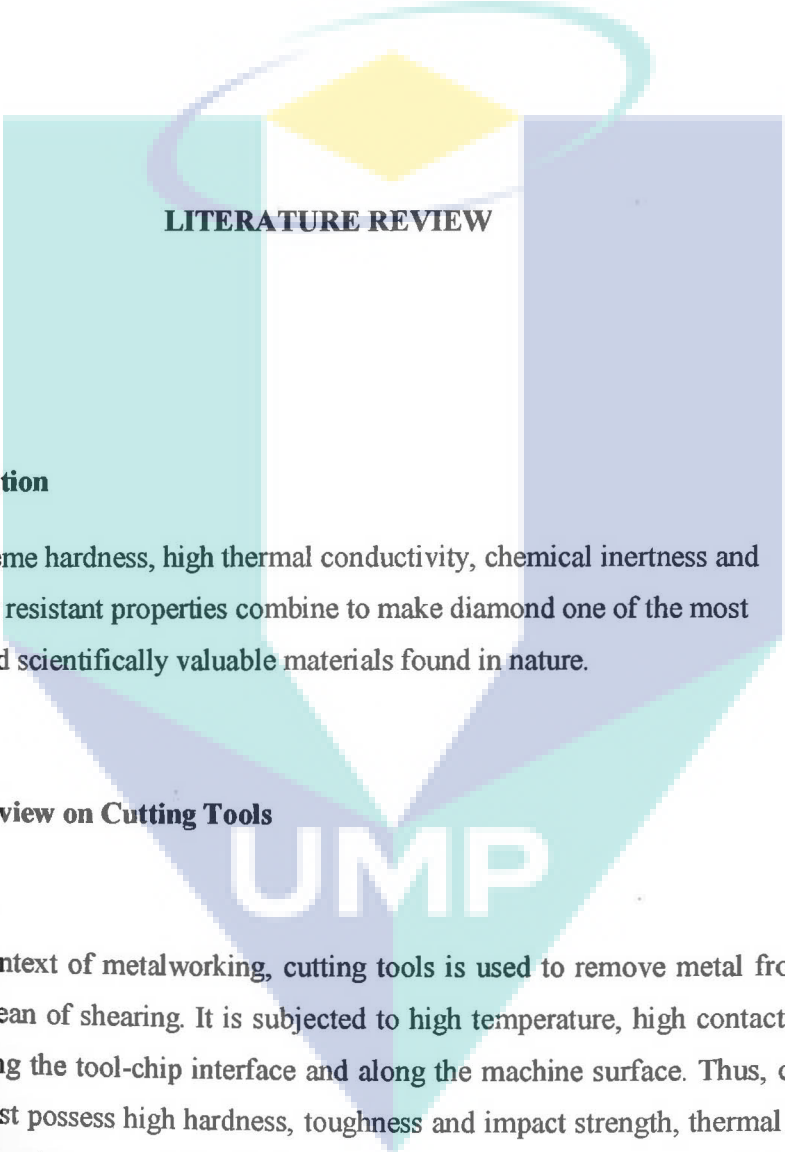
1.4 Significance of the Study

In an effort to enhance diamond nucleation and to control film growth morphology, the effect of surface conditions on nucleation processes will be investigated to select the optimum surface pretreatment method. The chemical properties and surface conditions of substrate materials critically influence surface nucleation processes of diamond in CVD. Thus, based on the output of this study, optimum surface treatment technique and deposition parameter will be determined to produce good quality polycrystalline diamond coating.

The logo for UMP (Universiti Malaysia Perlis) is a large, downward-pointing arrow shape. It is composed of four quadrants: top-left is light blue, top-right is light purple, bottom-left is light purple, and bottom-right is light blue. A yellow diamond is centered at the top of the arrow, and a light blue oval encircles it. The letters 'UMP' are written in white, bold, sans-serif font across the bottom of the arrow.

UMP

CHAPTER 2



LITERATURE REVIEW

2.1 Introduction

The extreme hardness, high thermal conductivity, chemical inertness and remarkable wear resistant properties combine to make diamond one of the most technological and scientifically valuable materials found in nature.

2.2 An Overview on Cutting Tools

UMP

In the context of metalworking, cutting tools is used to remove metal from the workpiece by mean of shearing. It is subjected to high temperature, high contact stress and rubbing along the tool-chip interface and along the machine surface. Thus, cutting tool material must possess high hardness, toughness and impact strength, thermal shock resistance, wear resistance and chemical stability. Various cutting tools material with a wide range of mechanical, physical and chemical properties has been developed to respond to the demanding requirement of cutting tool. Table 2.1 shows the common cutting tool material and their properties.

Table 2.1 General properties of common cutting tool materials [4]

Material	Hardness	Impact Strength, J	Modulus of elasticity, GPa	Coefficient of thermal expansion, $10^{-6}/^{\circ}\text{C}$	Melting temperature, $^{\circ}\text{C}$
High Speed Steel	83-86 HRA	1.35-8	200	12	1300
Tungsten Carbide	90-95 HRA	0.34-1.35	520-690	4-6.5	1400
Titanium Carbide	91-93 HRA	0.79-1.24	310-450	7.5-9	1400
Silicon Nitride	91-95 HRA	<0.1	310-410	6-8.5	2000
Cubic Boron Nitride	4000-5000 HK	<0.5	850	4.8	1300

2.2.1 Cutting Tool Materials

2.2.1.1 High Speed Steel

High speed steels are the most highly alloyed tool steels. There are two types of high-speed steels: Molybdenum (M-series) and tungsten (T-series). M-series contains up to about 10% Mo with Cr, V, W and Co as alloying elements while T-series contains 12-18% W with Cr, V and Co as alloying elements. The M-series made up 95% of all high-speed steel tools due to its higher abrasion resistance and is less expensive compared to T-series.

High speed steel can be hardened to various depth, has good wear resistance and relatively inexpensive. However, due to their low hot hardness, their cutting speeds are slow compared to others [4].

2.2.1.2 Carbides

To meet the challenge of increasingly higher cutting speeds, carbides were introduced in the 1930s. Carbides are among the most important and versatile tool due to their high hardness are wide range of temperature, high elastic modulus, high thermal conductivity and low thermal expansion. There are two major groups of carbides used for machining which is tungsten carbide (WC) and titanium carbide (TiC).[4]

Tungsten carbide consists of tungsten-carbide particles bonded together in cobalt matrix. Carbide cutting surfaces are often useful when machining through materials such as carbon steel or stainless steel, as well as in situations where other tools would wear away, such as high-quantity production runs. Most of the time, carbide will leave a better finish on the part, and allow faster machining. Carbide tools can also withstand higher temperatures than standard high speed steel tools.

Machining with carbide can be difficult, as carbide is more brittle than other tool materials, making it susceptible to chipping and breaking. To offset this, many manufacturers sell carbide inserts and matching insert holders. With this setup, the small carbide insert is held in place by a larger tool made of a less brittle material (usually steel). This gives the benefit of using carbide without the high cost of making the entire tool out of carbide. Most modern face mills use carbide inserts, as well as some lathe tools and endmills.

Titanium Carbide consists of a nickel-molybdenum matrix. It has higher wear resistance but lower toughness compared to WC.

2.2.1.3 Alumina based ceramic tools

Alumina based ceramic tools have very high abrasion resistance and hot hardness. It consists of fine-grained, high purity aluminum oxide with addition of titanium carbide and zirconia to help improve properties such as toughness and thermal shock resistance. Alumina based ceramic tools are more chemically resistant than high speed steel and carbides, thus have less tendency to adhere to metal during cutting. However, ceramics lack toughness and their use may result in premature tool failure such as chipping and catastrophic failure.[4]

2.2.1.4 Cubic Boron Nitride

Cubic boron nitride (cBN) is the hardest material available next to diamond. Cubic boron nitride is extremely hard, although less so than diamond and some related materials. Also like diamond, cubic boron nitride is an electrical insulator but an excellent conductor of heat. It is widely used as an abrasive for industrial tools.[5] Its usefulness arises from its insolubility in iron, nickel, and related alloys at high temperatures, whereas diamond is soluble in these metals to give carbides. Polycrystalline c-BN abrasives are therefore used for machining steel, whereas diamond abrasives are preferred for aluminium alloys, ceramics, and stone. Like diamond, cubic BN has good thermal conductivity, caused by phonons. In contact with oxygen at high temperatures, BN forms a passivation layer of boron oxide. Boron nitride binds well with metals, due to formation of interlayers of metal borides or nitrides.

2.2.1.5 Silicon Nitride based ceramic

Silicon nitride (Si_3N_4) is a hard, solid substance that can be obtained by direct reaction between silicon and nitrogen at high temperatures. Silicon nitride, which has relatively good shock resistance compared to other ceramics, is the main component in silicon nitride ceramics, with addition of alumina, yttria and titanium carbide [4].

2.2.2 Coated tool material

2.2.2.1 Titanium nitride coating

Titanium-nitride coatings have low friction coefficient, high hardness, resistance to high temperature, and good adhesion to substrate. These properties resulting in great improve in high-speed steel and carbide tools life.[4]

2.2.2.2 Diamond coatings

Diamond coatings have a great application as wear-resistant layers on tools. Polycrystalline diamond is being used widely as coating for cutting tools, especially tungsten carbide and silicon nitride inserts. Diamond-coated tools are effective when used to machine nonferrous and abrasive materials. It is also used when good surface finish and dimensional accuracy is required.

2.3 Overview of Diamond as Coating Material

The extreme hardness of diamond make it a very attractive material to be used as coating material for cutting tool. The structure of diamond, especially its very strong chemical bonding, leads to its unique mechanical and elastic properties. Beside its structure, nucleation and growth of diamond coating will be discussed. Substrate pretreatment and deposition parameter play important roles in obtaining high quality diamond coating.

2.3.1 Structures and properties of diamond

Diamond is a unique material because of its exceptional mechanical, thermal, optical and electronic properties. The structure of diamond, especially its very strong chemical bonding, leads to its unique mechanical and elastic properties. However, it has proved very difficult to exploit these properties, due to the cost and scarcity of large natural diamond and the fact that diamond only available in form of stones and grits.

Carbon is an element that exists in various polymorphic forms, as well as in the amorphous state. One of the polymorph of carbon is graphite; in the graphite lattice structure, as shown in Figure, each carbon atom combines with its three neighbors using hybrid sp^2 atomic orbitals, forming a series of continuous hexagonal structures, all located in parallel planes. The strong σ bonds are covalent, forming equal angles of 120° to each other; with a short bond length of 0.141 nm and a high strength of 524 kJ mol^{-1} . The fourth bonding electron participates in weak van der Waals type of bond between the layers of only 7 kJ mol^{-1} . As the consequences of these weak interplanar bonds, interplanar cleavage is facile, which give rise to the anisotropic characteristic of graphite.[6]

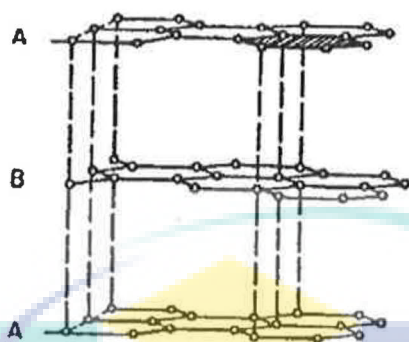


Figure 2.1 Schematic diagram of crystal structure of hexagonal graphite

Diamond is a metastable carbon polymorph at room temperature and atmospheric pressure. Diamond has two basic crystal structures, as shown in Fig. 2.2 : cubic symmetry (more common and stable) and hexagonal symmetry (rare but well established, found in nature as the mineral lonsdaleite). The closed packed layers, $\{111\}$ for cubic and $\{100\}$ for hexagonal, are identical [6].

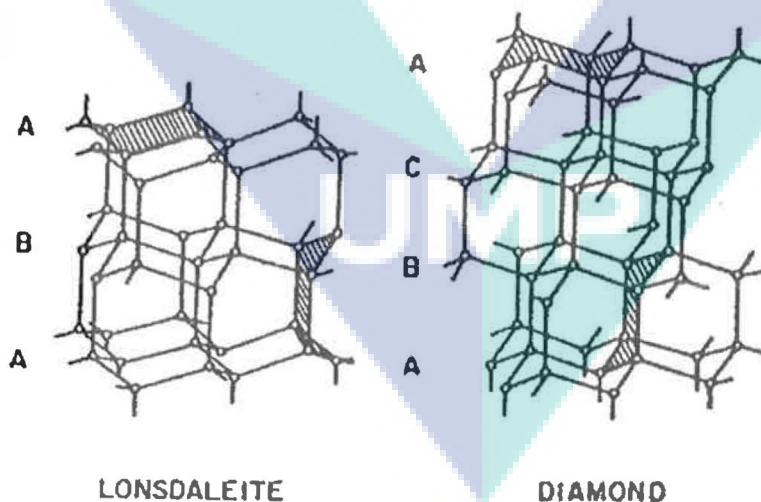


Figure 2.2: Schematic diagrams of two basic crystal structures of diamond: hexagonal lonsdaleite and cubic diamond

The cubic structure of diamond is the dominant crystal structure in both natural and synthetic since the staggered conformation is more stable due to slightly lower energy. Thus cubic diamond will simply referred as “diamond”. In the diamond lattice structure, each carbon atom is tetrahedrally coordinated, forming strong bonds to its four neighbor using hybrid sp^3 atomic orbital, with equal angles of $109^\circ 28'$ to each other. The covalent bonding between carbon atoms is characterized by short bond length of 1.54\AA and high bond energy of 711 kJ mol^{-1} . It short bond and the tetrahedral configuration are responsible for the high density of the crystal and its high Young's modulus [7]. Its crystal structure is a variant of the zinc blende, in which carbon atoms occupy all position, as shown in Fig. 2.3 [8].

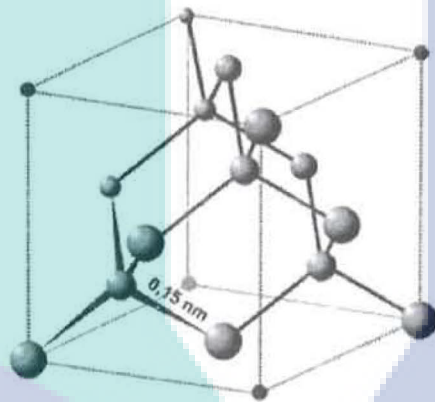


Figure 2.3: Schematic of unit cell of cubic diamond

UMP

Diamond has several crystal shapes which include $\{100\}$ cube, $\{110\}$ dodecahedron, $\{111\}$ octahedron and other more complicated shapes, as shown in Fig. 2.5. In CVD diamond, the octahedral faces are observed at low temperatures and low hydrocarbon concentration, while cubic faces predominate at high temperatures and high hydrocarbon concentrations. Cubo-octahedral crystal combining both these faces is commonly found [6].

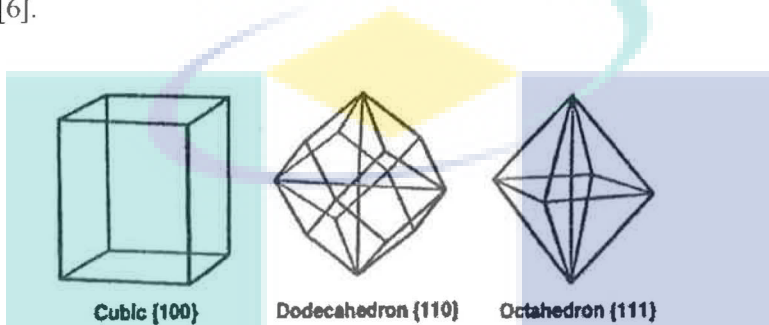


Figure 2.4: Schematic of the simple crystals shape of diamonds

The dependence of crystal shapes on deposition conditions has been correlated to the ratio of growth rates in $\langle 100 \rangle$ and $\langle 111 \rangle$ directions, defined as a growth parameter α , in which $\alpha = (v_{100}/v_{111})^{1/3}$. As shown in Figure 2.5, when value of α increases from 1 to 3, the crystal structure change from cube to cubo-octahedron and then to octahedron. The crystal grown with $\alpha > 1.5$ exhibit rough $\{111\}$ facets while crystals grown with $\alpha < 1.5$ show very smooth $\{111\}$ facets [9].

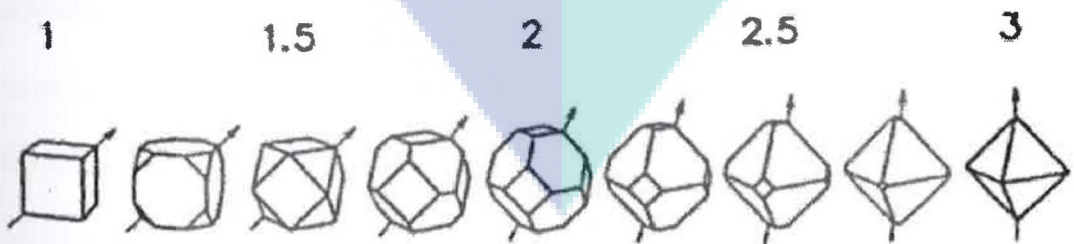


Figure 2.5: Idiomorphic crystal shapes of diamond for different values of the growth parameter, α .

Diamond probably the only material that in which size, morphology, shape and structure influence both type and efficiency of its applications as critically as they do. Modern diamond can be categorized into 4 categories: natural diamond, high pressure synthetic diamond, CVD diamond and diamond-like carbon (DLC). Single crystal synthetic diamond can be produced by high pressure high temperature method. CVD diamond is usually in form of polycrystalline thin coatings consisting of a dense network of high density carbon (diamond) crystallite, usually cubo-octahedral morphology. DLC films contain a good portion of sp^2 bonding, often up to 60% [10]. Table 2.2 shows comparison in term of properties for different kind of diamond.

Table 2.2: Comparison between typical properties of various categories of diamond [6, 10, 11]

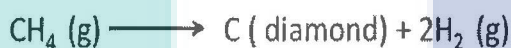
Properties	Single Crystal Diamond	CVD diamond	DLC
Density	3.515	2.8-3.51	1.8-2.8
Young Modulus, GPa	900-1250	250-1050	35-369
Thermal conductivity at 25°C, W/m·K	2200	>1300	400-1000
Bandgap, eV	5.45	5.45	0.8-3
Index of refraction at 10 μ m	2.4	2.34-2.42	1.8-2.4
Electrical resistivity, Ω ·m	10^6	$10^{12} - 10^{16}$	$10^5 - 10^{15}$
Vickers hardness, kg/mm ²	5700-10400	5000-10000	2000-9000
Coefficient of friction in air	0.035-0.3	0.05-0.15	0.01-0.3

2.3.2 Deposition Mechanism of Polycrystalline CVD diamond

Over the past few years, diamond in form of thin film has been produced by using film growth technique involving vapor-phase chemical reactions followed by the film deposition. The diamond is polycrystalline and consists of small or relatively large grain; amorphous carbon and graphite may present depending on the deposition parameter.

The basic reaction in CVD of diamond is seemingly simple. It involves the decomposition of a hydrocarbon such as methane as shown in Equation 1.

Equation 1



Although the complex interaction of deposition mechanism is not fully understood at this time, two essential conditions have been identified: (a) activation of carbon species and (b) the action of atomic hydrogen [11]. The identification of the critical species and mechanisms of the diamond CVD process will assist in the understanding and technological improvement of the process and materials. The generalized CVD diamond growth environment are presented in Fig. 2.6. The reactants, methane and hydrogen, enter a high temperature or energetic region in which the gas is activated by a plasma, a hot filament or a combustion flame front. Chemical reactions are initiated and the species participating in these reactions are transported by forced flow, diffusion and convection throughout the reactor, eventually reaching the substrate or being exhausted from the reactor. Near the substrate, species may diffuse through a stagnant flow region, called the boundary layer. On the substrate surface, various processes may occur such as adsorption, desorption, surface and bulk diffusion of species as well as the chemical reactions [12].

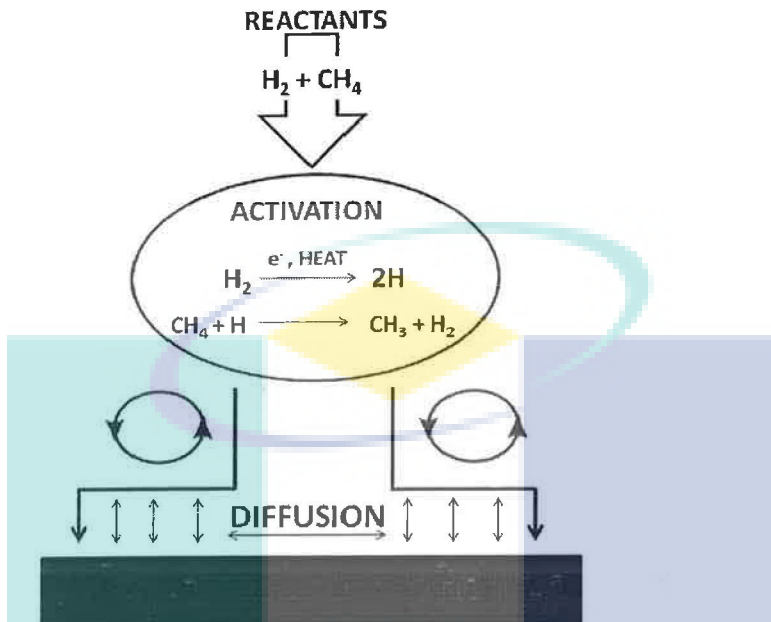


Figure 2.6 Generalized schematic of the physical and chemical process occurring in CVD diamond reactor

Diamond CVD differs from many other crystal growth processes in several important ways. First, carbon atoms can form different types of chemical bonds using sp , sp^2 , and sp^3 hybridization of its valence electrons. This characteristic results in the diverse nature of carbon-based materials and chemistries. Diamond is a crystalline form of carbon comprised solely of sp^3 bonds and is thermodynamically metastable relative to the sp^2 bonded graphite crystalline phase at the temperatures and pressures used in the CVD process. Second, it is probable that the gaseous and surface species in the growth environment will be molecular, not atomic, due to the affinity of carbon to form strong bonds and the prevalence of molecular and atomic hydrogen. Third, diamond CVD occurs at substrate temperatures which are low compared with the CVD of other high quality crystalline materials, when each is scaled to other characteristic temperatures or material properties [13].

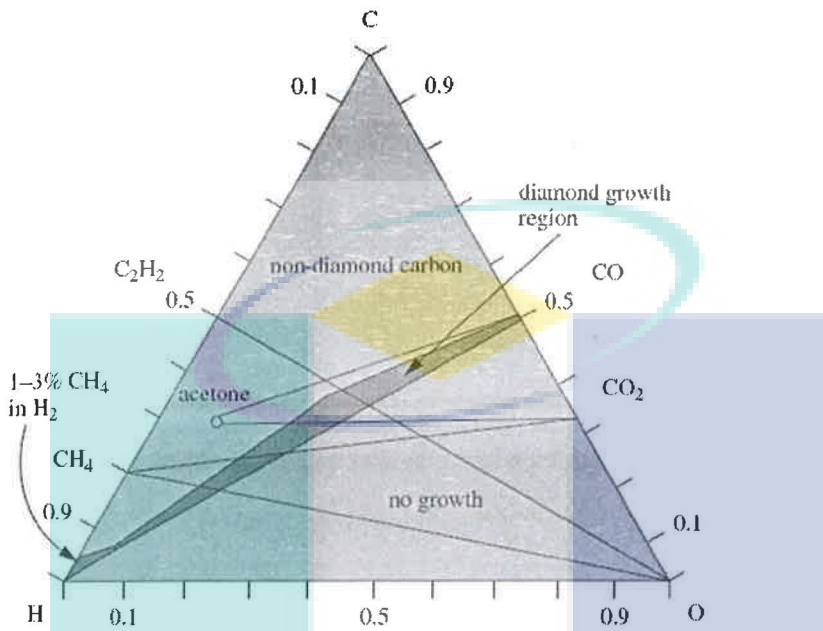


Figure 2.7 Simplified form of the Bachmann triangle C-H-O composition diagram in which below CO tie-line, no film growth will occur. Above the CO tie-line, non-diamond carbon is deposited except in a narrow window close to the tie-line which produces polycrystalline diamond films

2.3.2.1 Nucleation and Growth of CVD diamond

Nucleation is the first and critical step in CVD diamond growth. The control of nucleation is important in order to optimize the diamond properties such as grain size, orientation, transparency, adhesion and roughness.

The investigation of diamond nucleation not only can lead to the controlled growth of diamond films suitable for various applications, but also it can provide insight into the mechanism of diamond growth. To date, the understanding of diamond nucleation is very limited. Carbon atoms can form different types of chemical bonds via sp^1 , sp^2 , and sp^3 hybridization. Diamond consists solely of sp^3 bonds and is

thermodynamically meta-stable compared to graphite, which is composed of sp^2 bonds, under the experimental conditions used in CVD. It is an interesting and yet intriguing problem why metastable diamond can be grown on diamond or non-diamond substrates under CVD conditions

In order for nucleation to proceed, an incipient nucleus must form and be stable long enough for lattice growth to occur. The development of a critical nucleus, i.e., that size above which it is more probable that a nucleus will survive and grow, depends on the system free energy changes accompanying particle formation under growth conditions. The change in the system free energy must be negative for the process to occur. The nucleus free energy increases with the addition of atoms until the critical radius is attained, at which point the net free energy reaches a maximum and then declines as shown in Fig. 2.8 [13].

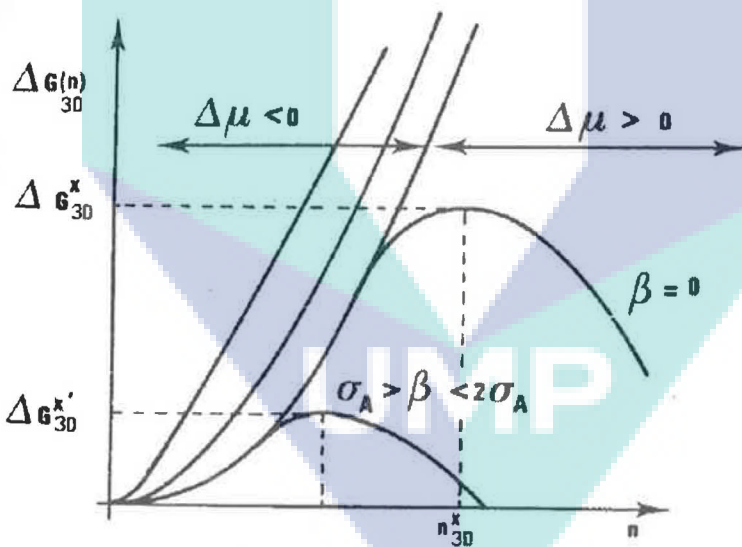
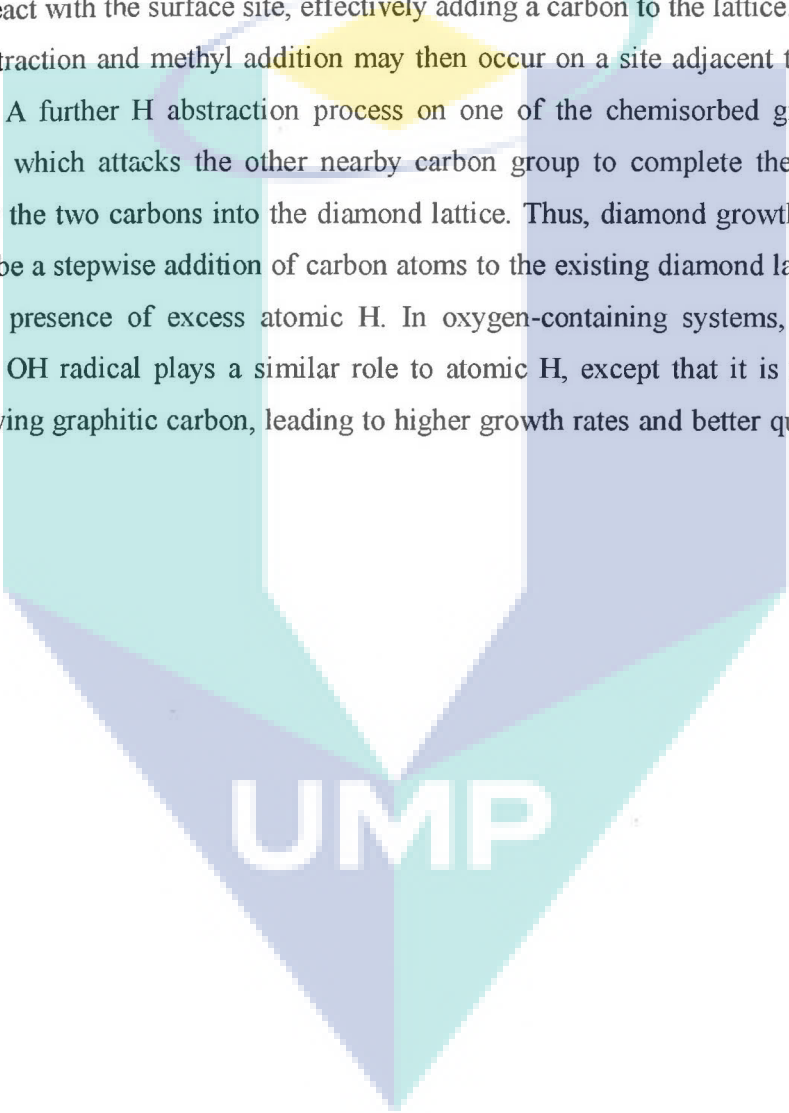


Figure 2.8 Free energy diagram of three dimensional crystal formation (ΔG_{3D}) at constant supersaturation ($\Delta\mu$) as a function of the number of its particle, n . [13]

Fig. 2.9 shows the simplified description of CVD diamond growth in which hydrogen atoms play an important role in CVD diamond formation process. Atomic H abstracts a surface H to form H_2 , leaving behind a reactive surface site. The most likely fate for this surface site is for it to react with another nearby H atom, returning the surface to its previous stable situation. However, occasionally a gas phase CH_3 radical can collide and react with the surface site, effectively adding a carbon to the lattice. This process of H abstraction and methyl addition may then occur on a site adjacent to the attached methyl. A further H abstraction process on one of the chemisorbed groups creates a radical, which attacks the other nearby carbon group to complete the ring structure, locking the two carbons into the diamond lattice. Thus, diamond growth can be considered to be a stepwise addition of carbon atoms to the existing diamond lattice, catalysed by the presence of excess atomic H. In oxygen-containing systems, it is believed that the OH radical plays a similar role to atomic H, except that it is more effective at removing graphitic carbon, leading to higher growth rates and better quality films [1].

The logo for UMP (Universiti Malaysia Perlis) is a large, downward-pointing arrow shape. It is composed of four triangular sections meeting at a central point. The top-left and bottom-right sections are light blue, while the top-right and bottom-left sections are light green. The letters 'UMP' are printed in a bold, white, sans-serif font across the center of the arrow.

UMP

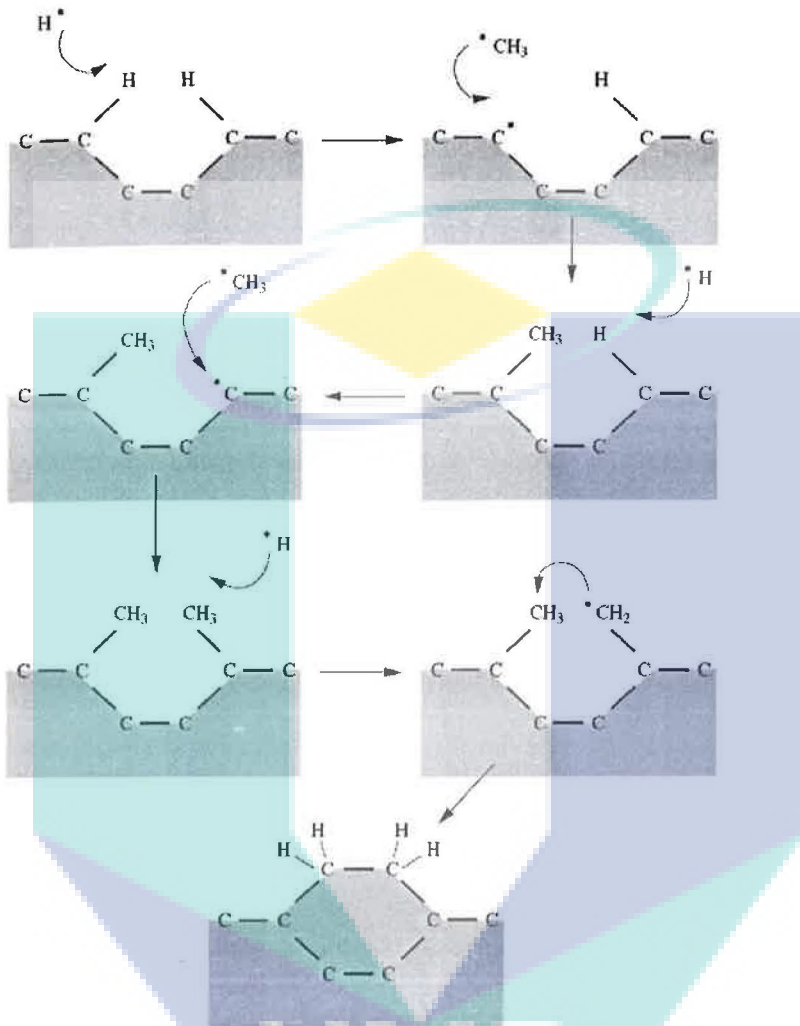


Figure 2.9: Schematic of the reaction process occurring at the diamond surface leading to stepwise addition of CH_3 species and diamond growth [1].

Although diamond can grow homoepitaxially on diamond surface without nucleation problem in HFCVD, MW PACVD and ECR PACVR from variety of carbon source, the diamond nucleation process will be very slow on non diamond surface [6]. Fig. 2.10 illustrate the growth process in conventional CVD polycrystalline diamond on non-diamond substrate. Before nucleation start, an incubation period (Fig. 2.10a) which may take few minutes up to hours may begin depend on substrate materials, surface

pretreatment and deposition parameters. Then the isolated sphere-like nuclei start to form. As the time increases, the nucleation density increases to certain value then the surface nucleation terminates allowing the isolated crystals to grow homogeneously in size and develops faceting. When the isolated crystals coalesce, a continuous diamond film is forms [3].

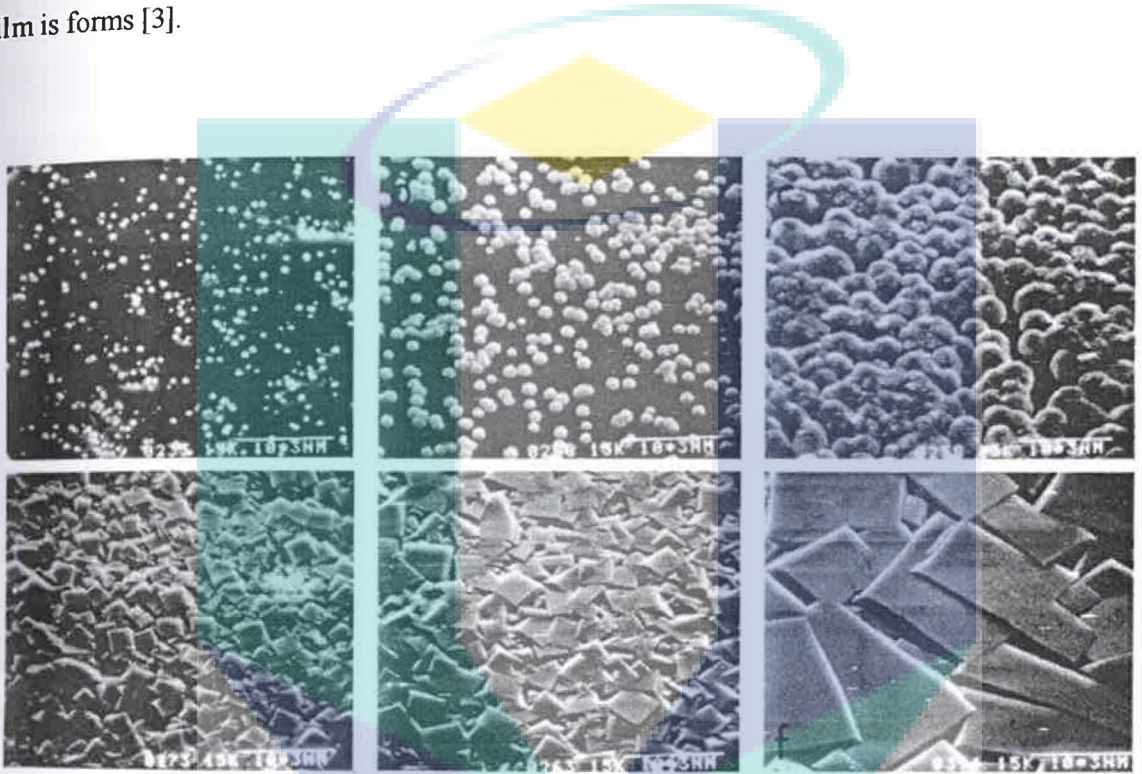


Figure 2.10: Growth process of a diamond film on a non-diamond substrates: (a) nucleation of individual crystallites (b-c) termination of nucleation, and growth of individual crystallite (d) faceting and coalescence of individual crystallites and formation of continuous film (e-f) some crystals grow faster and swallow their neighbours during growth of continuous film [6].

2.3.3 Polycrystalline diamond deposition of various substrates

Polycrystalline diamond has been deposited on various substrates to improve the properties of the substrate. As coating for cutting tools material, deposited diamond improves the fracture toughness of the material thus extend the tool life.

2.3.3.1 Deposition on cemented tungsten carbide

As discussed in Section 2.2.1.2, cemented tungsten carbide (WC Co) is used as cutting tool because it fulfilled the criteria of high performance machining tool to be able to withstand the static and dynamic loading requirement, satisfies the requirement in respect to wear and allow for easy manufacturing and processing [14].

Nevertheless, when used as cutting tools, it is found that WC-Co wear rapidly when machining some particular materials such as green ceramics, graphite or metal matrix composite[14-16]. Thus, diamond coating on WC-Co helps to enhance the machining effectiveness of WC-Co by improving the wear properties of WC-Co cutting tools.

However, diamond coatings deposited by CVD on cemented carbides generally have low adhesive-bond strength to the substrate due to (1) thermal expansion mismatch leading to thermal stress at interface and (2) interaction between the carbon and thin layer of cobalt on the surface of the tool. The surface of WC-Co substrate is composed of WC grains bound together by cobalt or cobalt alloy. Under typical diamond coating conditions, carbon exhibits a large solubility and diffusivity in cobalt. The dissolution of carbon into cobalt will extend the incubation period for diamond nucleation and enhance the accumulation of graphite at the diamond-graphite interface. The accumulated graphite will weaken the bond and degrade the quality of the diamond coating [17] . Thus, surface pretreatment must be done to remove cobalt from the surface.

Among common method in increasing diamond nucleation in WC-Co substrate are as follows [6]:

- Substrate scratching with abrasives
- Seeding substrate with diamond grit and other powders
- Electrical biasing
- Covering substrate surfaces with interlayers
- Chemical Etching
- Carburization of substrate surface

2.3.3.2 Deposition on silicon nitride

Silicon nitride (Si_3N_4) based ceramic tools are widely used as cutting tools because of their high hardness, high thermal conductivity and low thermal expansion coefficient, as discussed in Section 2.2.1.5. However, in some applications, silicon nitride surface can be damaged by particle impact or by oxidation. Thus, by coating the Si_3N_4 by a very hard, erosion resistant coating such as diamond film can reduce chemical wear of nitride ceramic and also protect the Si_3N_4 from failure [18, 19]. Si_3N_4 ceramic appears to be a favorable material to be diamond deposited considering its thermal expansion coefficient ($2.9 \times 10^{-6} < \alpha < 3.6 \times 10^{-6} \text{ K}^{-1}$ for $20 < T < 1500^\circ\text{C}$) is closer to that of diamond [20]. Also, the absence of graphite catalyser such as Co and others binders make Si_3N_4 suitable material as substrate for diamond deposition [21]. The quality of diamond deposited on silicon nitride substrate, however, strongly dependent and correlated with diamond nucleation and growth, presence of defect and interfacial stresses [18].

E. Cappelli et. al. [18] has discussed ways to improve diamond nucleation and adhesion on sintered nitride ceramics. Although Si_3N_4 is more stable compared to WC-Co in term of graphite formation that can reduce the adhesion strength of the diamond film, the carbide formation that helps in nucleation of diamond in such material also is unlikely, thus resulting in slow nucleation in Si_3N_4 substrate. The formation of matching

carbide layer in substrate materials such as Si, Mo and Ti acts as precursor for the onset of nucleation. In such materials, formation of carbide is thermodynamically favoured in conventional CVD conditions. However, for Si_3N_4 substrate, Si_3N_4 is more stable than SiC and the reaction



can only start at temperature above 1350°C . Furthermore, high activation energy required for heterogeneous nucleation also causes low nucleation density in Si_3N_4 [22]. Thus, various ways to improve nucleation of polycrystalline diamond deposited on Si_3N_4 has been done and will be discussed in section 2.3.4.

2.3.4 Surface pretreatment

Table 2.3 shows different Si_3N_4 substrate surface pretreatment that have been over this few years and its effect on the quality of the deposited polycrystalline. As discussed in Section 2.3.3.2, surface pretreatment is done to enhance the nucleation density that will in return improve the quality and adhesion strength of the diamond films.

Table 2.3 Surface pretreatment for silicon nitride substrate

CVD	Surface treatment method	Quality	References
HFCVD	As cut, rinsed acetone	Not continuous	[18]
	Polishing (abrasive SiC paper, diamond paste 1 μ m)	Continuous	
	Polishing (abrasive SiC paper, diamond paste 1 μ m), basic etching	Continuous	
	Acid etching (HF:HNO ₃ 1:1, 30 min) + ultrasound shaking	Continuous	
	Seeding by PLD	Not Continuous	
	Acid etching (HF:HNO ₃ 1:1, 30 min)	Not Continuous	
	Scratching with diamond paste	Almost continuous	
PACVD	Interlayer thickness 6.8 μ m, substrate temperature 910K	Nucleation density of 10 ⁸	[23]
	Interlayer thickness 5 μ m, substrate temperature 1080K	Nucleation density 6 x 10 ⁶	
MPCVD	Pretreated in strong acid (60% HNO ₃ and 47% HF (1:1))	Peeling after cutting amount of 50 cm ³	[24]
	Pretreatment followed by microflawing in diamond suspended ethanol solution	Normal wear after cutting amount of 320 cm ³	
	Pretreatment followed by deposition of DLC interlayer	Normal wear after cutting amount of 210 cm ³	
DC plasma jet CVD	Chemical etching with 40%HF and 15% HNO ₃ and scratched by 5 μ m	Good	[25]
	Chemical etching with 40%HF and 15% HNO ₃ and scratched by 1 μ m	Good	
HFCVD	CF ₄ addition	Nucleation density 10 ⁸	[21]

2.4 Deposition technique of polycrystalline diamond

2.4.1 Introduction

Diamond thin films have been synthesized by various method either using chemical vapor deposition (CVD) or physical vapor deposition (PVD). In CVD, the source of carbon is an activated gas phase that contains a mixture of molecules, atoms, radicals, ions and electrons which oscillate randomly in three dimensions and will condense as diamond only at suitable chemical composition and temperature. Physical vapor deposition techniques, on the other hand, involve the evaporation or sublimation of carbon from a solid source into gas phase. The evaporated carbon is chemically and energetically altered so that it condenses as diamond on the surface of the substrate.

2.4.2 Operating principle of CVD

Most method of CVD of diamond are based on these following principles [26]:

1. A gas phase is activated, either by high temperature and/or plasma excitation.
2. The gas phase contains a carbon-containing species such as hydrocarbon, carbon monoxide or carbon dioxide.
3. High concentrations of a species such as atomic hydrogen are needed to etches graphite or suppresses gaseous graphite precursor.
4. The substrate surfaces able to support the nucleation and growth of the diamond from the vapor phase by not having any catalyst that can promote formation of graphite.
5. The temperature gradient in the CVD processes will provide the driving force to transport the carbon-bearing species from the gas phase to the surface of the substrate.

All CVD techniques for producing diamond films required activating gas phase carbon-containing precursor molecules. While each CVD method differs in detail, they all share features in common. For example, growth of diamond normally requires that the substrate be maintained at temperature in the range 1000-1400 K and the precursor gas be diluted in an excess of hydrogen [2].

2.4.3 CVD diamond deposition techniques

Various CVD systems have been used in polycrystalline diamond deposition. Table 2.4 shows the comparison between various CVD systems in term of deposition rate, temperature control and main product.

Table 2.4 Characteristics of Diamond Deposition Processes [11]

Activation Method	Process	Substrate deposition rate	Temperature control	Main Product
Thermal	Hot Filament	Low (0.1-10 $\mu\text{m/hr}$)	Good	Coating
Glow Discharge plasma	Microwave RF	Low (0.1-10 $\mu\text{m/hr}$)	Good	Coating
Arc Plasma	DC Arc RF Arc	High (50-1000 $\mu\text{m/hr}$)	Poor	Coating
Combustion	Torch	High	Poor	Coating Powder

2.4.3.2 Arc-Discharge

Another common plasma deposition system for diamond coatings is based on plasma arc as shown in Fig. 2.11. Electrode usually consists of water-cooled copper

anode and a tungsten cathode. It also includes several gas-jet nozzles that can be operated simultaneously and have many design variations. When the gases are heated in the arc plasma, the gases will expand causing formation of a high-speed arc jet so that the atomic hydrogen and reactive carbon are transported almost instantly to the deposition surfaces.

Arc plasma system can produce rapid and efficient deposition, with high rates of deposition. However, temperature control and substrate cooling remains a problem in these systems.

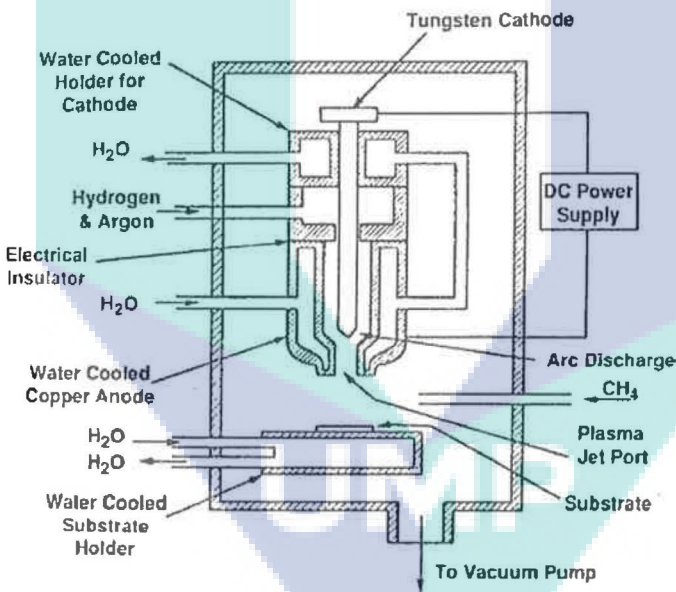


Figure 2.11 Schematic of arc-discharge apparatus for the deposition of diamond.

2.4.3.3. Microwave plasma-assisted CVD

A typical microwave plasma for diamond deposition has an electron density of approximately 10^{20} electrons/m³ and sufficient energy to dissociate hydrogen. The MPCVD reactor is shown in Figure 2.12. After the substrate is positioned at the lower end of the plasma, gases are introduced at the top of the reactor which will flow around and react around the substrate. For diamond to form, the substrate must be heated to 800 - 1000°C [11].

The advantage of MPCVD is its stability which allows uninterrupted deposition lasting for days if necessary.

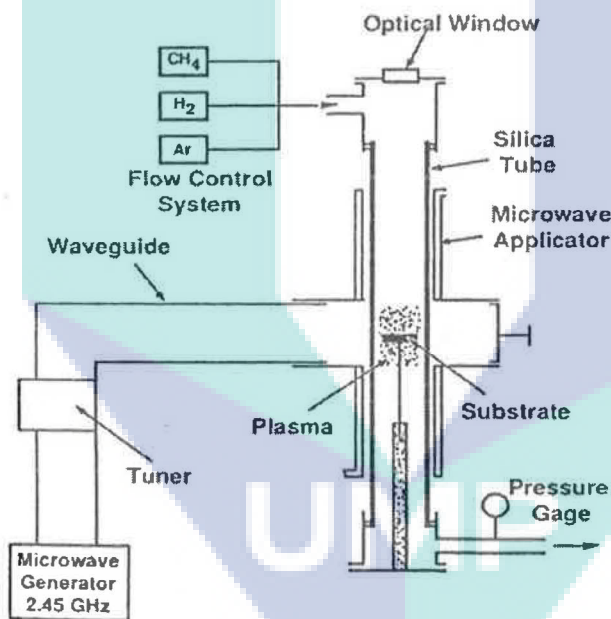


Figure 2.12 Schematic of microwave-plasma deposition

2.4.3.1 Hot Filament CVD

Hot filament CVD (HFCVD), as shown in Fig. 2.13, uses a vacuum chamber continually pumped using a rotary pump, while process gases are metered in at carefully controlled rates (typically a total flow rate of a few hundred sccm). Throttle valves are used to maintain the pressure in the chamber at typically 20–30 Torr, while a substrate heater is used to bring the substrate up to a temperature of 700–900 °C. The filament is made from a metal that will be able to survive these conditions and not react significantly with the process gas [1]. The hot filament transforms the input hydrocarbon such as methane (CH_4) into hydrocarbons stable at filament temperature such as acetylene (C_2H_2) and methyl (CH_3). The hot filament also dissociates H_2 into H^\bullet [26]. Metals such as tungsten and tantalum are most often used, although they do eventually react with the carbon-containing gases and carburize to form the metal carbide causing them to change their resistivity and makes them brittle. The HFCVD method is relatively cheap and easy to operate and produces reasonable quality polycrystalline diamond films [1].

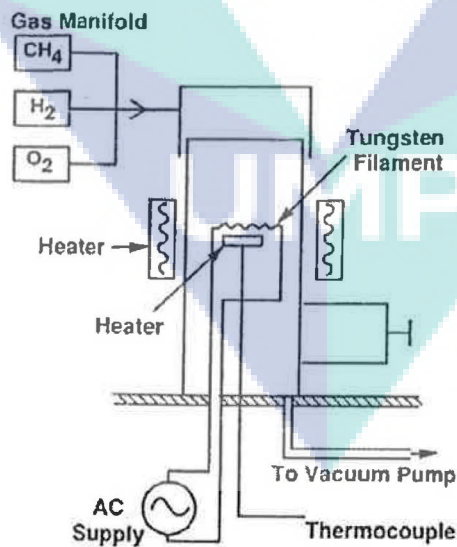


Figure 2.13 Hot Filament Apparatus for deposition of diamond

The usage of HFCVD in deposition of polycrystalline diamond on various substrates has been discussed in various publications. Table 2.5 shows the HFCVD parameter in depositing diamond in Si_3N_4 and WC-Co

Table 2.5: Deposition parameter of HFCVD on Si_3N_4 and WC-Co substrate.

Parameter	Cappeli et. al [18]	Sarangi et. al[27]
Substrate	Si_3N_4	WC
Pressure (Torr)	25	20
Methane concentration (vol%)	1	0.5
Total gas flow rate (sccm)	100	150
Substrate temperature ($^{\circ}\text{C}$)	810	730
Filament temperature ($^{\circ}\text{C}$)	2170-2250	2030-2130
Filament substrate distance (mm)	~0.8-1	5 - 6
Deposition time	2-35 hr	8

In general, although hot filament method have much slower growth rates (0.1-10 $\mu\text{m/hr}$), it produce high quality film. However, the filament method often suffers from contamination problems, since metal boiled off the filament can be incorporated into the diamond film [2]. Thus, by using lower filament temperature and slower deposition rate, contamination problem caused by the filament in the hot filament CVD reactor can be minimized [28].

The morphology of diamond films produced by HFCVD may also be controlled by various parameters in HFCVD. Substrate biasing, in which negative voltage is applied to the substrate during short period prior to normal growth, enhanced the diamond nucleation in HFCVD. This can be explained by bombardment of the substrate surface could enhance the surface mobility of atoms, thus carbon clusters would readily form. In addition, bias might cause a high concentration of atomic hydrogen and disassociated hydrocarbons near substrate surface by collision with accelerated ions,

resulting in increase nucleation [29] The mechanism for negative and positive substrate biasing are shown in Figure 2.14.

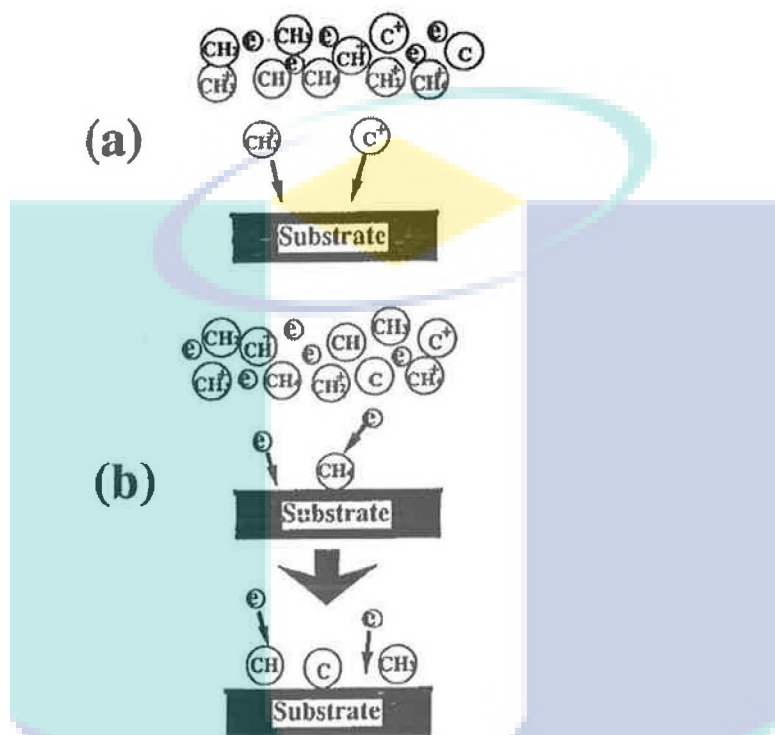


Figure 2.14 Schematic diagram showing the mechanisms of diamond nucleation enhancement on biased substrate. (a) Negative biasing: carbon containing cations are accelerated toward the substrate surface. (b) Positive biasing: electrons are accelerated toward the substrate surface and bombard carbon-containing molecules adsorbed on the surfaces [6].

Controlling the gas phase environment may also improve the quality of deposited diamond. Addition of CF₄ [21] and N₂ [30] into the HFCVD gas environment changes the surface morphology of the diamond film. W.Ahmed et. al. discussed about how addition of nitrogen can influence the surface morphology of the CVD diamond. The changes in the surface morphology and structure are related to the carbon supersaturation, which is controlled by the supply of carbon and creation of growth sites at the surface. Thus, small amounts of nitrogen are able to reduce carbon supersaturation which in turn improve the crystal quality [30].

CHAPTER 3

EXPERIMENTAL PROCEDURE

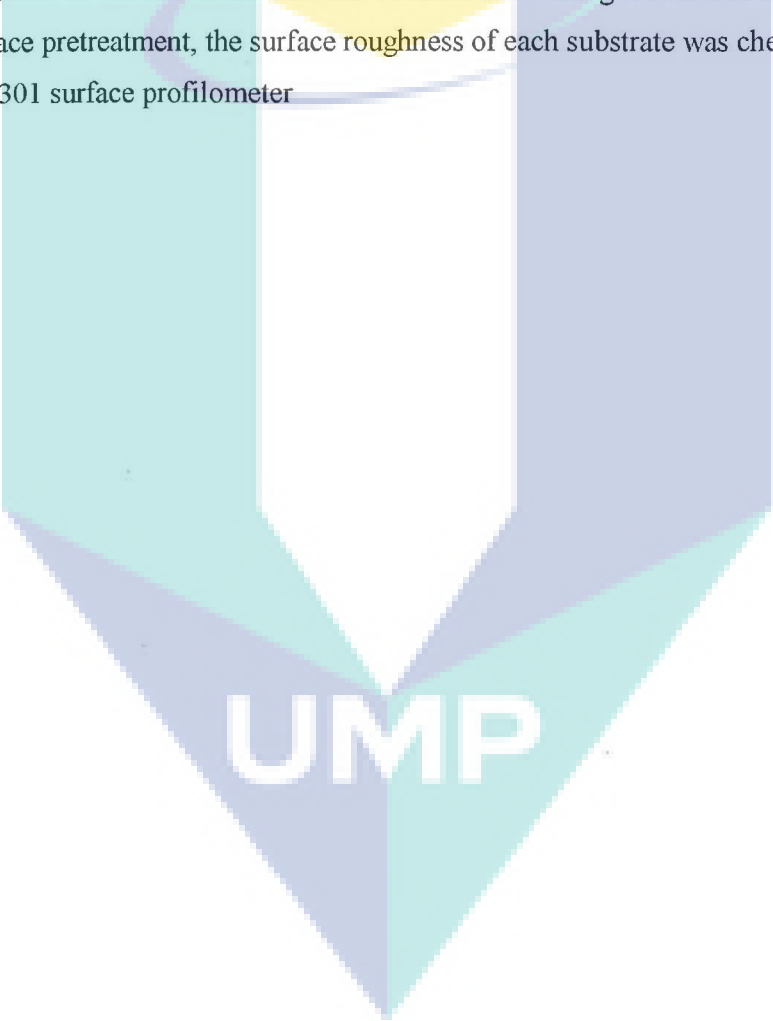
3.1 Introduction

In this chapter, detail description of equipment used and analysis method employed will be discussed. Various substrates pretreatment including cleaning, chemical etching and diamond seeding will be discussed in this chapter along with the principles of each machine used. The polycrystalline diamond coating is deposited using hot filament chemical vapor deposition machine followed by microstructural and mechanical characterization in order to investigate the properties and qualities of deposited diamond. Figure 3.1 shows the flow chart of the experiments.

3.2 Sample preparation and Pretreatment

3.2.1 Substrate Material

Silicon nitride (Si_3N_4) was used as substrate materials. As-received materials were characterized using XRD and EDX to determine its composition and crystal structure. The hardness of the substrate was also characterized using Vickers hardness tester. Prior to surface pretreatment, the surface roughness of each substrate was checked using Mitutoyo SJ-301 surface profilometer

The logo for UMP (Universiti Malaysia Perlis) is a large, downward-pointing arrow shape. It is composed of several geometric sections in shades of teal and light blue. The letters 'UMP' are printed in white, bold, sans-serif font across the bottom section of the arrow.

UMP

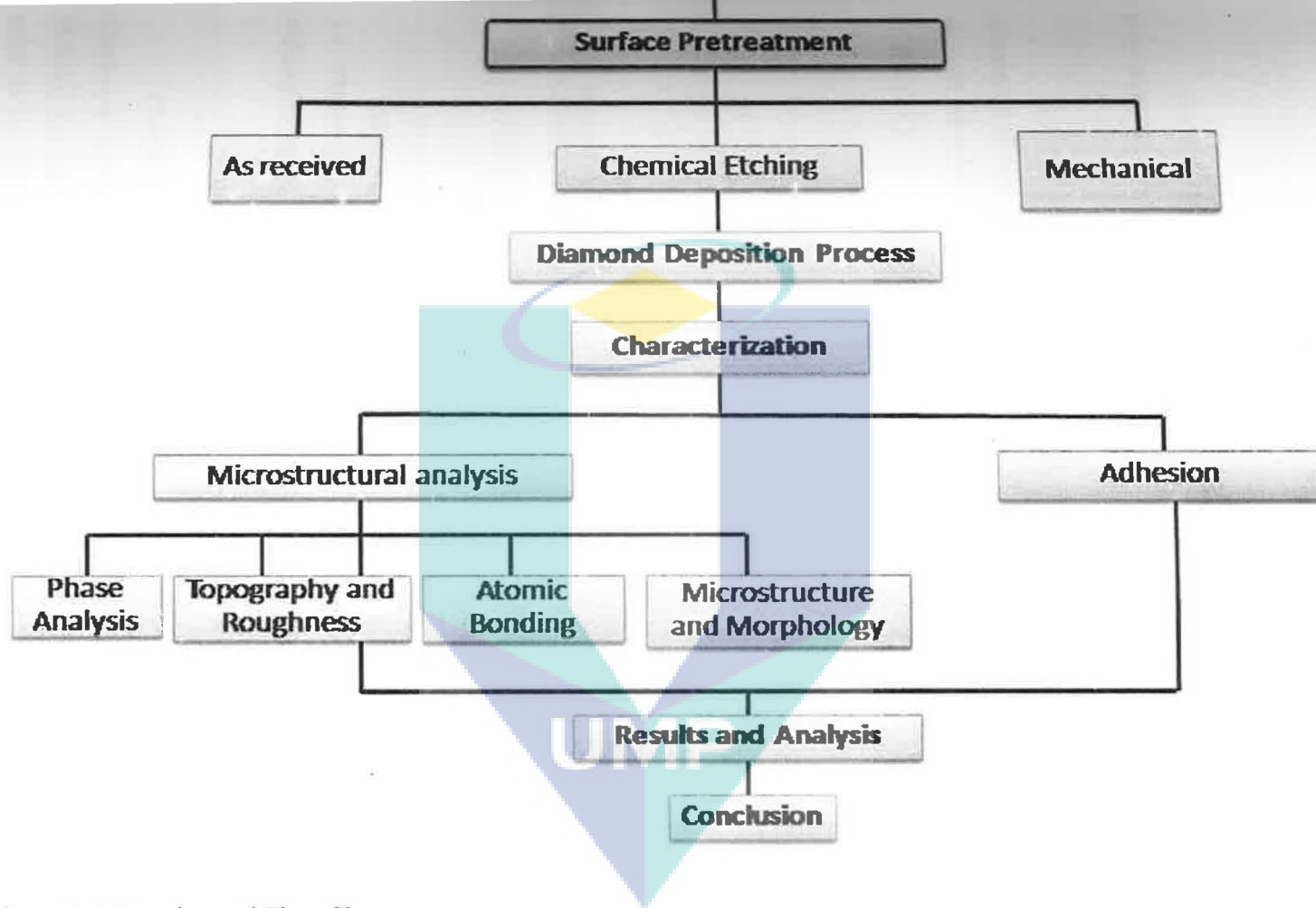


Figure 3.1 Experimental Flow Chart

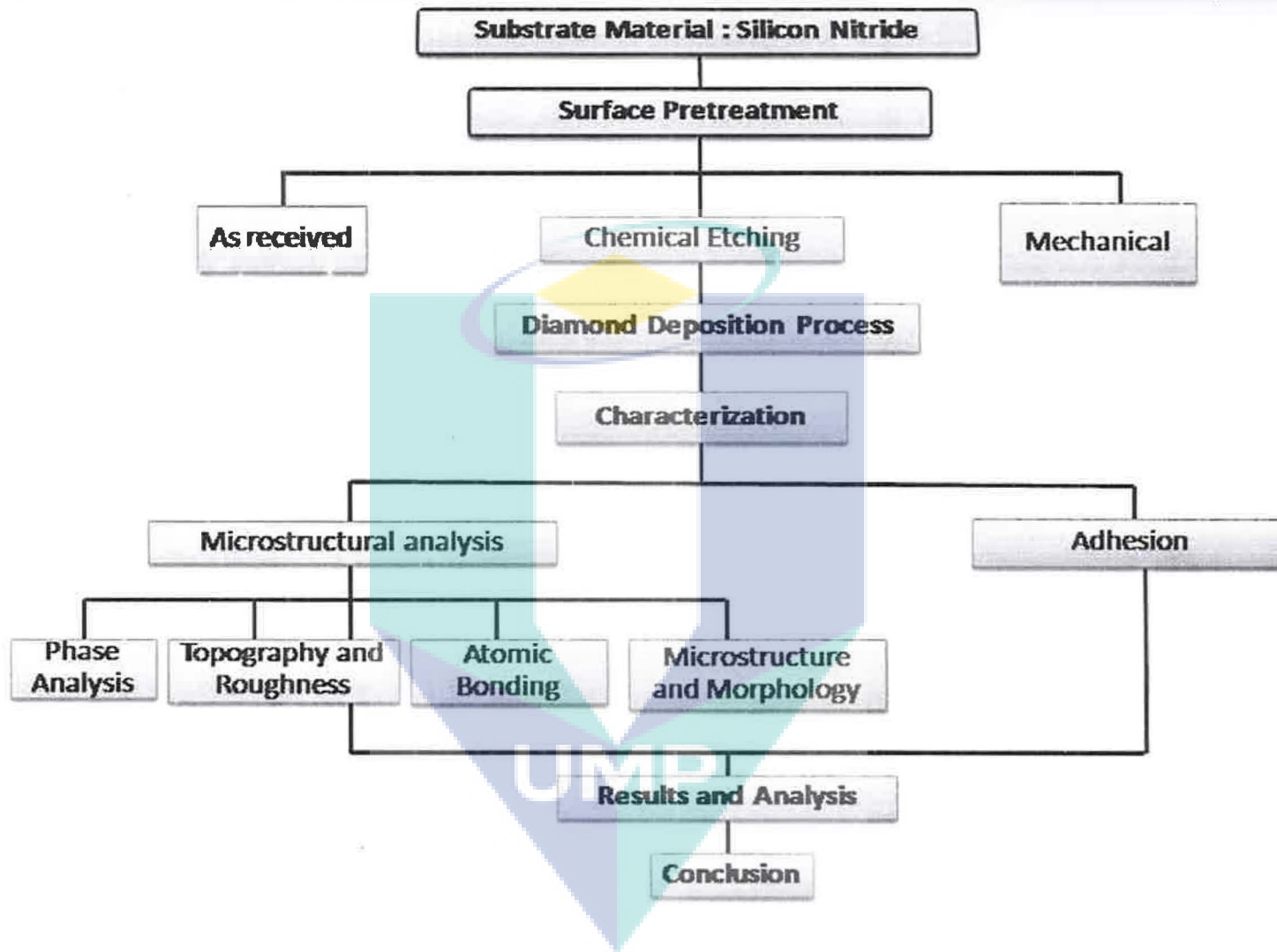


Figure 3.1 Experimental Flow Chart

3.2.2 Substrate Pretreatments

As-received silicon nitride substrate materials of dimension 12.69 x 12.69 x 7.95 mm were cut into half using ISOMET 5000 linear precision saw.

The cut sample then was cleaned with ethanol using a Bandelin SONOREX ultrasonic cleaner, as shown in Figure 3.2, to removes surface impurities, grease, oil and dust on the substrates.

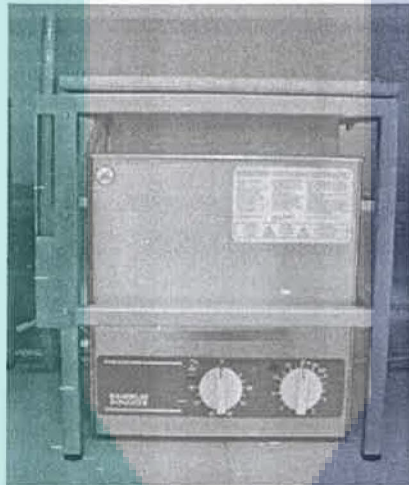


Figure 3.2 Ultrasonic cleaner used to clean the sample

Then, the substrates were subjected to various pretreatment as shown in Table 3.1. Chemical etching process was carried out by immersing the substrate in various etching solution. Mechanical pretreatments, on the other hand are described on Table 3.2.

Chemical etchings and mechanical pretreatments were done to introduce surface roughness on the substrate surface prior to deposition. Thus, following the chemical etching, the surface roughness of the samples was verified using stylus profilometer prior to seeding process. Prior to seeding process, samples were cleaned with distilled water ultrasonically to remove reagent due to etching.

Table 3.1 Chemical Treatment of Si_3N_4 substrates

Sample No.	Etching Reagent	Etching Time (min)	Seeding
1	40% HF: 15% HNO_3 (1:1), 50°C	10	Yes
2	40% HF: 15% HNO_3 (1:1), 50°C	10	No
3	40% HF: 15% HNO_3 (1:1), 50°C	20	Yes
4	40% HF: 15% HNO_3 (1:1), 50°C	20	No
5	40% HF: 15% HNO_3 (1:1), 50°C	30	Yes
6	40% HF: 15% HNO_3 (1:1), 50°C	30	No
7	Strong Acid etching 65% HNO_3 and 49% HF (1:1), 50°C	10	Yes
8	Strong Acid etching (65% HNO_3 and 49% HF (1:1), 50°C	10	No
9	Strong Acid etching (65% HNO_3 and 49% HF (1:1), 50°C	20	Yes
10	Strong Acid etching (65% HNO_3 and 49% HF (1:1), 50°C	20	No
11	Strong Acid etching (65% HNO_3 and 49% HF (1:1), 50°C	30	Yes
12	Strong Acid etching (65% HNO_3 and 49% HF (1:1)	30	No
13	Basic Etching, 30% KOH, 60°C	10	Yes
14	Basic Etching, 30% KOH, 60°C	10	No
15	Basic Etching, 30% KOH, 60°C	20	Yes
16	Basic Etching, 30% KOH, 60°C	20	No
17	Basic Etching, 30% KOH, 60°C	30	Yes
18	Basic Etching, 30% KOH, 60°C	30	No

Table 3.2 As-received and mechanically treated sample

Sample No	Surface treatment method	Seeding
19	As cut, rinsed acetone	Yes
20	As cut, rinsed acetone	No
21	Blast with SiC 180 for 30 sec	Yes
22	Blast with SiC 180 for 30 sec	No
23	Grinding with 180 grit for 5 minutes followed by 600 grit for 5 minutes	Yes
24	Grinding with 180 grit for 5 minutes followed by 600 grit for 5 minutes	No

Seeding is done by immersing the pretreated substrates into seeding solution described in Table 3.3. The SiC powder in seeding solution will further helps with roughen the surface for the diamond seed to be implanted onto the surface. The diamond seed will enhance the nucleation and growth of diamond film.

Table 3.3 Seeding process for pretreated substrates

Base Chemical	10% of TR13/ Tickopur in distilled water
	0.8 g/L diamond powder 5g/L SiC powder
Temperature	Room temperature
Vessel	Ultrasonic Basin
Time	5 minutes

3.2.3 Surface Roughness

Surface roughness of the substrates was checked before and after pretreatment using Mitutoyo SJ-301 surface profilometer. Profilometers are instruments for measuring (or visualizing) the surface morphology [50]. A stylus profilometer uses a diamond tip dragged on a surface with very light pressure to get information about surface topography. The movement of the tip actuates a LVDT (Linear Variable Differential Transducer) that converts movement in electrical signal. A LVDT is a very sensitive transducer but the tip of the profilometer is conical and has a finite rounded shape, which interacts with the sample being scanned. The vertical sensitivity is in the nanometer range but steep edge profiles are distorted because of the shape of the tip as indicated in the illustration. Small radius tips are better but more likely to be damaged by mishandling.

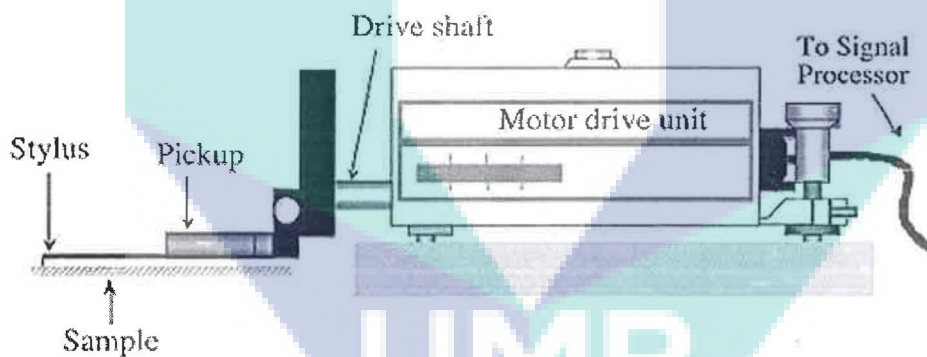


Figure 3.3 Schematic of a profilometer used to determine the surface roughness of the materials

3.3 Polycrystalline Diamond Deposition by Hot Filament Chemical Vapor Deposition Technique

Deposition on the substrate surface was conducted in UTM, Skudai by CC800®/Dia low pressure Hot Filament Chemical Vapor Deposition machine as shown in Figure 3.3. Table 3.2 shows the HFCVD deposition parameter used during the experiments.

Table 3.4 HFCVD deposition parameter

Parameter	
Substrate	Si ₃ N ₄
Pressure (mBar)	10.2
Methane concentration (vol%)	1
H ₂ gas flow rate (sccm)	3000
CH ₄ gas flow rate (sccm)	30
Filament temperature (°C)	2290±5
Deposition time (hr)	22

UMP

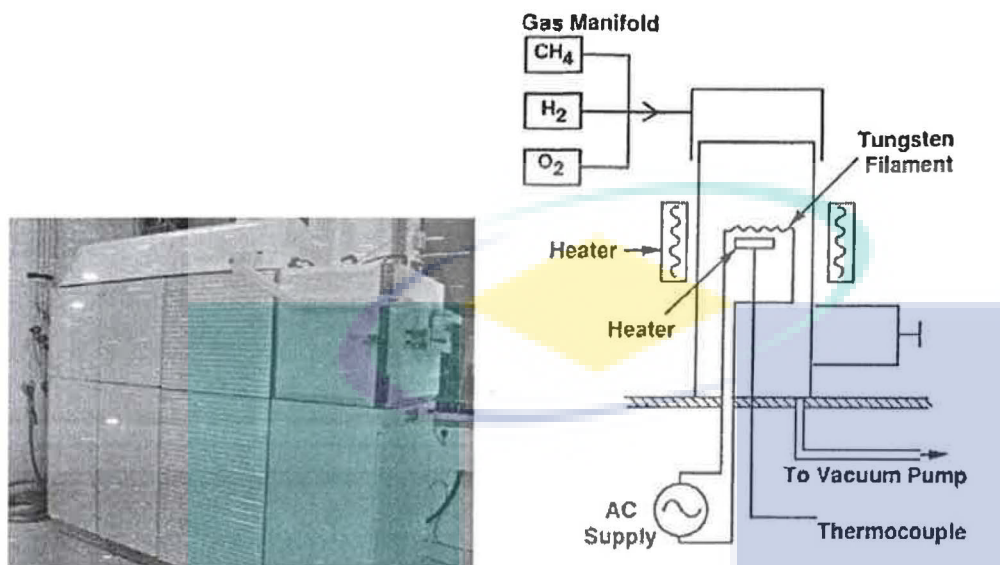


Figure 3.4 Hot filament chemical vapor deposition (a) actual equipment and (b) schematic drawing of HFCVD equipment.

The process chamber of the HFCVD machine is made of fine steel with dimensions $800 \times 600 \times 700$ mm. The chamber utilizes copper rail with slide in tungsten filaments (diameter = 0.4mm , length = 135mm , 6 in a row). The substrates were placed on a copper tube which has been placed on a graphite holder as shown in Figure 3.5.

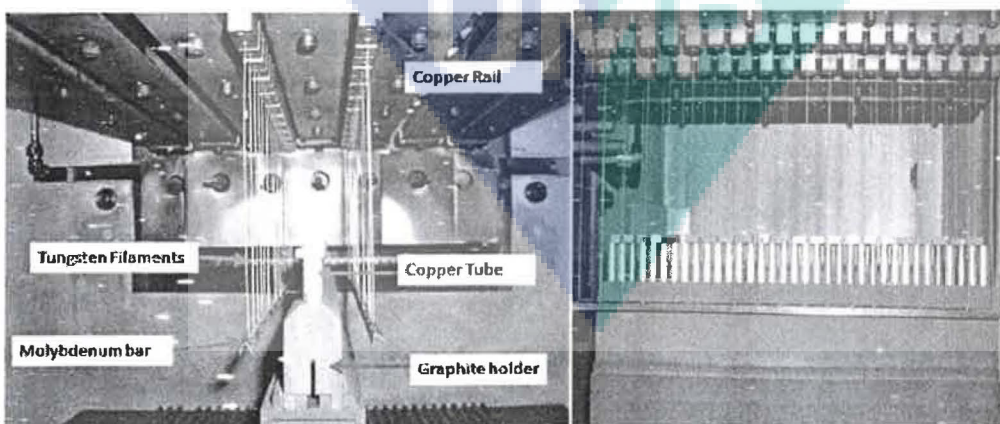


Figure 3.5 HFCVD chamber configuration showing (a) front view and (b) side view.

3.4 Microstructural Characterization

Microstructural analysis of film morphology were done using Scanning Electron Microscope (SEM) and Atomic Force Microscope (AFM) while film characterization was done using X-Ray Diffractometer (XRD) and Raman Spectroscopy.

3.4.1 Surface Morphology and Thickness by Scanning Electron Microscopy

The Supra 350V scanning electron microscope (SEM), as shown in Figure 3.6, is used to determine surface morphology, microstructure and grain size of the coating.



Figure 3.6 Scanning Electron Microscopy used to investigate the morphology of deposited polycrystalline diamond

SEM uses a focused beam of high-energy electrons to generate a variety of signals at the surface of solid specimens. The signals that derive from electron-sample interactions reveal information about the sample including external morphology (texture), chemical composition, and crystalline structure and orientation of materials making up the sample. In most applications, data were collected over a selected wera of

the surface of the sample, and a 2-dimensional image is generated that displays spatial variations in these properties.

3.4.2 Surface Topography and Surface Roughness by Atomic Force Microscopy

Surface topography and surface roughness of deposited film were characterized using Ambios Technology Universal SPM atomic force microscopy (AFM) as shown in Fig. 3.7. AFM measurement was done in Hi-Tech Instrument Sdn. Bhd, Selangor.

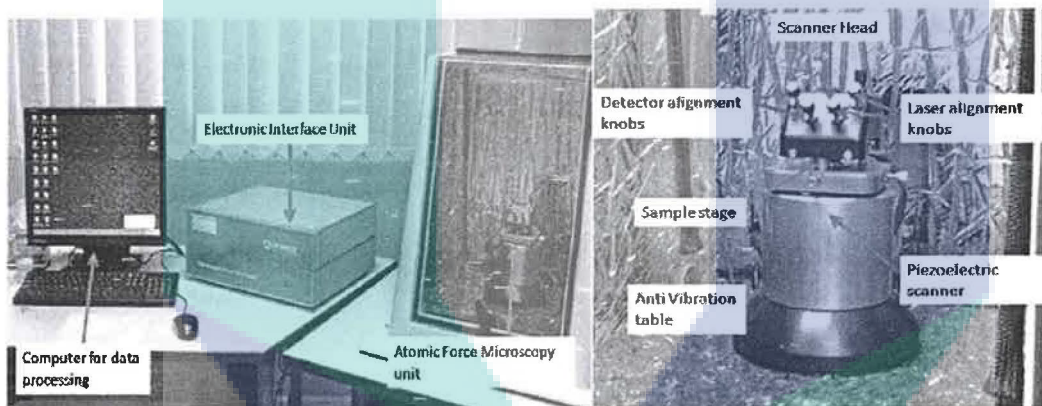


Figure 3.7 Atomic Force Microscopy used for topography and surface roughness analysis

3.4.3 X Ray Diffraction

X-ray diffractometer can be used to determine accurately the atomic spacing, structure and crystal orientation of the CVD diamond films. Diffraction peak of coating that correspond to peak (111), (220), (311) and (400) are reflective to diamond crystal structure

X-ray powder diffraction (XRD) is a rapid analytical technique primarily used for phase identification of a crystalline material and can provide information on unit cell dimensions. The X-ray radiation most commonly used is that emitted by copper, whose characteristic wavelength for the K radiation is $\lambda = 1.5418 \text{ \AA}$. When the incident beam strikes a powder sample, diffraction occurs in every possible orientation of 2θ as shown in Fig 3.8.

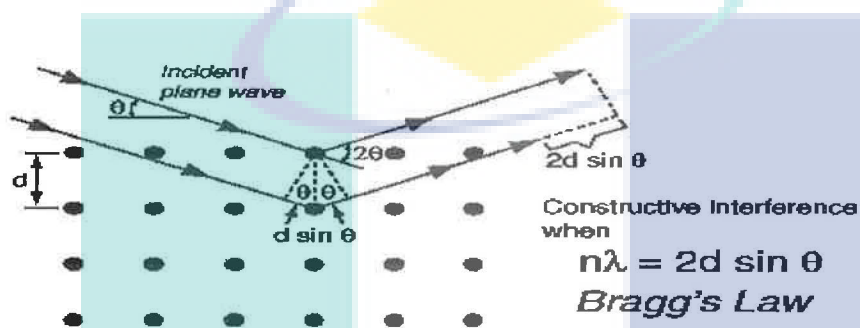


Figure 3.8 Bragg's Law explaining the diffraction of crystals

The X-ray radiation most commonly used is that emitted by copper, whose characteristic wavelength for the K radiation is $\lambda = 1.5418 \text{ \AA}$. When the incident beam strikes a powder sample, diffraction occurs in every possible orientation of 2θ . The diffracted beam may be detected by using a moveable detector such as a Geiger counter, which is connected to a chart recorder. An example of XRD equipment is as shown in Fig 3.9.

In normal use, the counter is set to scan over a range of 2θ values at a constant angular velocity. Routinely, a 2θ range of 5 to 70° is sufficient to cover the most useful part of the powder pattern. The scanning speed of the counter is usually 2θ of 2 min^{-1} and therefore, about 30 minutes are needed to obtain a trace.

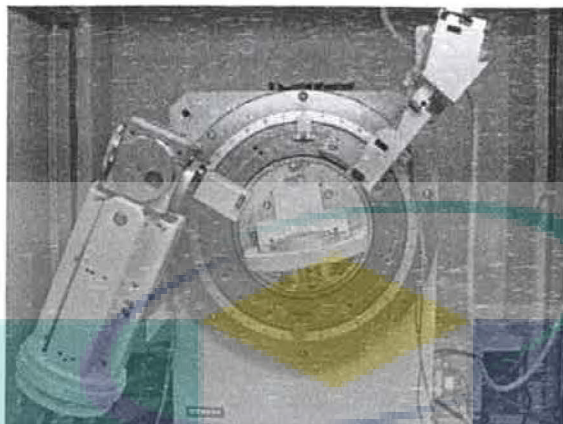


Figure 3.9 X-Ray Diffractometer (XRD) used to determine composition and phase analysis of the coating

3.4.4 Diamond Quality and Residual Stress by Raman Spectroscopy

Raman investigation was done using Raman Spectrometer in AMREC, Sirim Bhd, Kulim, Kedah with the help of Mr Shahru Nizam. Raman spectra analysis is used to investigate diamond or non diamond atomic bonding. The equipment, as shown in Fig. 3.10, can be used to investigate the crystalline diamond (sp^3) and non-diamond/graphite (sp^2) in which the peaks of each structure are 1332 cm^{-1} and 1580 cm^{-1} respectively. It also can be used to determine the presence of other types of carbon species such as nanocrystalline and microcrystalline diamond

Raman spectroscopy is a spectroscopic technique used in condensed matter physics and chemistry to study vibrational, rotational, and other low-frequency modes in a system. It relies on inelastic scattering, or Raman scattering, of monochromatic light, usually from a laser in the visible, near infrared, or near ultraviolet range. The laser light interacts with phonons or other excitations in the system, resulting in the energy of the laser photons being shifted up or down. The shift in energy gives information about the phonon modes in the system. Infrared spectroscopy yields similar, but complementary, information. Typically, a sample is illuminated with a laser beam. Light from the illuminated spot is collected with a lens and sent through a monochromator.

Wavelengths close to the laser line, due to elastic Rayleigh scattering, are filtered out while the rest of the collected light is dispersed onto a detector.

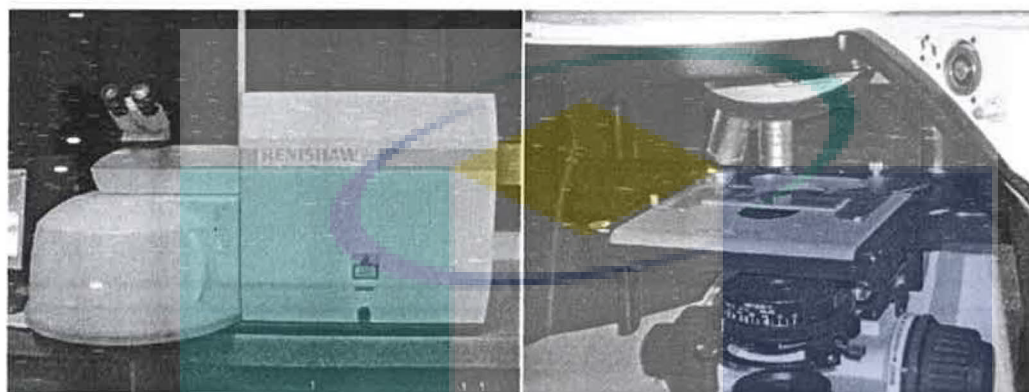


Figure 3.10 Raman Spectroscopy Equipment

3.5 Adhesion properties by Vickers hardness tester

The polycrystalline film adhesion on the various pre-treated ceramic nitride substrates has been evaluated by the indentation technique (Vickers' indenter). A Vickers' indentation test was utilized to obtain an estimation of adhesion between polycrystalline thin films of various thickness and the ceramic surfaces. In the test method, the coating sample is indented at various increasing loads. When the load is sufficiently high, some lateral cracks initiate and propagate along the coating-substrate interface. Lateral crack lengths increase with the indentation load. The minimum load at which the coating fracture is observed is called critical load and is employed as measure for coating adhesion [30].

However, since the diamond coating will be very hard and brittle (as hard as the Vicker's indenter), it is not easy to quantify the exact value of the crack length. Thus only qualitative estimation is made based on the shape of tip imprinting, kind of failure and extension of the lateral cracks [30].

The Vickers hardness test method consists of indenting the test material with a diamond indenter, in the form of a right pyramid with a square base and an angle of 136 degrees between opposite faces subjected to a load of 1 to 100 kgf as shown in Figure 3.11. The full load is normally applied for 10 to 15 seconds. The two diagonals of the indentation left in the surface of the material after removal of the load are measured using a microscope and their average calculated. The area of the sloping surface of the indentation is calculated. The Vickers hardness is the quotient obtained by dividing the kgf load by the square mm area of indentation [4].

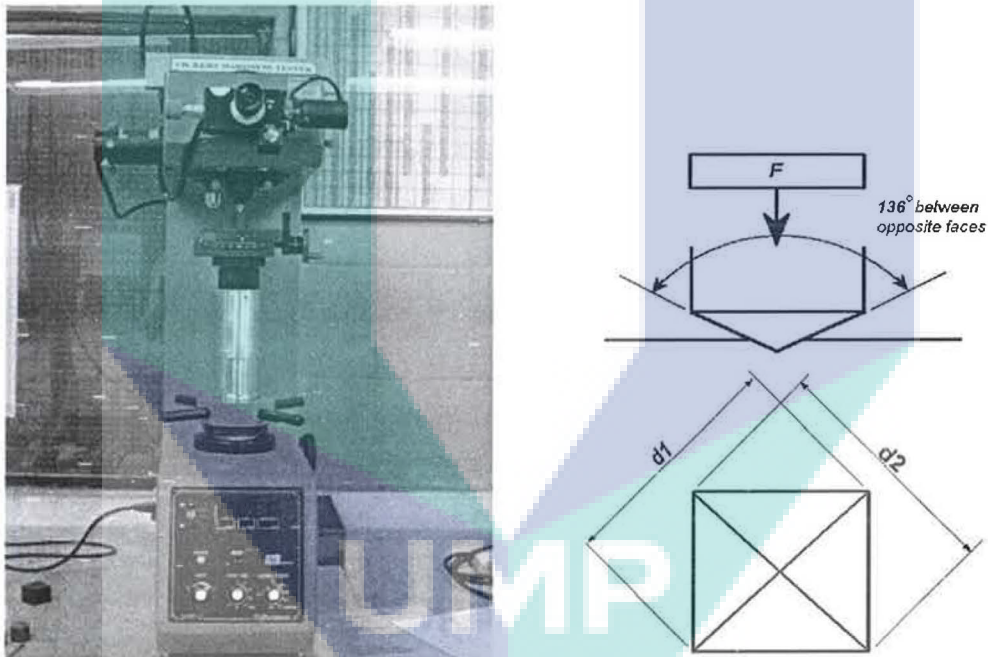


Figure 3.11 Vickers Hardness Tester indenter (a) actual equipment and (b) schematic of hardness measurement

CHAPTER 4

RESULTS AND DISCUSSION

4.1 Materials

4.1.1 Composition and Phase Analysis

Si_3N_4 was used as substrates material. Fig 4.1(a) shows the substrates with the dimension of 12mm x 12mm x 4 mm. Fig. 4.1 (b) shows the optical micrograph of the as-received substrates surface.

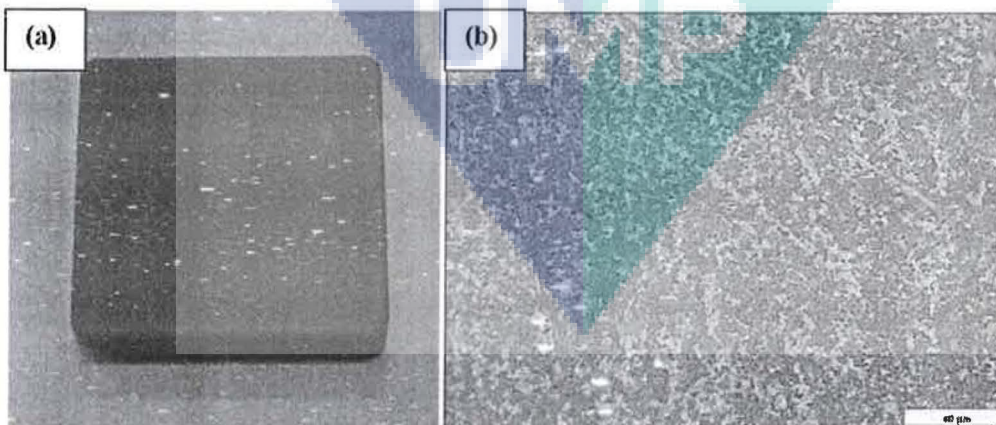


Figure 4.1 (a) As-received Si_3N_4 substrates and (b) optical micrograph of Si_3N_4 (x200)

EDX and XRD were done to determine the composition and structure of the as-received Si_3N_4 . Fig. 4.2 shows the EDX spectrum of the Si_3N_4 showing the surface composition of as-received.

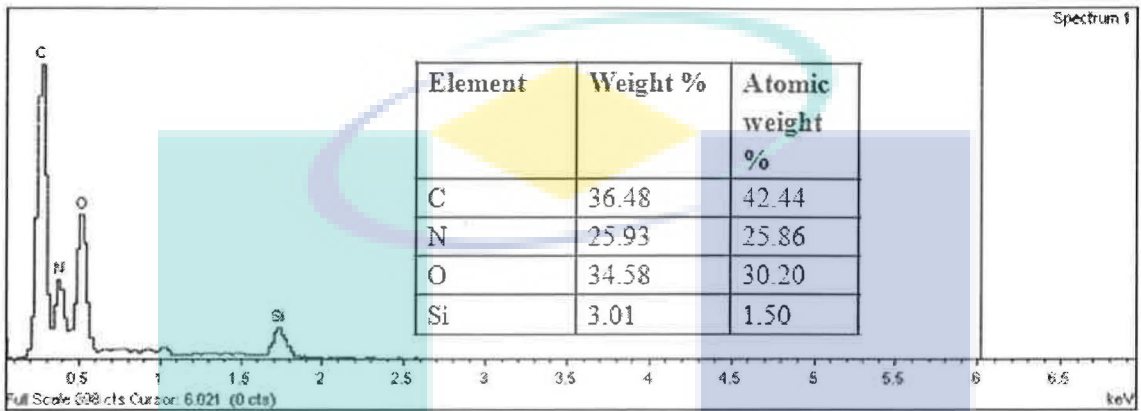


Figure 4.2 EDX spectrum of Si_3N_4

Fig. 4.3 shows the XRD spectra of as-received Si_3N_4 sample. From XRD, it is found that the Si_3N_4 sample have hexagonal (space group $P63/M$) with $a=7.6044\text{\AA}$ and $c=2.9075\text{\AA}$ indicating that the sample is β - Si_3N_4 .

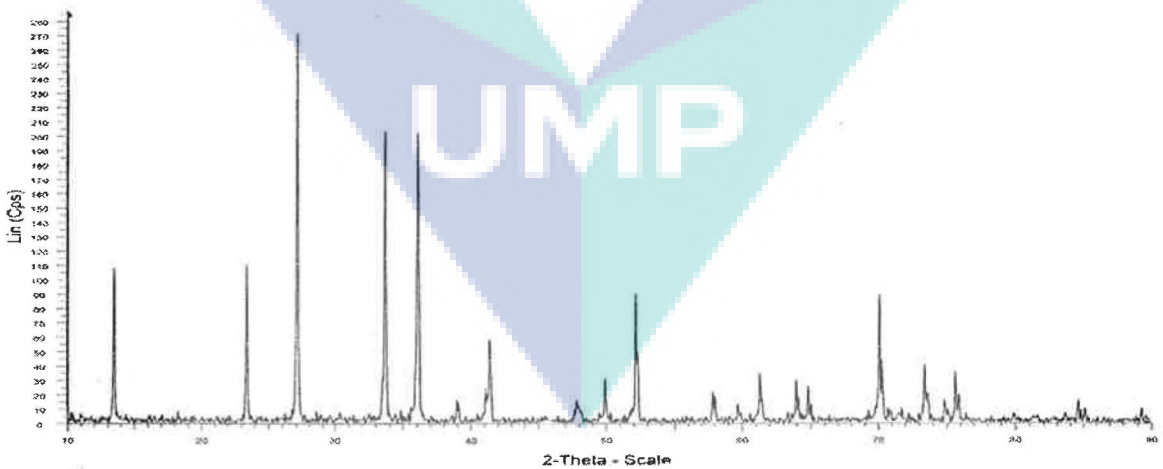


Figure 4.3 XRD spectrum of as-received Si_3N_4

4.1.2 Hardness analysis

The hardness of Si_3N_4 that was measured using Vicker Hardness Tester gives mean value of 2157 HV. Typical Vickers indentation on Si_3N_4 is as shown in Fig. 4.4.



Figure 4.4 Vickers indentation on Si_3N_4

4.2 Pretreatment Analysis

Pretreatment analysis was carried out to observe the effect of surface pretreatment on the surface of the substrates prior to deposition.

4.2.1 Effect of pretreatment on surface roughness and morphology

4.2.1.1 Substrates morphology after pretreatment

Chemical etching is a conventional method to reveal microstructure by selective corrosion. Fig. 4.5 shows the SEM micrograph of Si_3N_4 surface morphology after wet

chemical etching while Fig 4.6 shows the AFM image analysis of substrate pretreated under strong acid etching for 10 minutes. Although the chemical etching capable to expose the surface of the substrates, the slow etch rate was unable to etch entirely the bigger, rod-like particles thus leaving the larger particle protruding while the smaller grain being etched deeper. Chemical etching removed most of the intergranular phase in the Si_3N_4 , thus leaving behind rod-like particle of $\beta\text{-Si}_3\text{N}_4$ [1].

Chemical etching is a nontraditional machining process in which material removal is carried out by using strong chemical solution, called "etchant". This is simply the "accelerated and controlled corrosion" process[1] Acid etching using hydrofluoric acid (HF) and nitric acid (HNO_3) is an isotropic process in which the material is removed non-directionally from the surface substrates. Basic etching, on the other hand, is an anisotropic etching in which the etching rate is orientation dependant especially in silicon wafer [2].

Another challenge is maintaining an isotropic etch, i.e., one in which the etch rate is the same in any direction. In particular, silicon nitride materials deposited on a substrate are not necessarily planar, which mandates an isotropic etch. Applying bias to the substrate results in an anisotropic etch, often resulting in residual nitride that forms "mini-spacers." Thus, an isotropic process with no or minimal bias is needed to laterally etch silicon nitride[3].

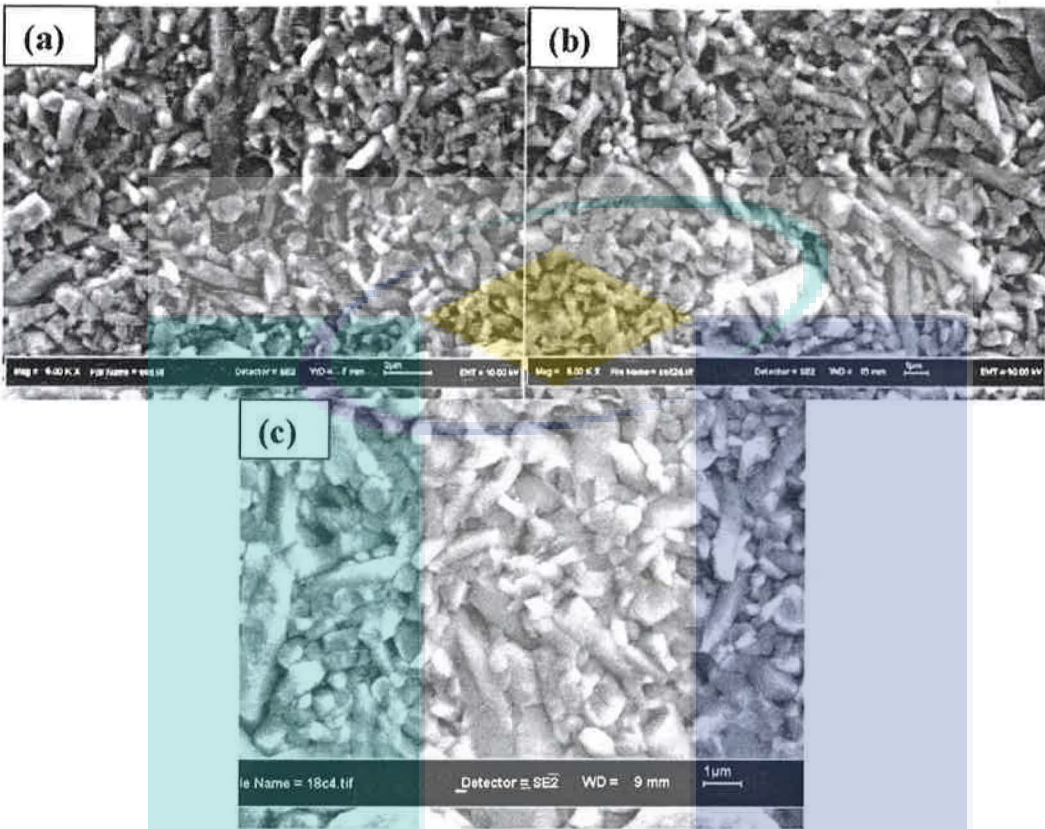


Figure 4. 5 FE-SEM micrograph of substrates surface due to (a) acid etching, (b) strong acid etching and (c) basic etching.

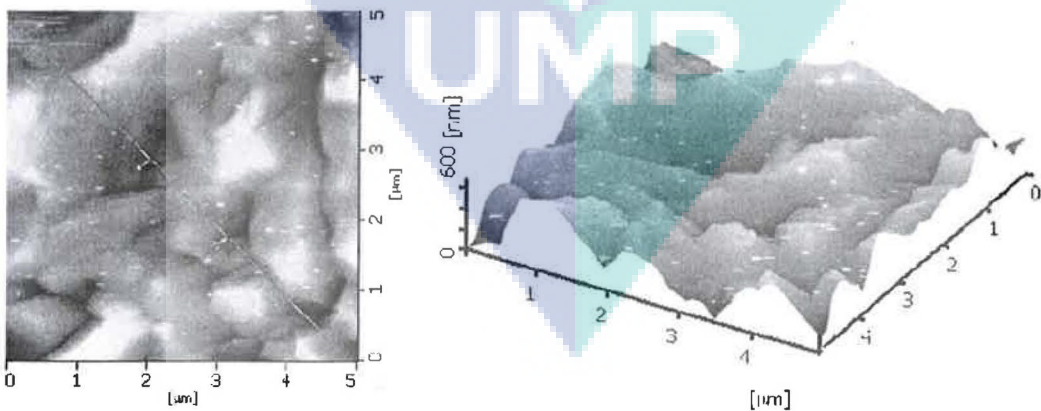


Figure 4. 6 AFM image analysis showing (a) top view and (b) 3-dimensional view of substrates undergoes strong acid etching for 20 minutes.

Fig. 4.7 shows the mechanism of wet chemical etching. There are three important steps, the reactants are transported by diffusion to the reacting surface, chemical reactions occur at the surface and the products from the surface are removed by diffusion. As the wet chemical etching usually done by immersion with mechanical agitation, the uniformity and consistency of etching rate can be ensured[4].

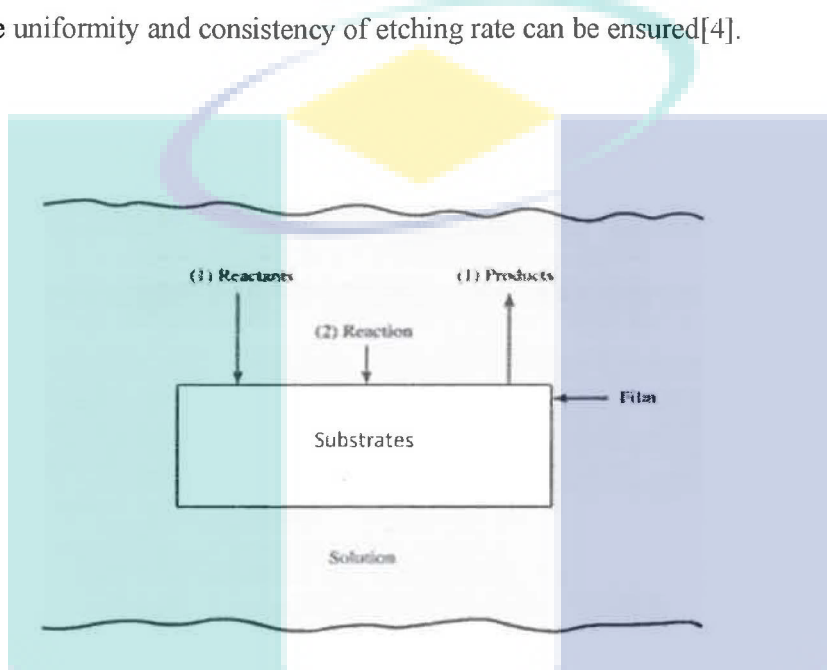


Figure 4. 7 Mechanism of wet chemical etching

Fig. 4.8 shows the topography of mechanically pretreated substrates showing very irregular surface with various depth due to impact erosion.

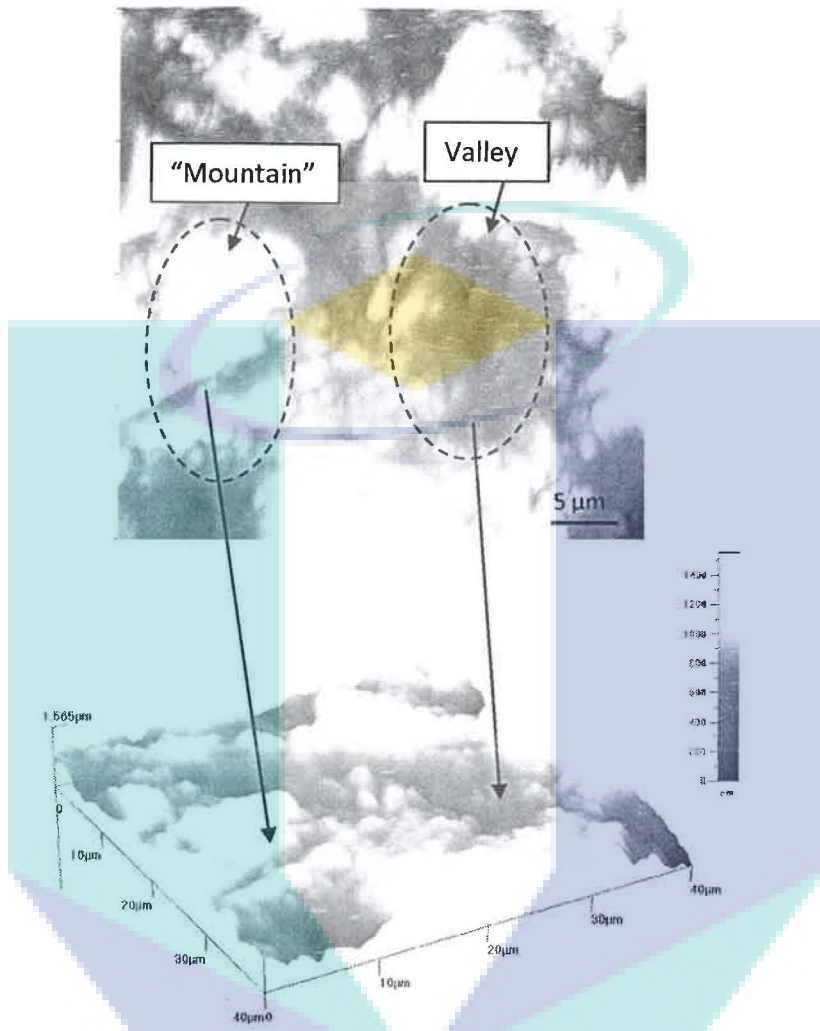


Figure 4. 8 AFM images of surface topography of Si_3N_4 substrate pretreated by sand blasting.

Fig. 4.9 shows the mechanism of sand blasting. Sand blasting is process where high velocity jet of abrasive particle and carrier gas is impinged onto target surface. As the particles impact the surface , they cause a small fracture and the gas stream carries both the abrasive particles and fractured particles away [5]. Upon impact, the grains 'dig' into and then rebound out off the surface leaving a rugged, miniature 'mountain-and-valley' finish.

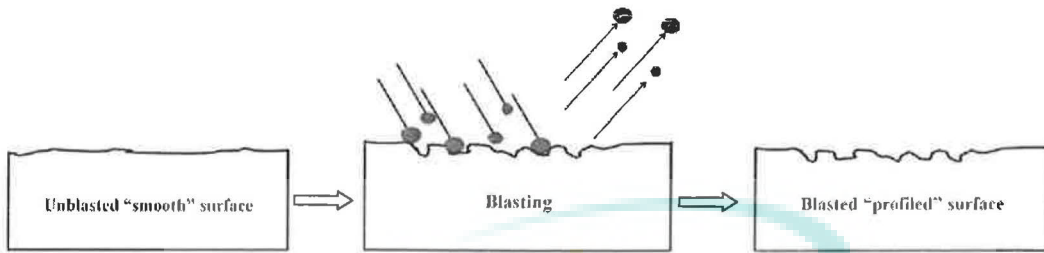


Figure 4.9 Schematic diagram of blasting mechanism

Fig. 4.10, on the other hand, is showing AFM images of more flat surface with apparent porosity. The flat surface was due to removal of surface of Si_3N_4 by grinding process. Fig. 4.11 shows schematic drawing of grinding mechanism.

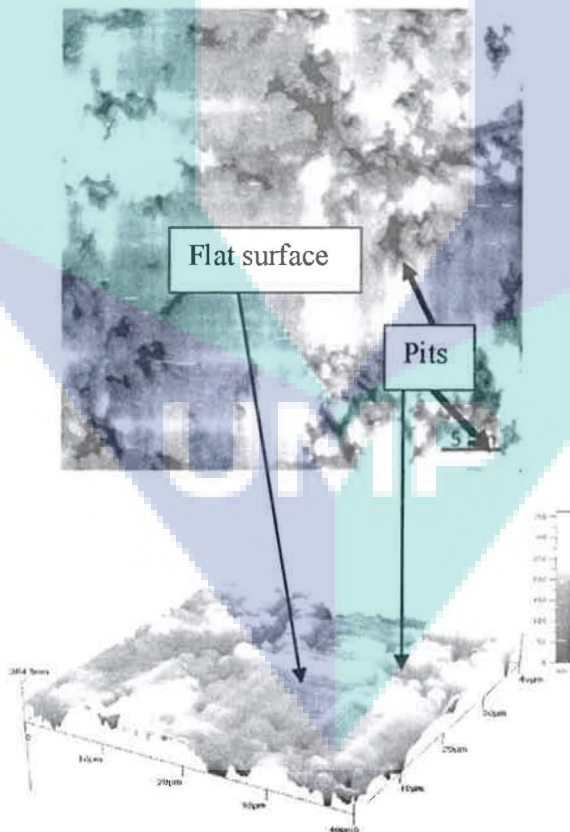


Figure 4.10 AFM images of surface topography of Si_3N_4 substrate pretreated by grinding process

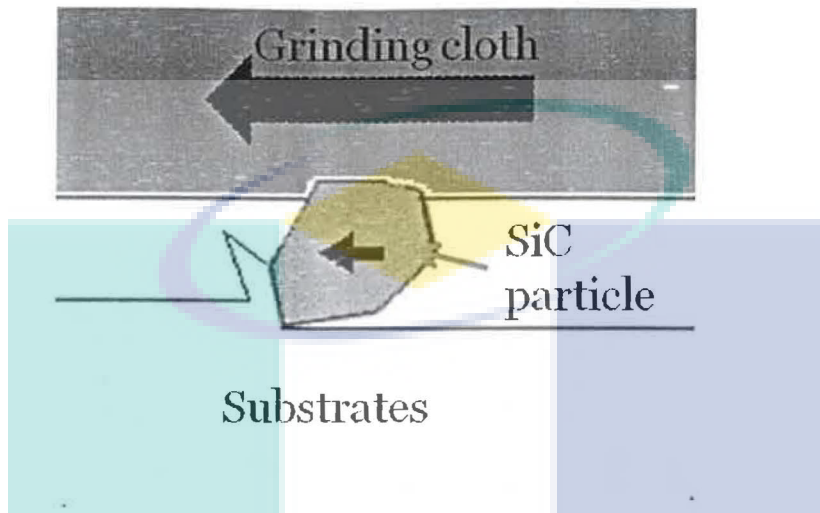


Figure 4.11 Schematic diagram of grinding mechanism

By subjecting the substrates to mechanical and chemical etching, surface roughness before and after is compared as shown in Fig. 4.12. Surface roughness of each sample was measured before and after pretreatment to investigate the effect of each pretreatment. Fig. 4.12(a) shows the changes in sample pretreated with acid etching showing that the highest surface roughness is achieved when the samples were etched for 20 minutes. Fig. 4.12(b), which shows the sample pretreated in strong acid etching, have the same trend with acid etching. As explained before, acid etching is an isotropic process. When the substrates were exposed to the acid etchants at longer period, the surface starts to rounded up, thus decreases the surface roughness. However, for sample pretreated with basic etching shown in Fig. 4.12(c), the surface roughness of the samples increases with etching time with highest surface roughness at etching time of 30 minutes. This can be attributed to the selective etching due to anisotropic properties of basic etchant. Fig. 4.12(d) on the other hand is showing the surface roughness differences of mechanically pretreated samples. The highest surface roughness are obtained by subjecting the substrate to sandblasting using SiC while grinding did not introduces much surface roughness on the substrates.

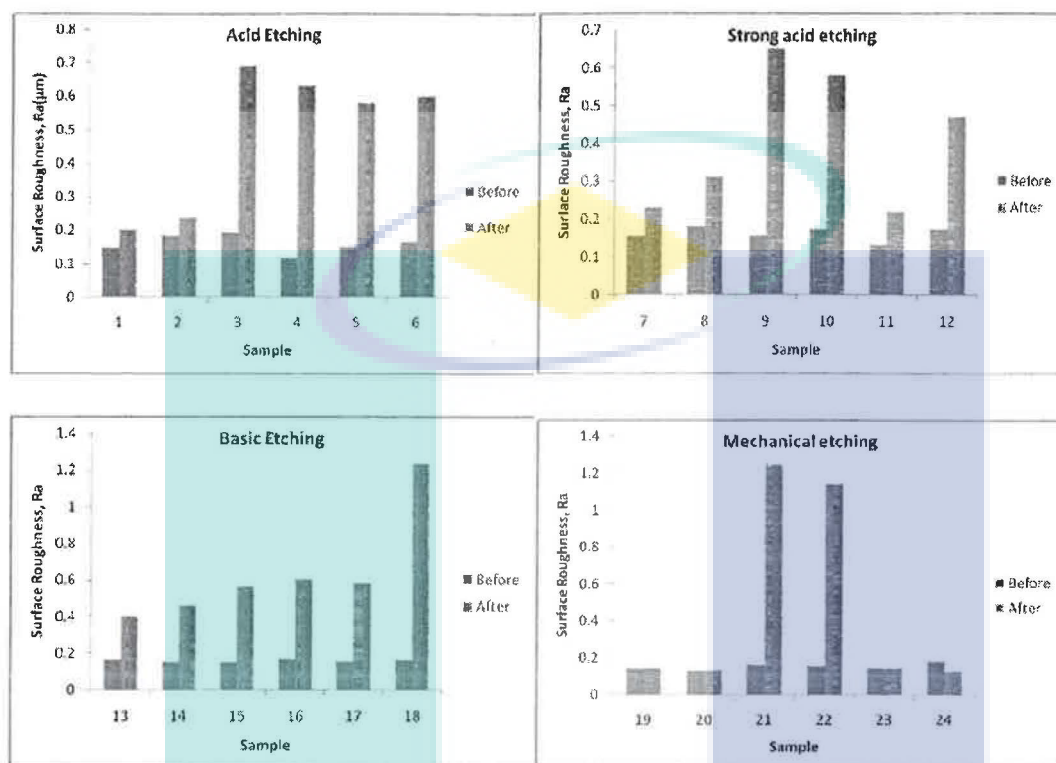


Figure 4.12 Surface roughness (Ra) before and after surface pretreatment

4.2.1.2 Effect of seeding on diamond nucleation

Diamond seeding was carried out to increase diamond nucleation rate and improve adhesion of formed diamond film to the substrates. The non-seeded substrates were investigated to explain the importance of seeding to formation of diamond film.

Fig. 4.13 shows the diamond deposited on the chemically pretreated substrates illustrate clearly the individual diamond crystal due to the growth of diamond nuclei. As can be observed, the diamond crystals have cauliflower morphology with smaller crystallite. The nucleation density on chemically pretreated substrates was low.

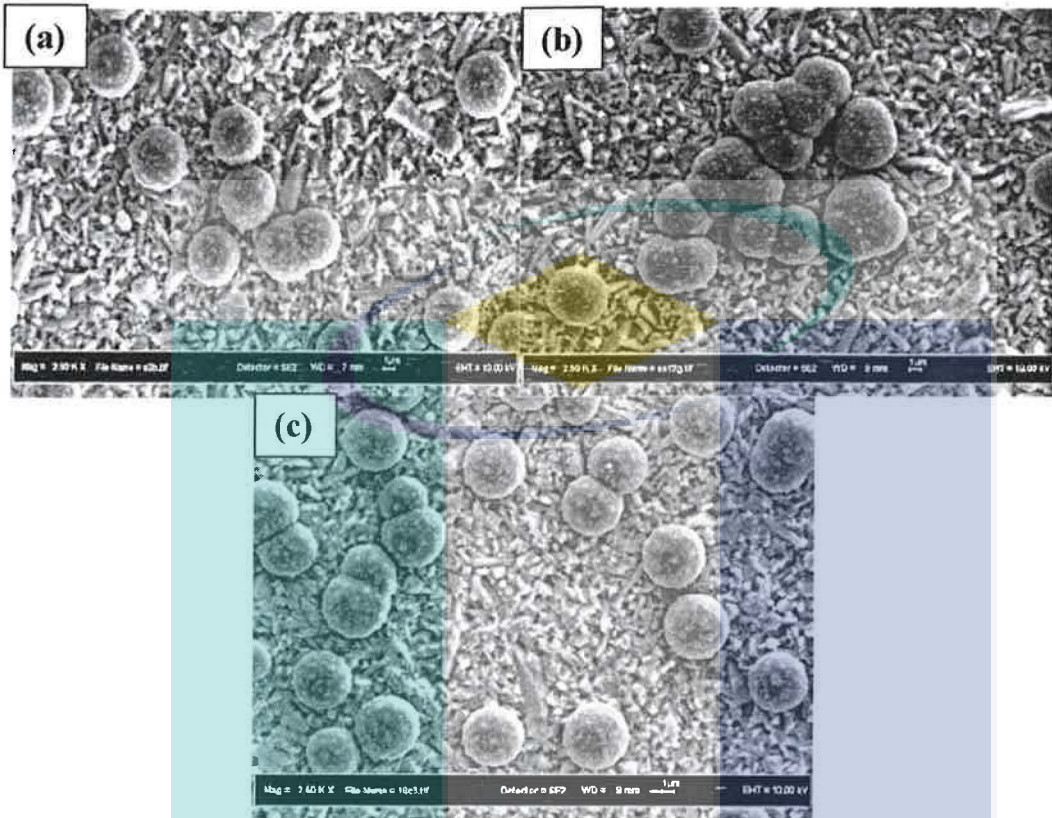


Figure 4.13 Diamond nucleation on substrates pretreated with (a) acid etching (b) strong acid etching and (c) basic etching

Nucleation is usually observed mostly on defects such as scratches, grain boundaries and dislocation. However, chemical etching did not introduce enough grooves for nucleation to occur in mechanical pretreatment. Nucleation on chemical etching substrates are driven by low pressure HFCVD. Low pressure CVD greatly increases the mean free path of atomic H, thus increases the nucleation density by creating favorable environment for diamond nucleation [6].

On the other hand, non-seeded mechanical pretreated substrates shows higher rate of nucleation based on SEM inspection. Fig. 4.14 shows that sample have almost continuous film with distinct feature of diamond crystals. Due to higher rate of

nucleation compared to samples in Fig. 4.13, higher number of diamond crystal coalesced with each other to form diamond film with distinct crack showing at which each crystal touches each other.

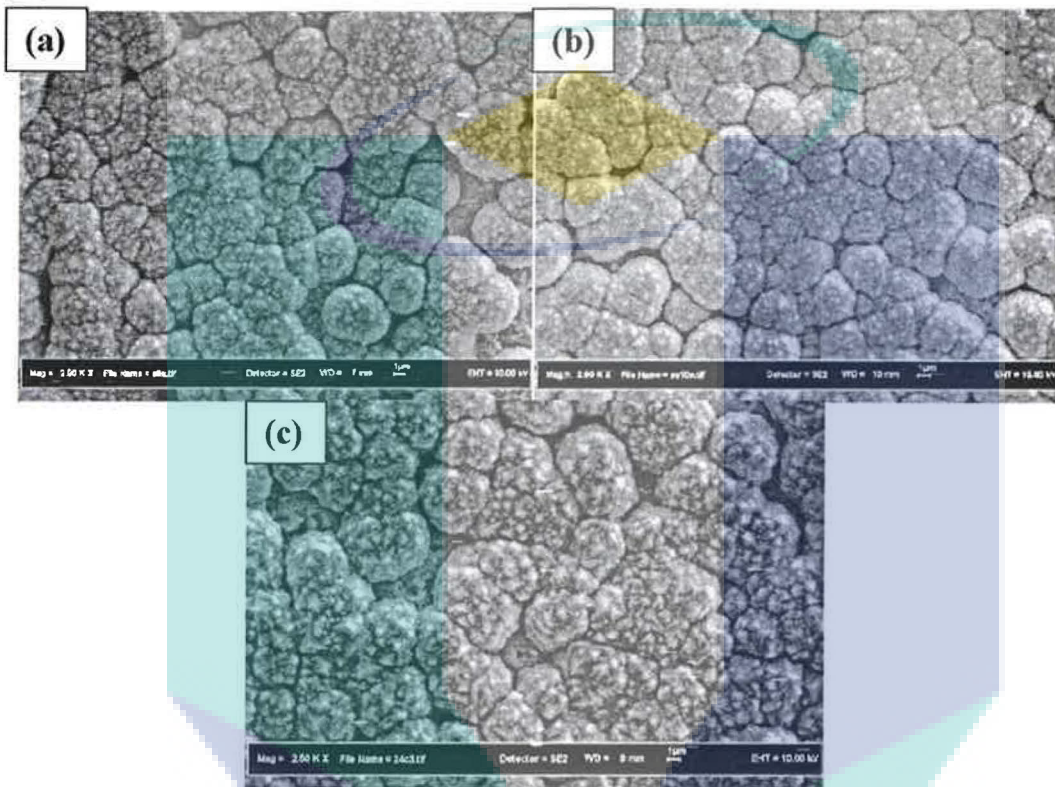


Figure 4.14 Diamond nucleation on non-seeded, (a) as-received (b) pretreated by blasting and (c) pretreated by grinding substrates.

Fig. 4.15 shows the mechanism of nucleation on mechanically pretreated substrates. Mechanical pretreatment introduces grooves and highly disordered surfaces that create high energy sites which are the preferred nucleation sites for diamond nucleation. It is because high surface energy minimized the interfacial energy by formation of diamond on sharp convex surfaces and presence of dangling bonds at sharp edge favored the chemisorptions of nucleating species [7]. This factor when coupled with low pressure CVD obviously increased the nucleation density in the mechanically pretreated substrates.

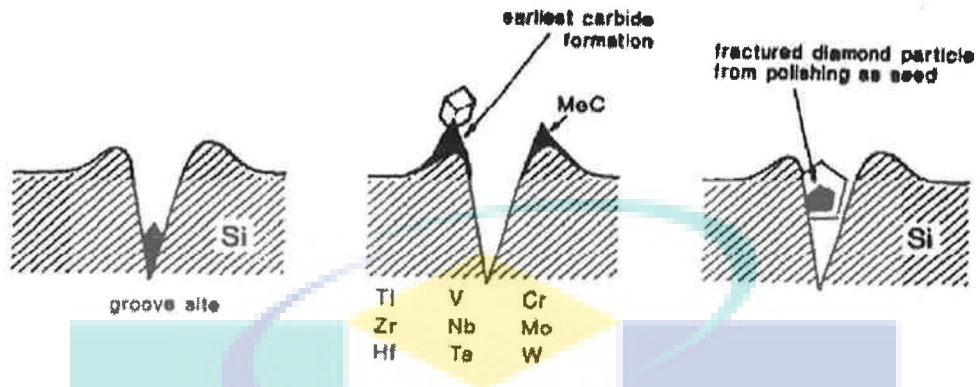


Figure 4. 15 Schematic diagram of mechanisms for diamond nucleation enhancement of scratched substrates [7]

Fig. 4.16 shows the Vickers indentation on substrates pretreated by grinding at 10kgf done for seeded and unseeded substrates. As observed from Fig. 4.16 (b), the adhesion of diamond film on unseeded sample is very low showing obvious spallation, exposing the substrates underneath.

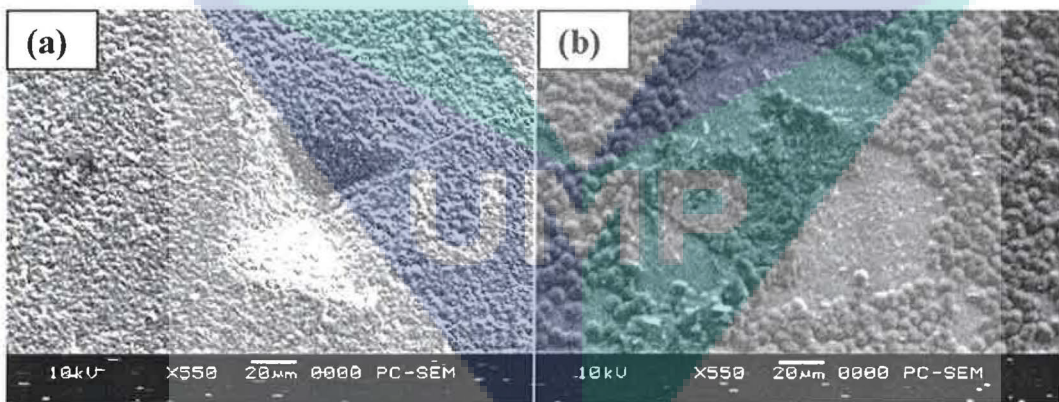


Figure 4.16 SEM micrograph of Vickers indentation on Si_3N_4 substrates pretreated by grinding on (a) seeded and (b) unseeded sample.

Thus, due to poor nucleation and formation of diamond in the unseeded substrates, both in chemically and mechanically pretreated substrates, diamond seeding is really necessary in order to investigate the effect of surface pretreatment on the quality of diamond formed.

4.3 Effect of chemical etching time

4.3.1 Introduction

In order to choose the best optimum etching time, chemical etching are done at three different duration; 10, 20 and 30 minutes. Surface roughness of the samples was taken before and after each pretreatment, which has been discussed in Section 4.2.1. After the deposition, each sample was characterized to find the best etching time for each pretreatment.

4.3.2 Effect of etching time on the morphology of the diamond film

Fig 4.17 to 4.19 shows the FE-SEM images of deposited diamond film. It can be seen from the micrographs that the diamond film is composed of large diamond cluster with 300-350 nm in size that contain tiny diamond crystals. This type of morphology is described as “cauliflower” or ballast morphology [8-10]. Fig 4.17(b) on the other hand is showing smooth continuous diamond film with well-faceted crystallite which contains much finer grain in between large grain. Fig 4.17 (c) has the same surface morphology with Fig 4.17(a). Diamond film deposited on strong acid and basic etched substrates also shows the cauliflower morphology as shown in Fig 4.17.

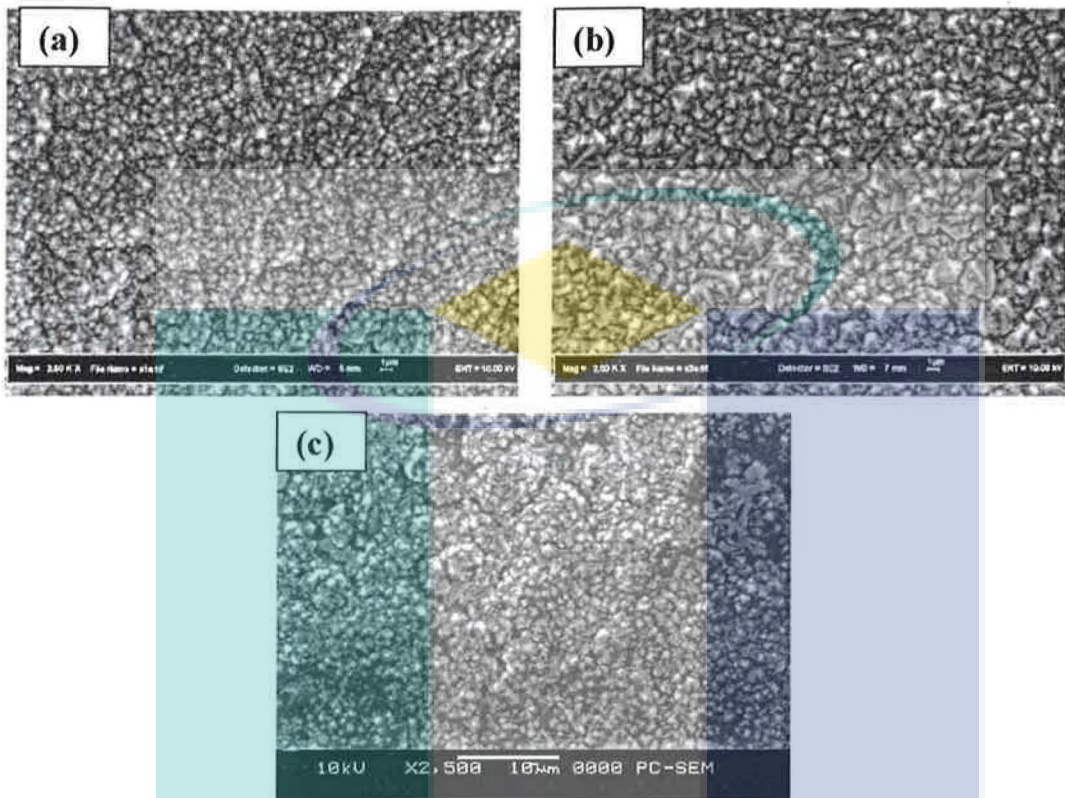


Figure 4.17 SEM showing diamond film deposited on substrate pretreated with acid etching for (a) 10 (b) 20 and (c) 30 minutes.

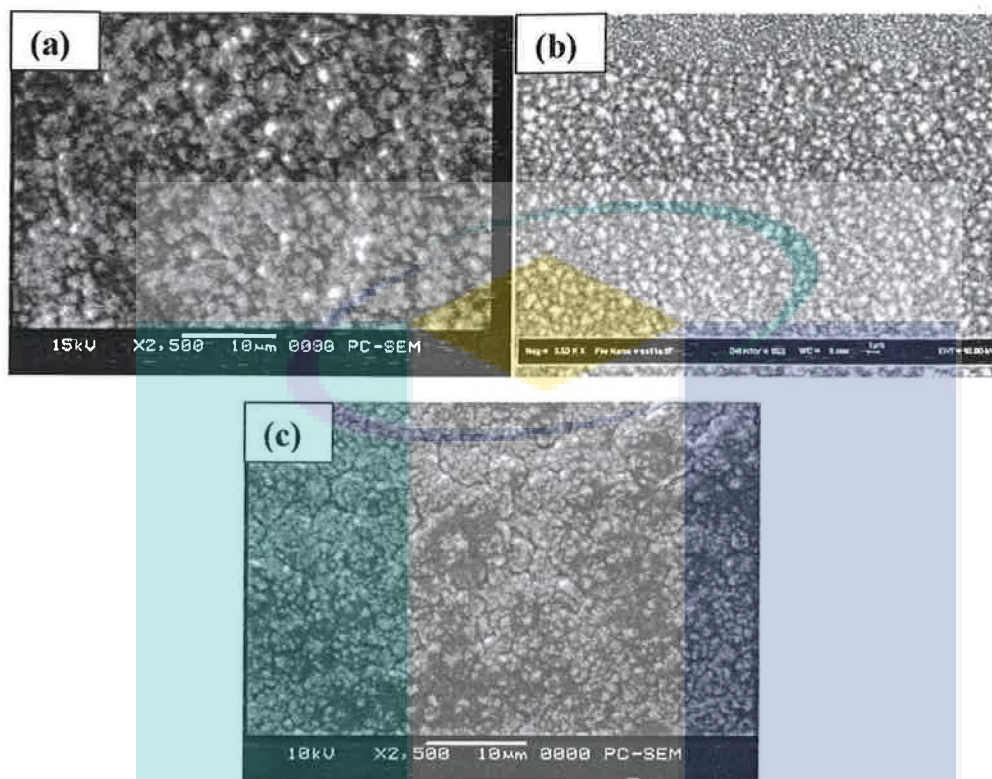


Figure 4. 18 SEM showing diamond film deposited on substrate pretreated with strong acid etching for (a) 10 (b) 20 and (c) 30 minutes.

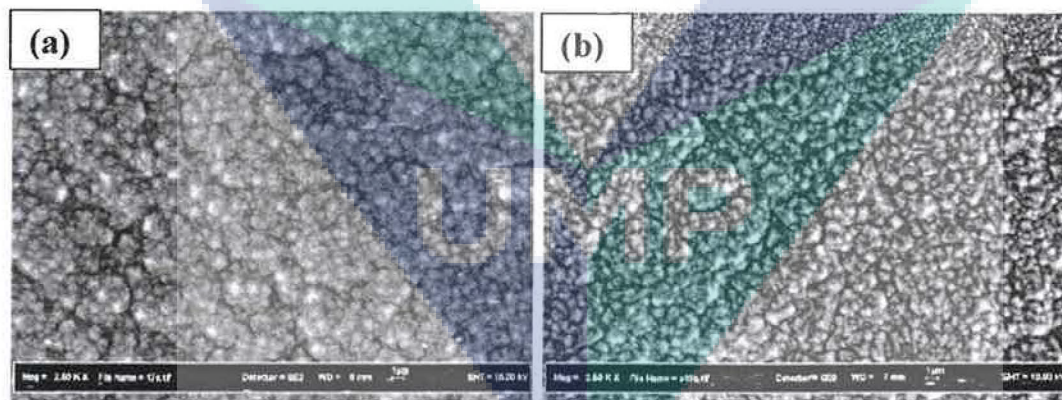


Figure 4. 19 SEM showing diamond film deposited on substrate pretreated with basic etching for (a) 10 (b) 20 and (c) 30 minutes.

The diamond films deposited on chemical etched substrates shows cauliflower-like morphology which showing diamond clusters composed on nano-metric crystallites with size between 30-50nm. The sizes of crystallites was calculated according to full width half maximum of (111) diffraction peak of XRD [11].

Formation of this NCD morphology is due to [10, 12]:

- Steady re-nucleation processes from ballas particle that grows on the nucleation sites due to surface pretreatment.
- Before a diamond crystal can grow further, new growth center is formed and the growth of the former crystal is inhibited. Some of those growth sectors develop randomly and have their fastest growth orientation in radial direction as shown in Fig. 4.20

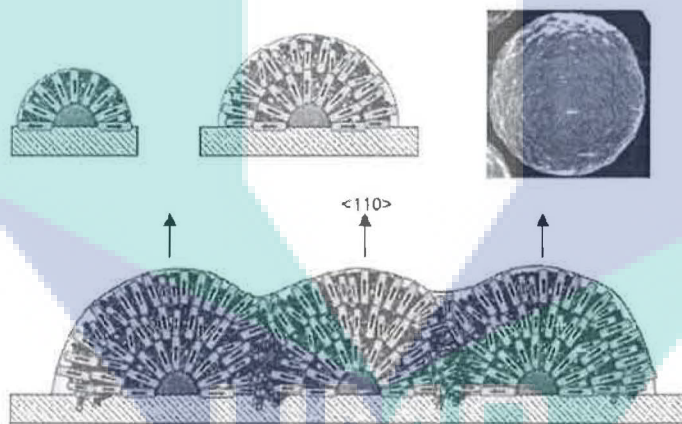


Figure 4.20 Schematic of ballas-like particle growth suggesting preferential $\langle 110 \rangle$ orientation during NCD film deposition [10].

4.3.3 Surface topography and surface roughness by atomic force microscopy (AFM)

Atomic force microscopy (AFM) was used to study the effect of etching on surface topography and surface roughness. Fig. 4.21 shows the 3D topography of diamond deposited on acid etched substrates for 10, 20 and 30 minutes in a $5 \times 5 \mu\text{m}$ square area. In Fig. 4.21 (a) the diamond film is shown to have sharp peak compared to slightly rounded grain in Fig. 4.21(b) and (c). The surface roughness, R_a , values decreases with etching time, from 60.76 to 42.4 and 37.3 nm for 10, 20 and 30 minutes respectively. This may due to decreases in grain cluster size from 5413 nm to 2475 followed by 1926 nm.

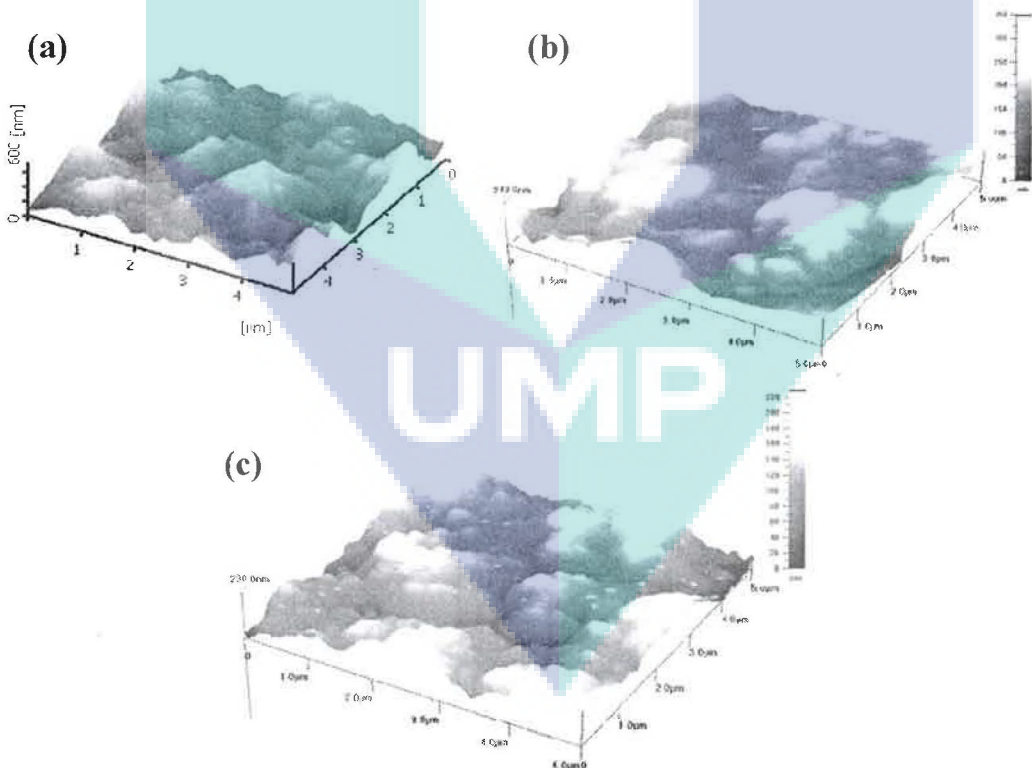


Figure 4.21 AFM 3D topography of diamond film deposited on acid etched substrates for (a) 10 (b) 20 and (c) 30 minutes.

Fig. 4.22 shows the 3D topography of diamond deposited on strong acid etched substrates for 10, 20 and 30 minutes in a $5 \times 5 \mu\text{m}$ square area. The surface roughness of diamond films deposited decreases with increasing etching time from 73.39 nm to 67.72 and 60.38 nm subsequently for 10, 20 and 30 minutes respectively.

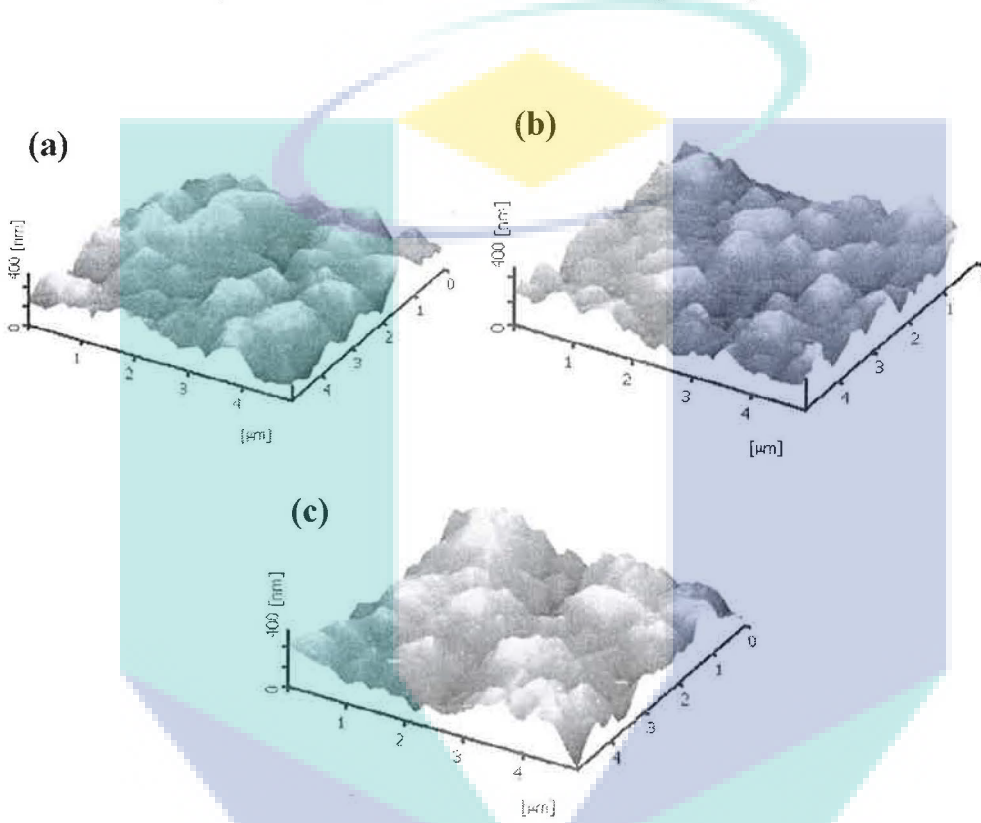


Figure 4.22 AFM 3D topography of diamond film deposited on strong acid etched substrates for (a) 10 (b) 20 and (c) 30 minutes.

Fig. 4.23 shows the 3D topography of diamond deposited on basic etched substrates for 10, 20 and 30 minutes in a $5 \times 5 \mu\text{m}$ square area. The surface roughness of diamond films deposited decreases with increasing etching time from 73.39 nm at 10 minutes to 67.72 and 60.38 nm 10, 20 and 30 minutes respectively.

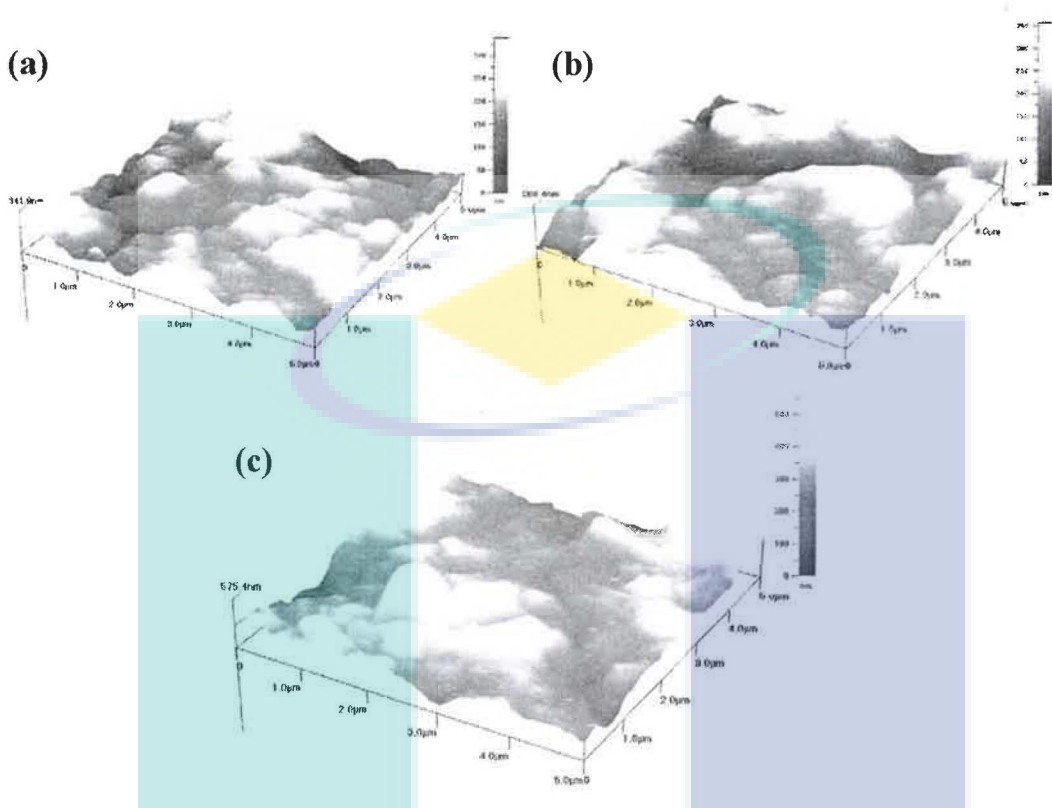


Figure 4. 23 AFM 3D topography of diamond film deposited on basic etched substrates for (a) 10 (b) 20 and (c) 30 minutes.

Fig. 4.24 shows the surface profile of diamond film obtained from atomic force microscope. Fig. 4.24 (a) shows diamond film with highly faceted and sharper diamond peak, thus explain higher surface roughness. Fig. 4.24(b) on the other hand shows the diamond with smooth, granular surfaces of cauliflower morphology and lower surface roughness. Decreases in surface roughness indicate decreases in grain size [6, 13-15].

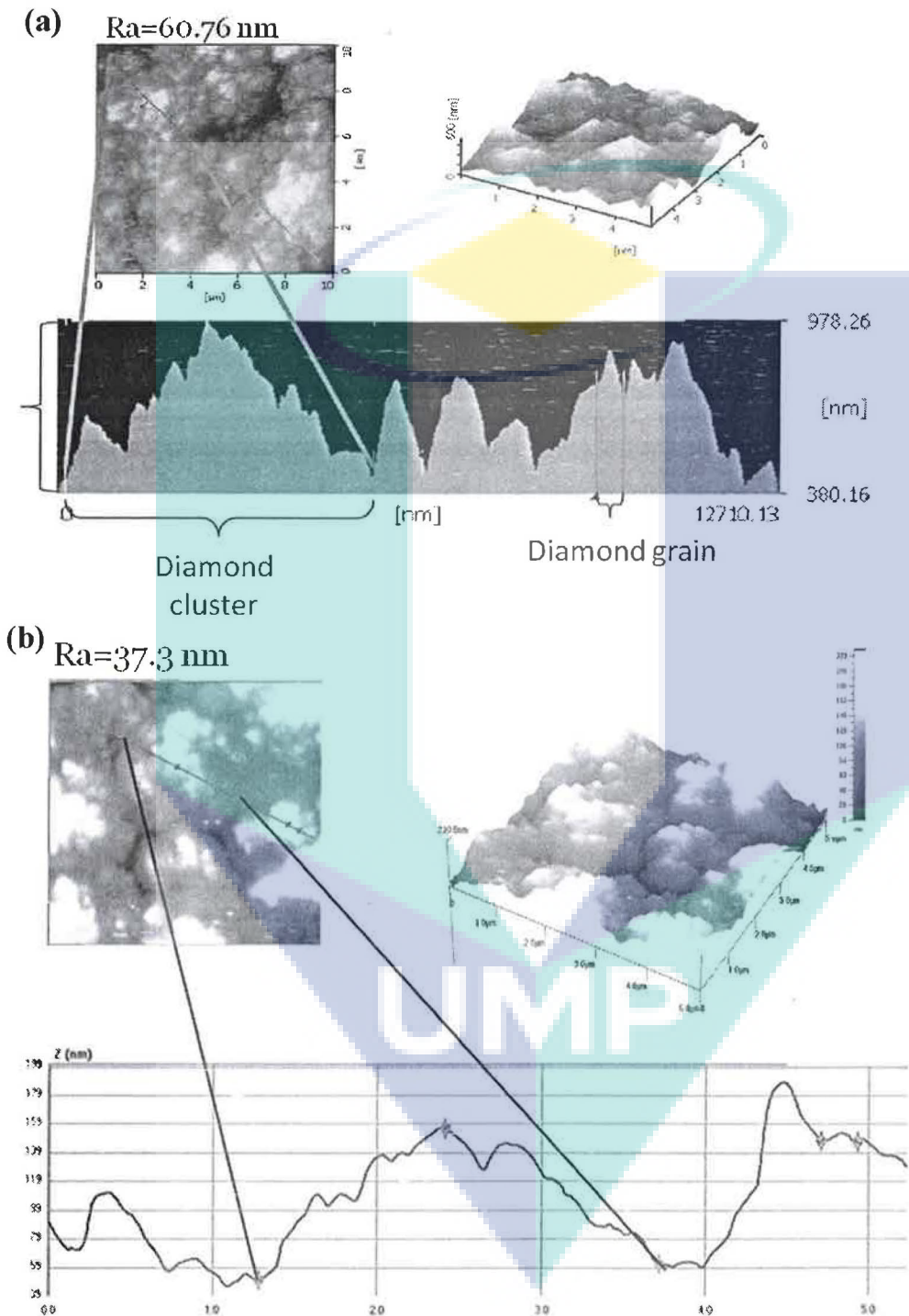


Figure 4. 24 AFM profile of diamond film deposited on acid etched substrates showing (a) highly faceted crystalline morphology and (b) cauliflower morphology

Surface roughness of deposited diamond films influence mechanical properties of the film in term of hardness and Young's modulus value [14]. Since lower surface roughness indicates smaller crystallite, it also indicates increases in the grain boundaries thus resulting in the increase of amorphous carbon content [6]. This explains why diamond with cauliflower morphology has lower surface roughness compared to well faceted diamond. Various tribological studies on diamond film indicates that reduced surface roughness in beneficial in decrease in cutting resistance and friction coefficient [16-18].

Table 4.1 summarized the SEM and AFM evaluation of each diamond film.

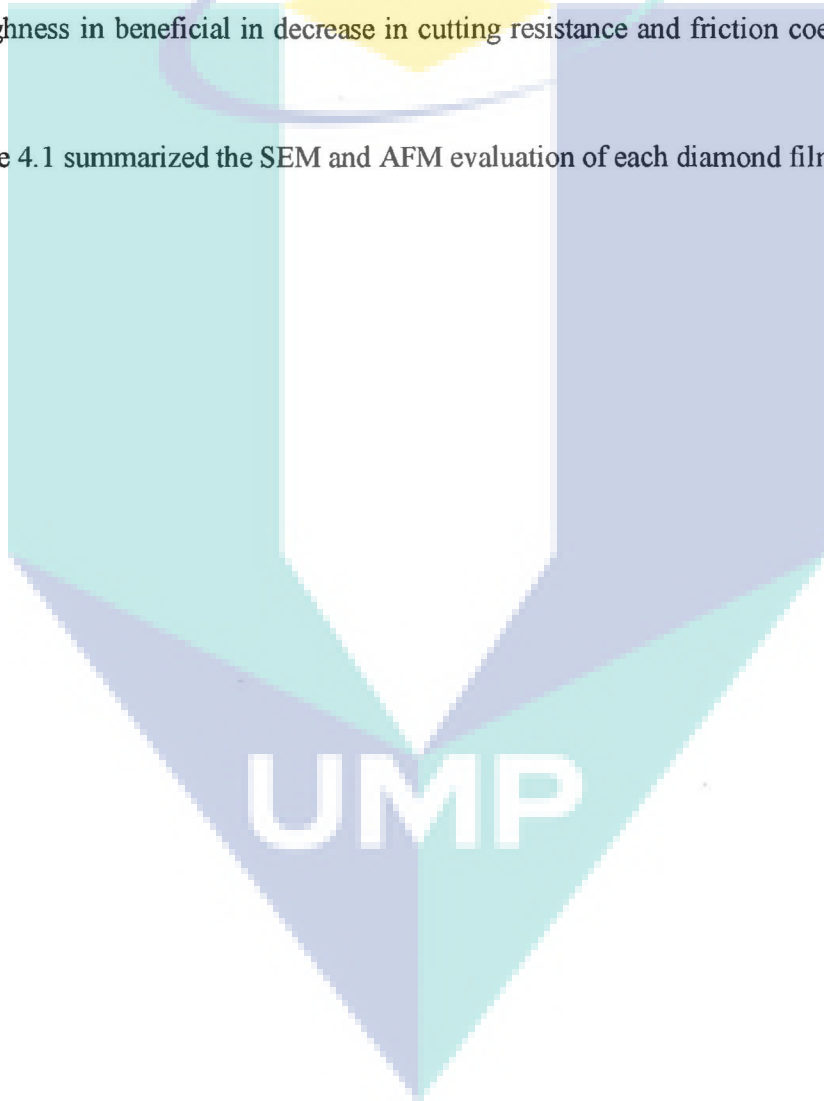


Table 4. 1 Summary of SEM and AFM evaluation for diamond film deposited on substrates pretreated with chemical etching

Characterization	SEM	AFM				
		Ra	RMS	Cluster size, ΔD	Cluster height, ΔZ	Crystallite size
Acid Etching						
1	Cauliflower morphology	60.76	160.6	5413	539.58	496
3	Smooth film with well faceted diamond	42.4	169.8	2475	198.8	516
5	Cauliflower morphology	37.3	172.7	1926	164.5	391.8
Strong Acid Etching						
7	Cauliflower morphology	73.39	136.5	164.1	5440	589
9	Smooth film with well faceted diamond	67.72	123.8	136.5	3593	439
11	Cauliflower morphology	60.38	164.1	123.8	7473	540
Basic Etching						
13	Cauliflower morphology	32.8	236.6	236.6	1549	208.2
15	Cauliflower morphology	38.9	221	221	1517	242.8
17	Cauliflower morphology	57.7	335.9	335.9	2417	295.9

4.3.4 Phase analysis using X-ray diffraction

Fig. 4.25 to 4.27 shows the comparison of X-ray diffraction pattern of diamond film deposited on acid, strong acid and basic etched substrates respectively. Due to the low thickness of diamond films produced at only around 7 μm , Si_3N_4 substrate peaks were more intense than those of diamonds. It is shown that diamond (111) and (2 2 0) diffractions could be identified at around 44.2° and 75.8° respectively, in addition to those of Si_3N_4 peaks in the substrate. These peaks were observed in all samples indicating that the films produced on the substrates consisted of diamond crystals. Furthermore, there was no evidence for the presence of graphitic carbon from the XRD peaks. This gives further evidence that the deposited films were composed of diamond grains only. However, X-ray diffraction could not detect the non-crystalline phase such as amorphous carbon in the diamond film.

The (111) and (110) ratio of diffraction peak of the cubic diamond were investigated and their ratio were compared to determine the preferred orientation of each diamond films. The broadening of full width at the half maximum (FWHM) of (111) peak is correlated to small grain sizes of the films [19]. The crystallite size of diamond film can be calculated using Debye-Scherrer equation:

$$t = \frac{K\lambda}{B_{1/2} \cos \theta_B} \quad (1)$$

t = crystallite size

K = unit cell geometry dependant constant whose value typically between 0.85 and 0.99

λ = wavelength of the x-ray

Θ_B = Bragg angle

$B_{1/2}$ = full-width-half-maximum of the peak

Based on broadening of FWHM of (111) peak, the crystallite size of diamond film were calculated using Equation (1). The crystallite size was found to be in range of 30-50 nm. Also observed is that there is no apparent shift due to strain that may be caused the either thermal or intrinsic stress.

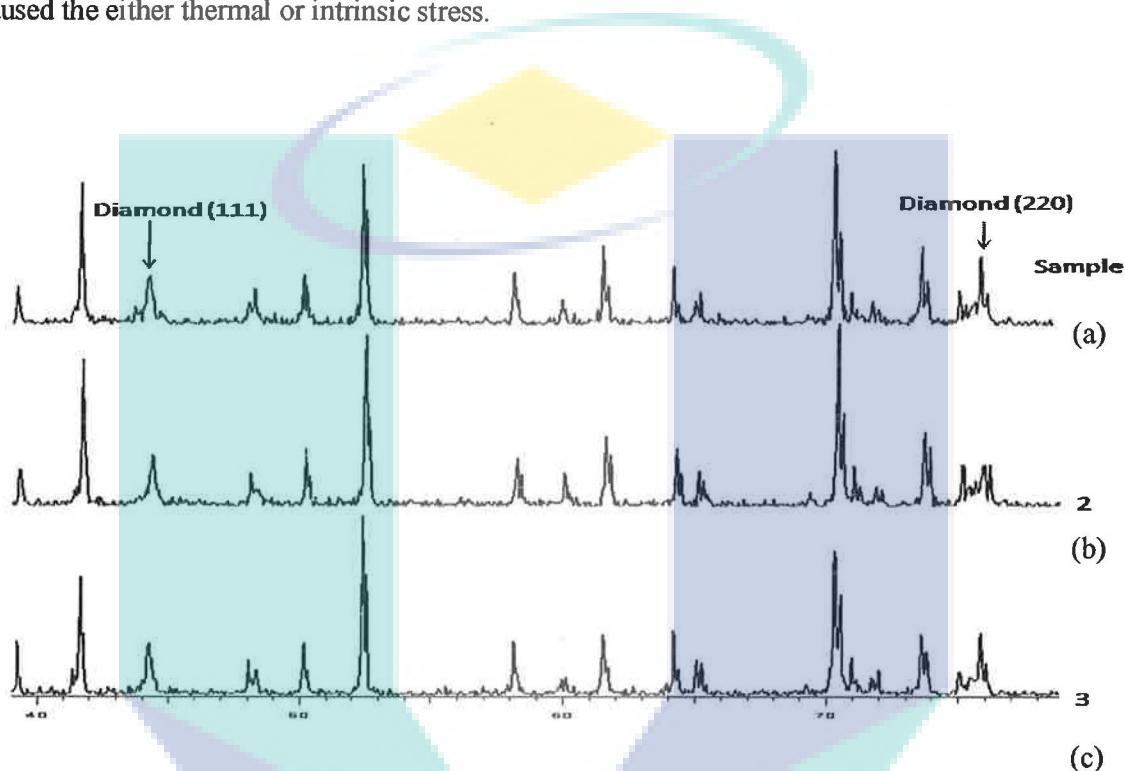


Figure 4.25 X-ray diffraction pattern of diamond film deposited on acid etched substrates for (a) 10 (b) 20 and (c) 30 minutes

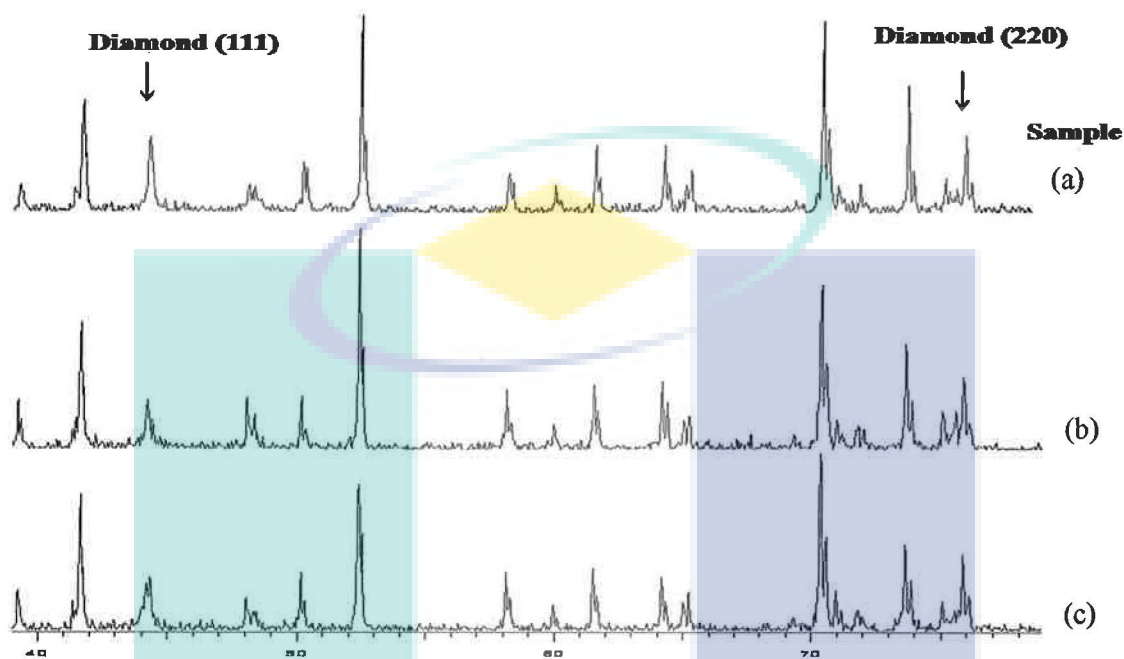


Figure 4.26 X-ray diffraction pattern of diamond film deposited on strong acid etched substrates for (a) 10 (b) 20 and (c) 30 minutes

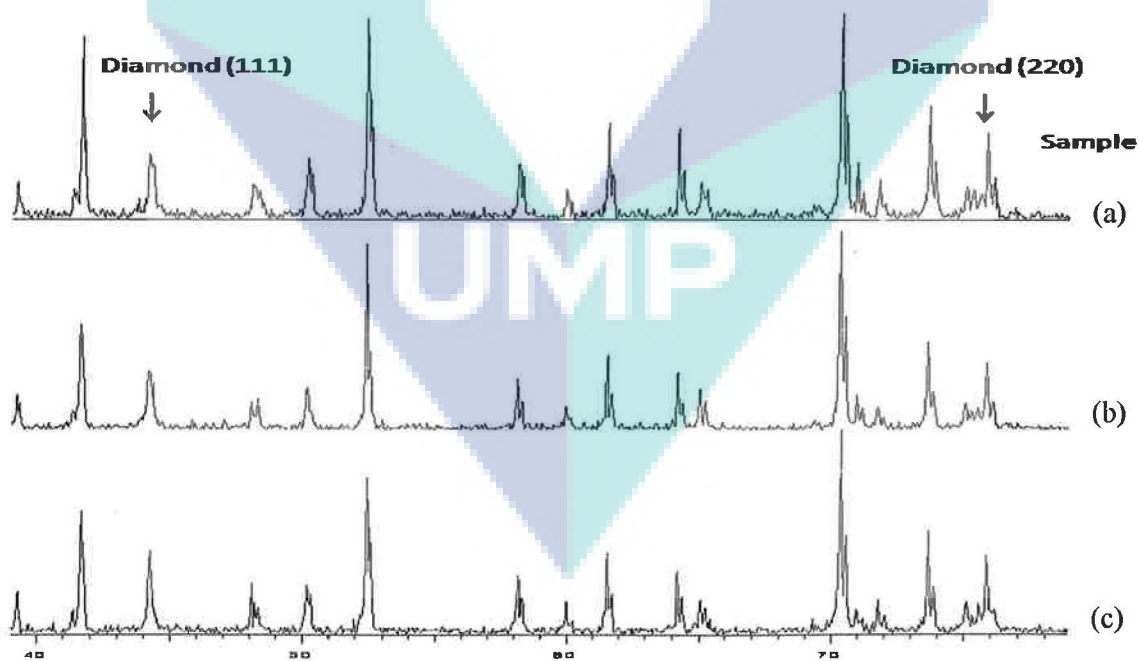


Figure 4.27 X-ray diffraction pattern of diamond film deposited on basic etched substrates for (a) 10 (b) 20 and (c) 30 minutes

The absence of graphite in all samples indicating that maybe initially formed graphitic phase undergoes complete amorphization and recrystallization to diamond and nanodiamond phase [20].

The ratio of (110) to (111) in the samples ranges from 0.66 to 1.283; the values are higher compared to natural diamond at 0.25 JCPDS Data Card No. 6-675. This shows that the nanocrystalline diamond have preferred orientation at (110). This can be attributed to the nanometric (110) growth sectors develop faster than the others as explained in nanocrystalline diamond formation in Section 4.2.3.

Summarizing from the XRD measurement, it can be concluded that different pretreatments have no influence on the crystalline properties of the diamond film. This is in agreement with the finding from Azevedo, A.F., et al [21].

4.3.5 Diamond quality analysis using Raman spectra

Raman analyses shown in Fig 4.28 to 4.30 were done to evaluate the quality of diamond film. Fig. 4.28 shows the Raman spectra of the diamond films deposited on the Si_3N_4 . The important feature is the diamond band at 1330 cm^{-1} . Compared to the value of 1332 cm^{-1} that is usually associated with diamond sp^3 bonding, observed negative shift in the Raman peak is associated with the low thickness of the deposited diamond film ($\sim 7\mu\text{m}$) [22]. However, the diamond shift values also corresponds to very low tensile stresses using the expression [23]

$$\sigma(\text{GPa}) = -0.567\Delta\nu(\text{cm}^{-1})$$

where $\Delta\nu$ is the difference between measured and natural stress-free diamond peak shifts.

Other important feature that can be seen in the Raman spectra is soft peak at 1140 cm^{-1} and broad peak with maximum at 1480 cm^{-1} assigned to C–H chain structures as transpolyacetylene [trans-(CH) $_n$] and widely accepted as typical spectra of nanocrystalline diamond [23],[24].

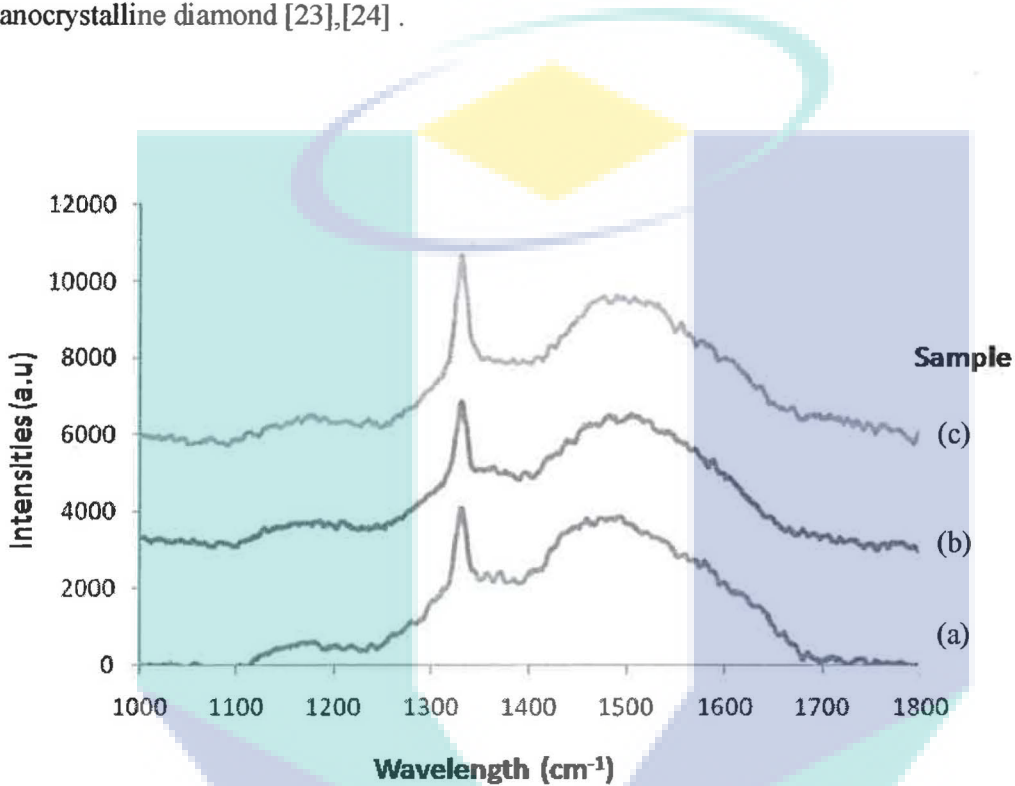


Figure 4.28 Raman spectra comparison between substrates pretreated in acid etching for (a) 10 (b) 20 and (c) 30 minutes.

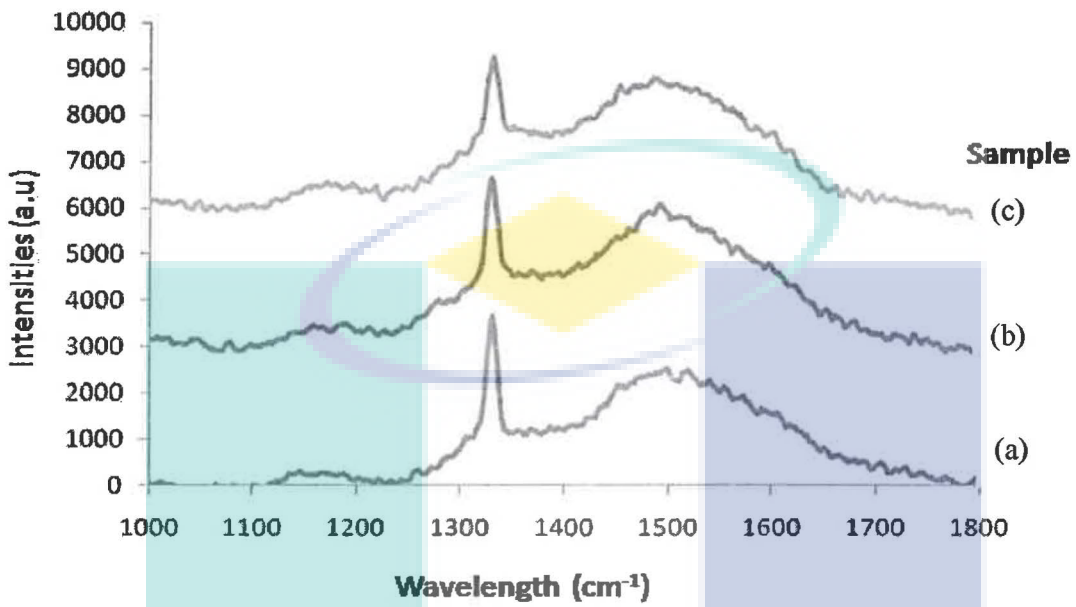


Figure 4.29 Raman spectra comparison between substrates pretreated in strong acid etching for (a) 10 (b) 20 and (c) 30 minutes.

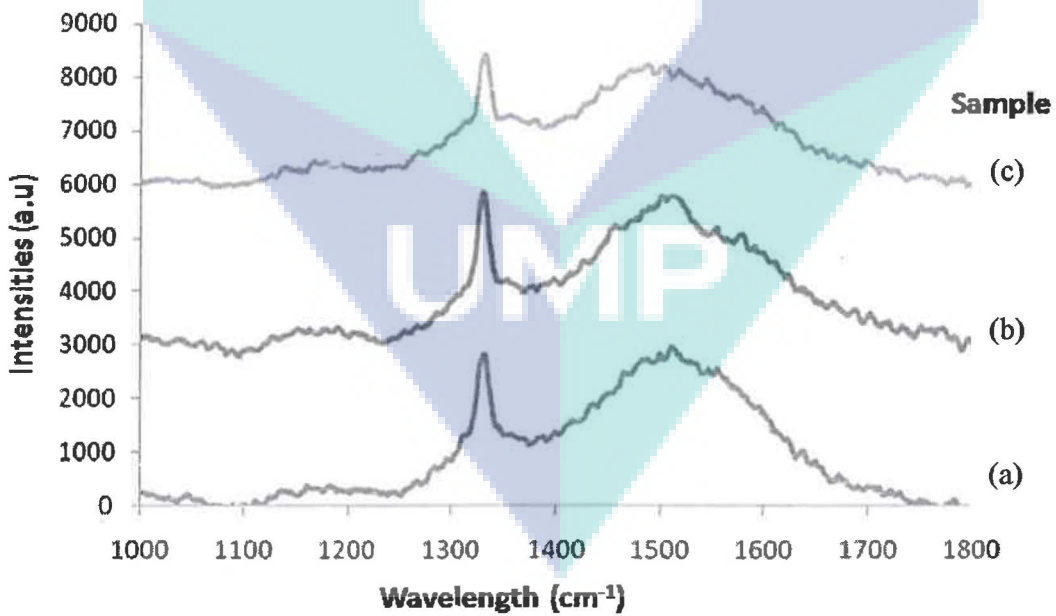


Figure 4.30 Raman spectra comparison between substrates pretreated in basic etching for (a) 10 (b) 20 and (c) 30 minutes.

The ratio of intensity of diamond peak, (I_D) at 1330cm^{-1} over intensity of nanocrystalline diamond phase (I_{ND}) at 1480 cm^{-1} was calculated for each sample. The influence of etching time to the value I_D/I_{ND} of is varied for different etching reagent. The ratio of I_D/I_{ND} increases with etching time during acid etching. But for strong acid etching, I_D/I_{ND} is highest when etching time is 10 minutes. Value of I_D/I_{ND} of basic etching, on the other hand, is highest when etched for 20 minutes.

The intensity ratio of I_D/I_{ND} is generally a measure for zone edges or border phonons of the carbon clusters, which depend on cluster sizes and distributions. The increase in the I_{ND} peak content is an indication of the state of development of the sp^2 phase and that the sp^2 sites are beginning to organize into small graphitic clusters[25]. The increase in I_D/I_G ratio indicates a decrease in the sp^3 content [26]. This are due to decrease in crystallite size of the diamond films thus larger proportion of the grain boundaries are sp^2 -bonded[27].

To determine the sp^2/sp^3 bonds ratio, McNamara et al. formula were used:

$$f = 100 \times \frac{I_{ND}}{(75 \times I_D + I_{ND})}$$

Where I_D is the intensity of diamond peak at 1332.5 cm^{-1} , and I_G is the intensity of the non-diamond peak at about 1480 cm^{-1} [28]

During chemical etching, the surface roughness induced during the process did not introduce much surface roughness as when compared to mechanical pretreatment. The surface of the substrates were much smoother, thus the surface energy of the surface also much less. The effect of decreases surface energy will promote the formation of sp^3 bonds, hence higher quality were obtained while larger surface energy will lead to sp^2 bond formation[29] .

Table 4.2 summarized the evaluation of chemical etching time on the morphology and phase analysis based on SEM and X-ray diffraction pattern . Based on ratio of $I_{(100)}/I_{(110)}$ and value of β , the best chemical etching time was selected. Table on the other hand summarized the evaluation based on AFM and Raman spectroscopy analysis.

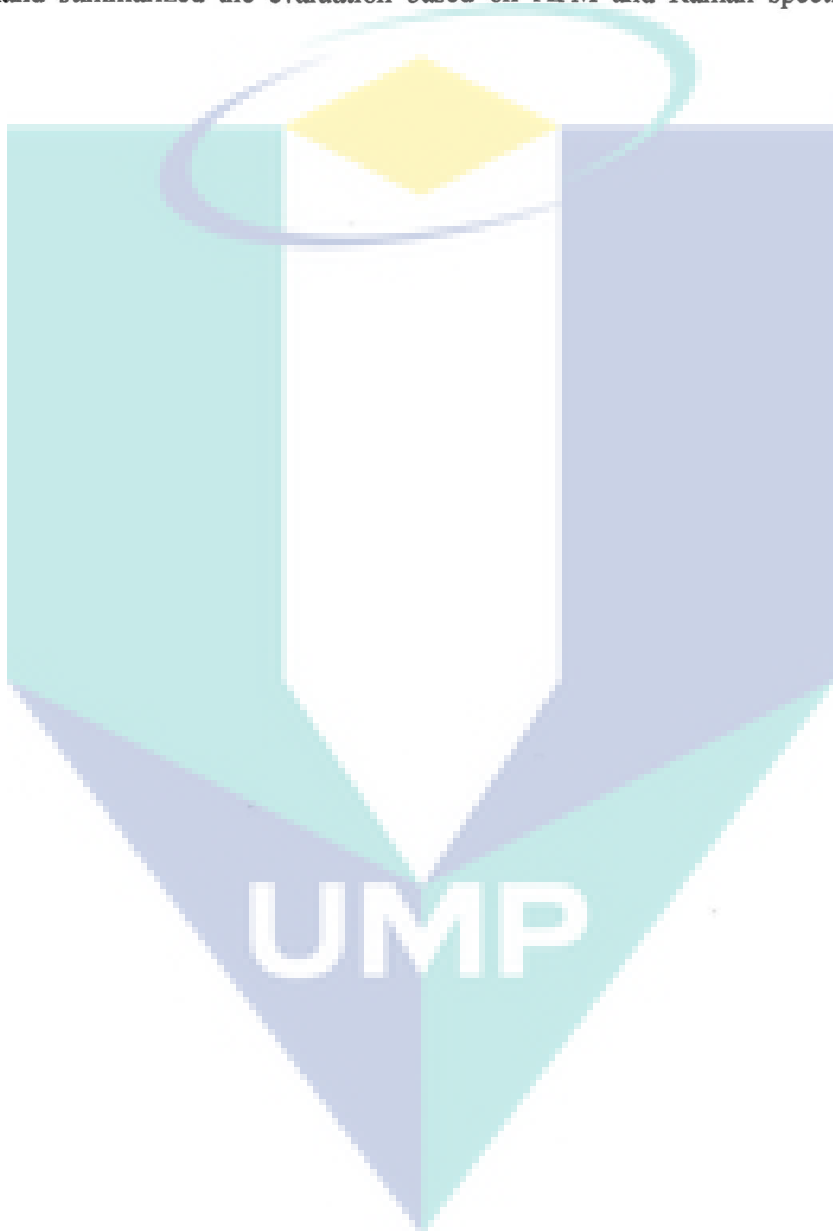


Table 4.2 Summary of XRD and Raman Spectroscopy characterization on diamond deposited on substrates pretreated with chemical etching

Characterization	XRD			Raman Spectroscopy				
	Crystallite size (nm)	Intensity		$I_{(110)}/I_{(110)}$	I_D/I_{ND}	sp^2/sp^3 ratio (%)	Tensile stress (GPa)	FWHM
(111)		(220)						
Acid Etching								
1	38.95414	31.6	43.6	0.725	1.0648	1.236669	0.81081	13.8966
3	34.14815	33.1	25.8	1.283	1.112	1.190525	0.81081	14.0133
5	34.55964	37	44	0.841	1.329	0.993265	0.81081	13.9572
Strong Acid Etching								
7		46	42	1.095	1.526	0.866273	0.81081	11.9842
9		30	45	0.66	1.199	1.100016	1.67832	13.4901
11		30.5	50	0.61	1.223	1.078328	-0.06237	15.0514
Basic Etching								
13	31.8575	33.7	42.6	0.791	0.949	1.385055	-0.06237	
15	38.95717	45.5	44.7	1.018	1.183	1.114558	1.67832	13.7565
17	47.8849	46.9	45.1	1.040	1.089	1.058156	-0.06237	

4.4 Mechanical pretreatment

4.4.1 Introduction

The effect of mechanical pretreatment on diamond morphology, phases and quality will be examined.

4.4.2 Effect of etching time on the morphology of the diamond film

Fig. 4.31 shows the morphology of diamond film deposited on as-received, pretreatment by blasting and grinding. Fig. 4.31 (a) shows cauliflower morphology with apparent grain boundary due to coalescent of nuclei. Fig. 4.31 (b) shows continuous and well faceted diamond film with no apparent cauliflower morphology. Fig. 4.31 (c) on the other hand also shows cauliflower morphology, only smoother compared to Fig. 4.31 (a).

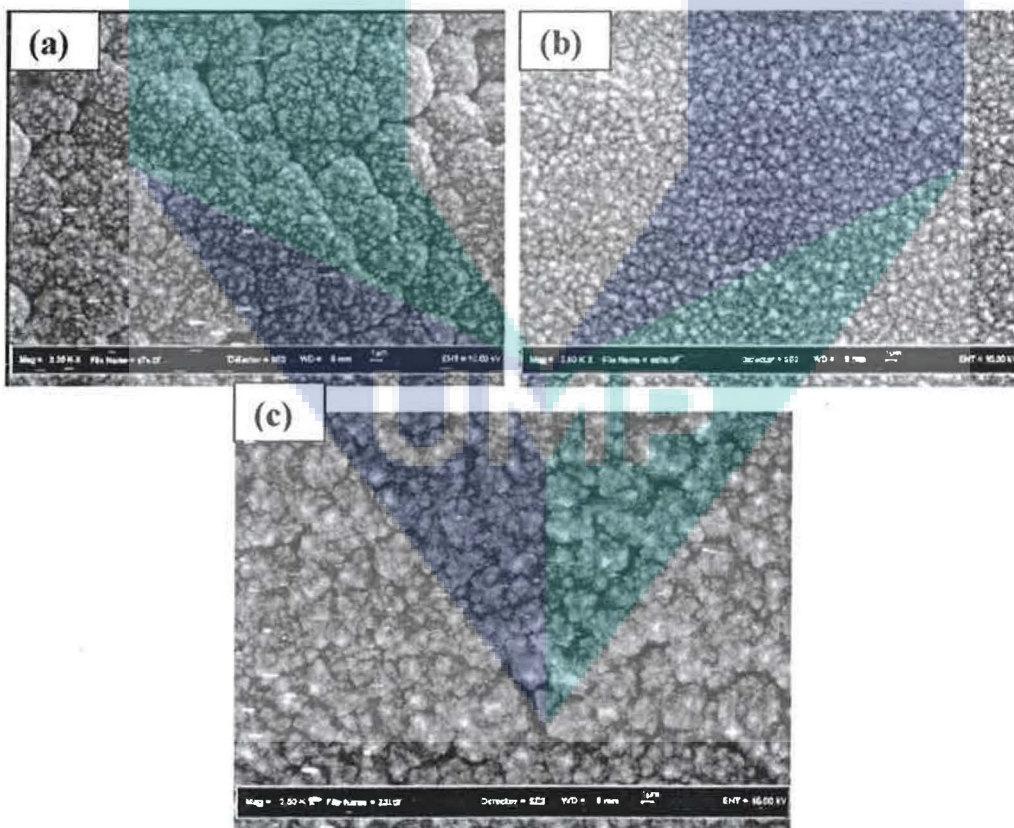


Figure 4.31 Fe-SEM micrograph of diamond film deposited on (a) as-received (b) pretreated by blasting and (c) pretreated by grinding substrates.

4.4.3 Surface topography and surface roughness by atomic force microscopy (AFM)

Fig. 4.32 is showing 3D topography view of as-received and mechanically treated substrates. The surface roughness of diamond film deposited on as-received is 60.76 nm, followed by 42.4nm (sand blasted substrate) and 37.3 nm (ground substrates).

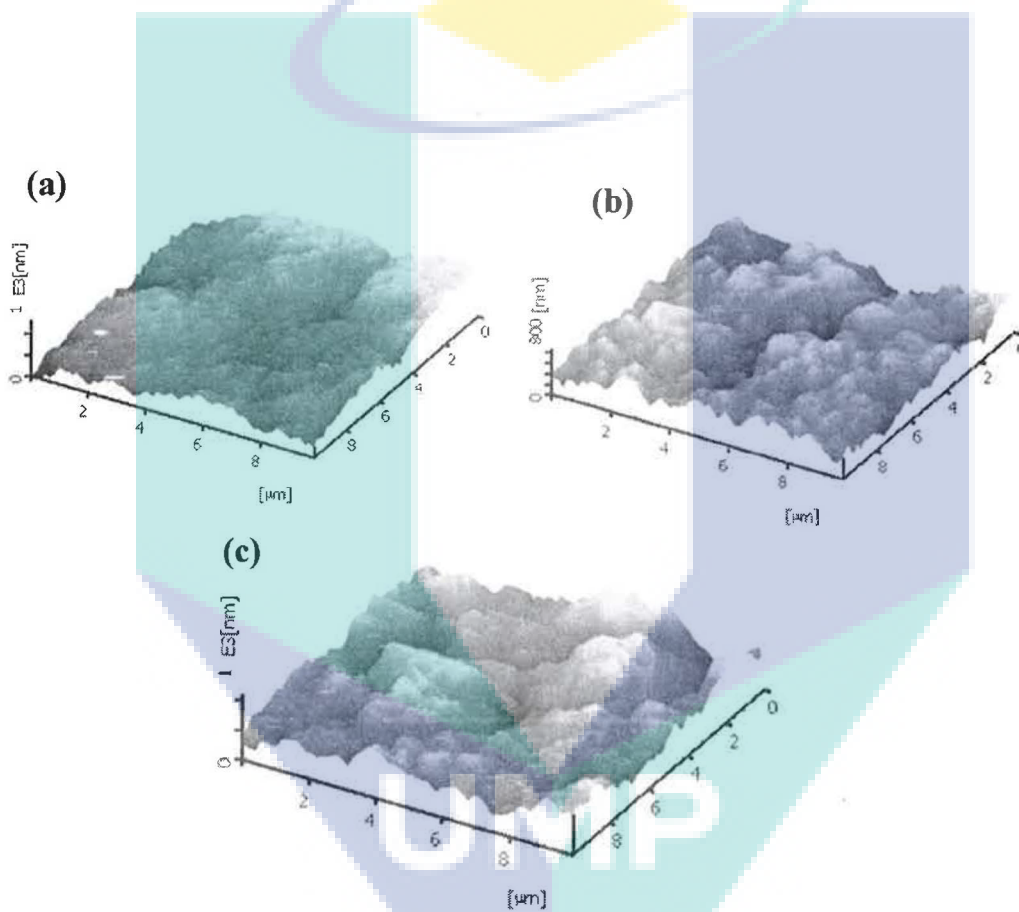


Figure 4. 32 3D topography of diamond film deposited on (a) as-received (b)pretreated by blasting and (c) pretreated by grinding substrates.

4.4.4 Phase analysis and quality of diamond using X-ray diffraction

Fig. 4.33 are showing the comparison of x-ray diffraction peaks of as-received and mechanically treated substrates. As-received and grinded substrates are showing preference in (111) direction compared to blasted surface.

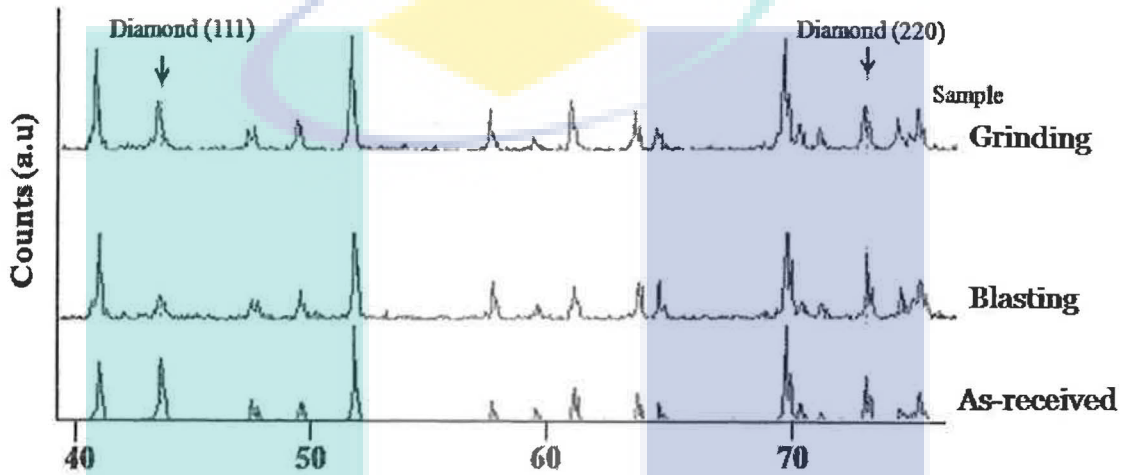


Figure 4. 33 XRD peaks comparison of diamond film deposited on as-received, pretreated by blasting and pretreated by grinding substrates.

Raman spectra comparison, on the other hand, is shown in Fig. 4.34

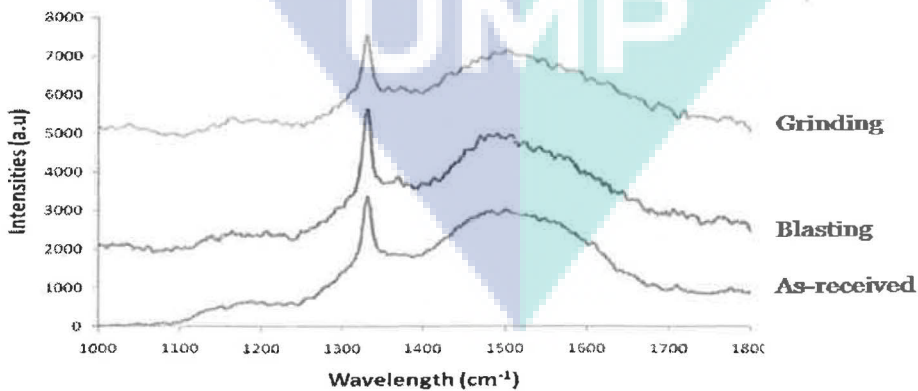


Figure 4. 34 Raman spectra of diamond film deposited on as-received, pretreated by blasting and pretreated by grinding substrates.

Table 4. 3 Summary of SEM and AFM evaluation for diamond film deposited on as received and substrates pretreated with mechanical etching

Characterization	SEM	AFM				
		Morphology evaluation	Ra (nm)	RMS (nm)	Cluster size, ΔD , (nm)	Cluster height, ΔZ , (nm)
As-Received						
	Cauliflower	60.76	76.33	1131.69	140.26	442
Sand Blasting						
3	Smooth film with well faceted diamond	95.68	118.8	3212.96	398.93	516
Grinding						
5	Cauliflower	103	127.5	2341.43	243.11	468.29

Table 4. 4 Summary of XRD and Raman Spectroscopy characterization on diamond deposited on as received and substrates pretreated with mechanical etching

Characterization	XRD				Raman Spectroscopy				
	Sample No.	Crystallite size (nm)	Intensity		$I_{(100)}/I_{(110)}$	β	sp^2/sp^3 ratio	Tensile stress (GPa)	FWHM
(111)			(220)						
Acid Etching									
1	38.95414	31.6	43.6	0.725	0.5706	1.1827	1.61595	15	
3	34.14815	33.1	25.8	1.283	0.5471	1.0919	0.74277	12.8545	
5	34.55964	37	44	0.841	0.5549	1.0581	1.67832	13.9174	

UMP

4.5 Adhesion analysis of diamond film deposited on various pretreated substrates.

4.5.1 Introduction

Adhesion strength plays an important role in performance of final product. Indentation test based on well defined tips was done on the diamond film to quantify its adhesive strength. The cracking behavior of the diamond films were inspected using SEM and optical microscope.

4.5.2 Adhesion behavior due to different indentation loads

In indentation method, the diamond coating was indented at increasing load of 5kgf, 10kgf and 30kgf. When the load is sufficiently high, some lateral cracks initiate and propagate along the coating-substrates interface. This minimum load is called critical load and is used to measure the coating adhesion. However, due to hard and brittle nature of diamond film, it is hard to quantify the exact value of critical load. Thus, qualitative estimation of adhesion can be made from shape of tip imprinting, kind of failure and extensions of the lateral cracks [22].

Fig. 4.35 shows response of diamond coating on substrates pretreated with acid etching for 20 minutes to various load of Vickers indentation. At 5kgf, no apparent failure was observed except for partial spalling at Vickers imprinting and radial crack. However, as the load increases to 10 and 30kgf, the diamond film start to delaminate and spallation occurs. Radial cracks lengths also increases with increasing loads.

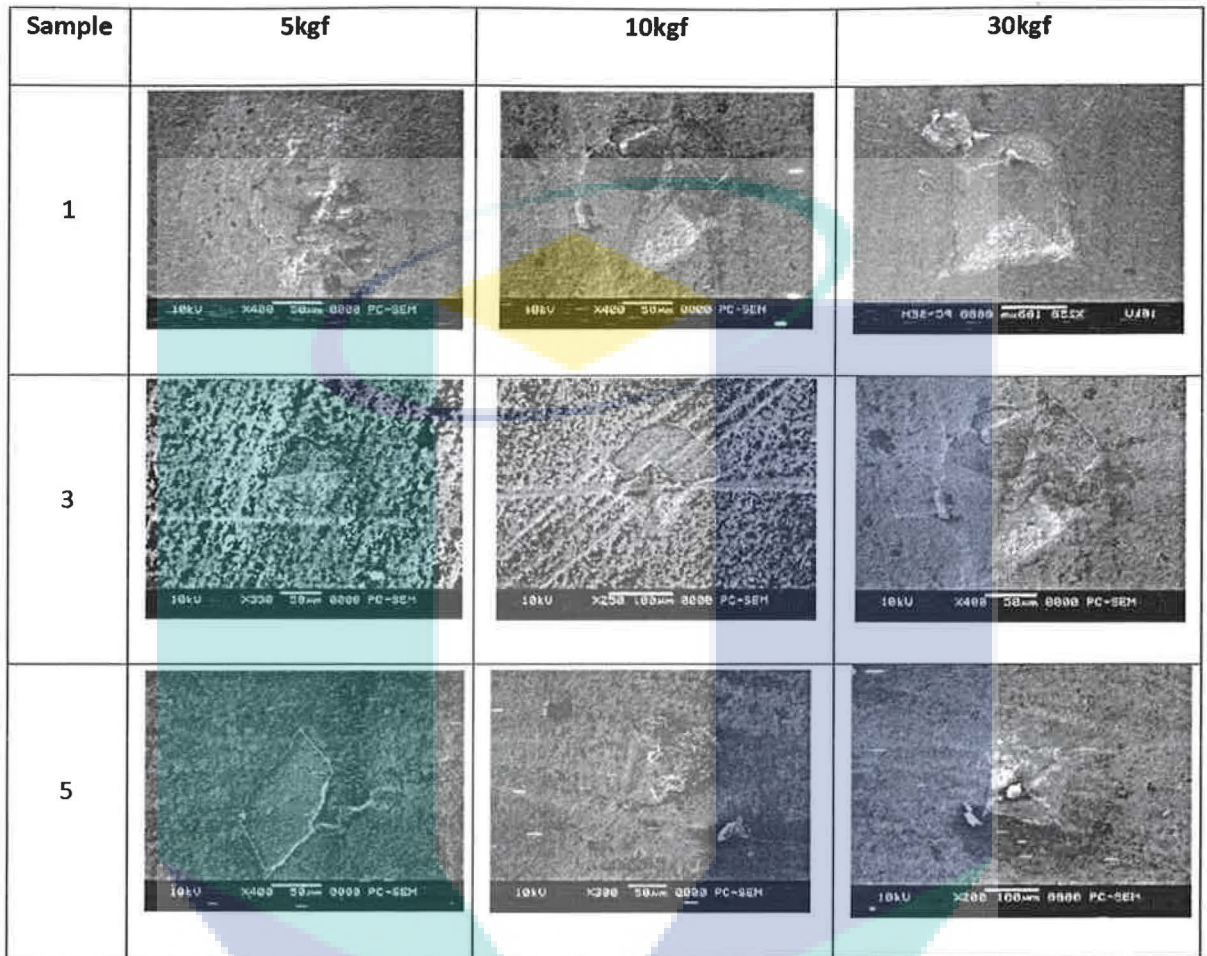


Figure 4.36 SEM images of Vickers indent on acid etched pretreated samples

UMP

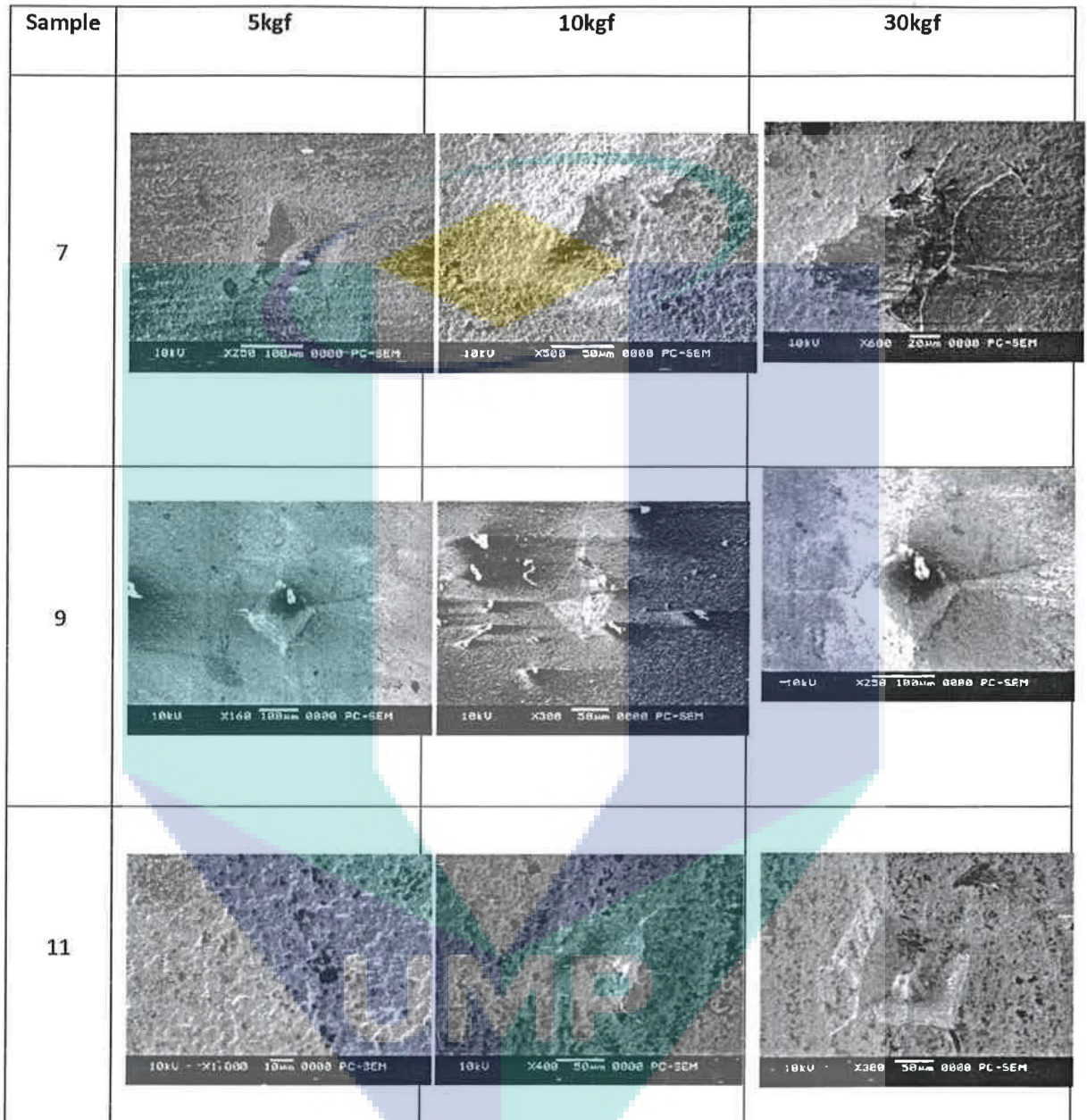


Figure 4. 37 SEM images of Vickers indent on strong acid etched pretreated samples

Crack response of diamond film deposited on basic etched substrates are shown in Fig. 4.38. At 5kgf, the diamond films peeled off from the substrates and this continues under 10 and 30kgf. This behaviors show that the diamond film on basic etched substrates have poor adhesive strengths.

Based on SEM investigation, strong acid are showing better adhesion compared to acid and basic etching. Higher HF and HNO₃ concentration used during acid etching leading to deeper pit on the substrates, thus provide more anchoring sites for the diamond film [30]

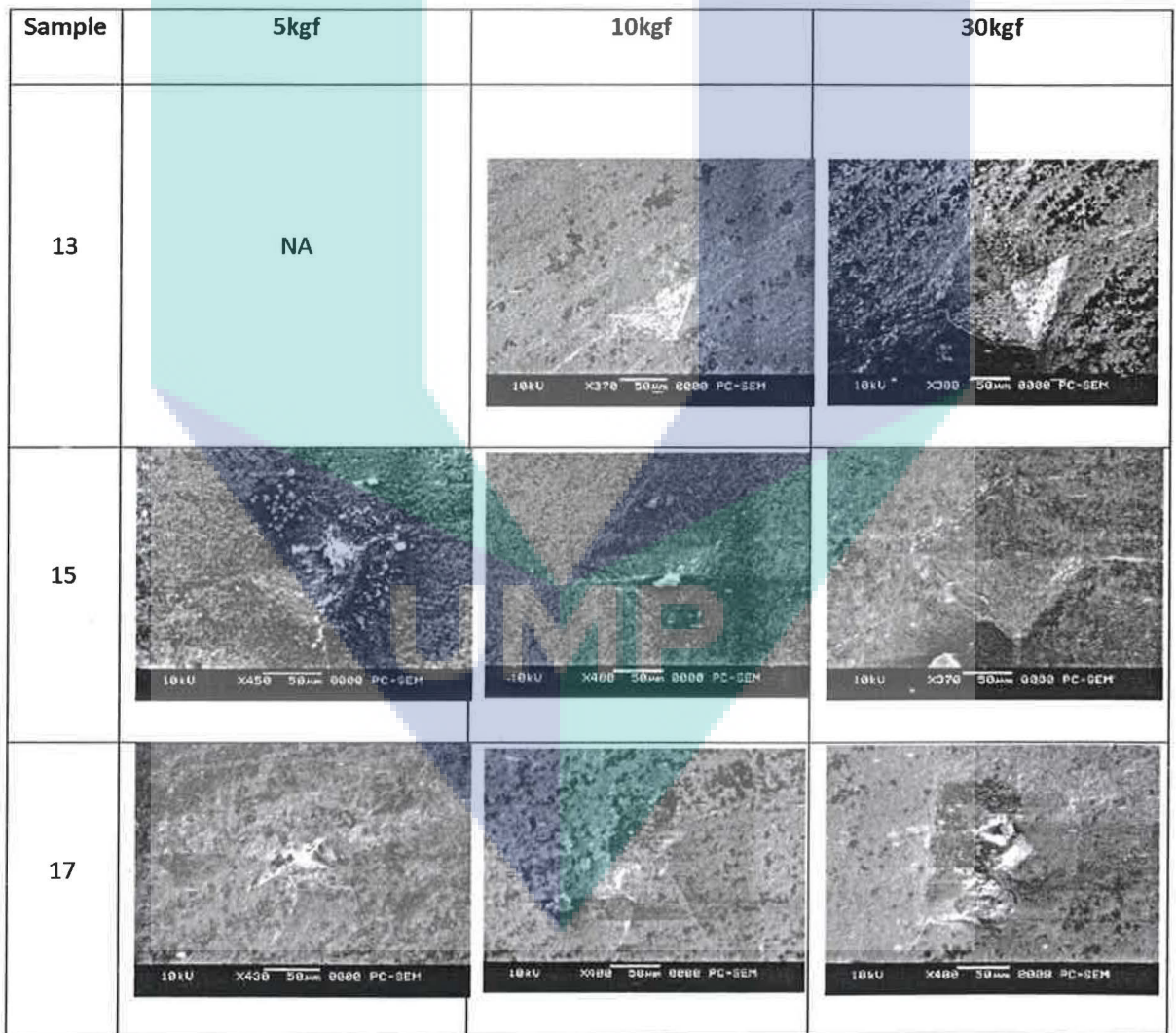


Figure 4.38 SEM images of Vickers indent on basic etched pretreated samples

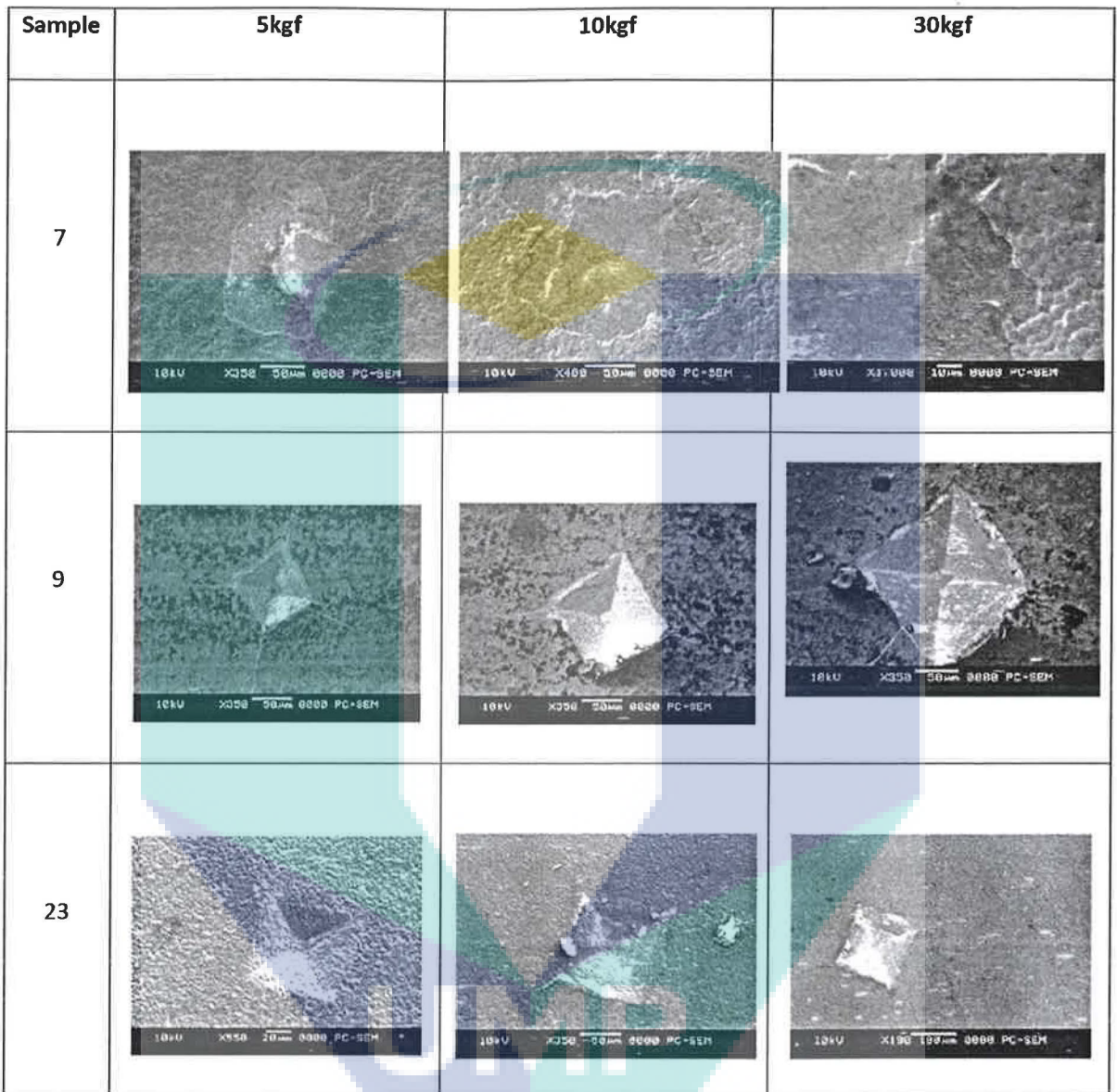


Figure 4. 39 SEM images of Vickers indent on as-received and mechanically pretreated substrates

Based on SEM investigation shown in Fig. 4.39, the adhesion was very good in both blasted and ground substrates with no spallation observed even at higher load. The adhesion on as-received substrate, however, were very poor, showing complete peel off even at 5kgf.

4.5.3 Determination of adhesive strength

4.5.3.1 Adhesive strength determination based on radial crack

The adhesion strength of diamond film was examined based on work done by C.R Lin, et. al [31]. The radial crack length versus indentation load for selected samples are plotted in Fig. For low load, all films behaves similarly except for as-received substrates. However, as the load increases the crack length of each samples behaves differently due to different adhesion strength along substrate/film interface. The inverse slope of linear fit has been used as measure of interfacial cracking resistance of diamond film/ substrates system [1].

The value of dP/dx obtained from Fig.4.41 then is shown in Fig. 4.42. Diamond film deposited on chemical pretreated substrates has higher adhesive strength compared to mechanically pretreated substrates with highest adhesive strength were obtained by substrates undergoes basic etching (651 kgf/mm) followed by acid etching (411 kgf/mm) and strong acid etching (313 kgf). Blasted and grinded substrates have diamond film with adhesive strength of 148 and 129 kgf/mm respectively. As-received substrates, as expected, has lowest dP/dx value at 43 kgf/mm.

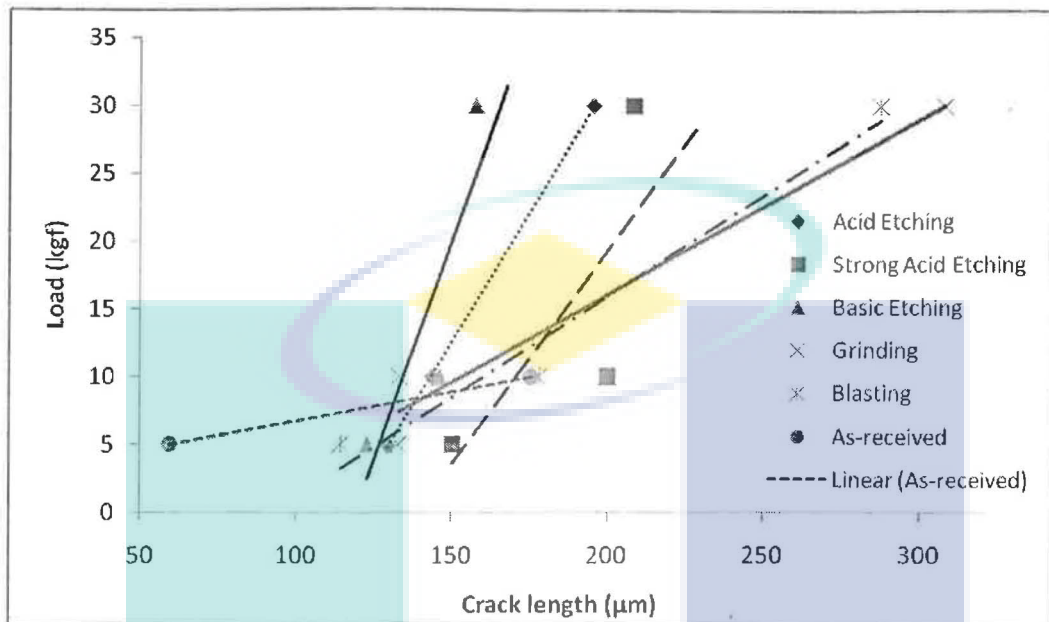


Figure 4.40 Indentation load versus crack length curves for diamond films with different surface pretreatment

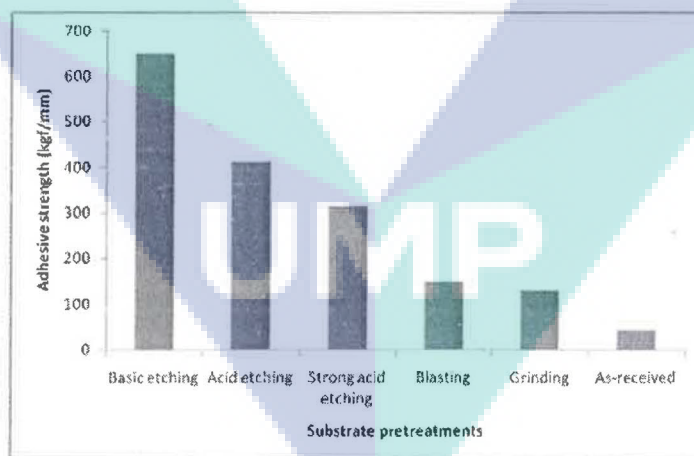


Figure 4.41 Adhesive strength of diamond film deposited on various surface pretreated substrates

Buijnsters et al., however argue that the usage of crack length as measurement of adhesive strength is not appropriate due to hard and brittle nature of diamond film. The formation of radial crack is common in hard and brittle film, thus not a measure of adhesive failure [32]. Further investigation shows that the value of dP/dx obtained from Fig. 4.41 did not reflect the real behavior of diamond film under indentation load. Fig. 4.42 shows comparison between diamond film that undergoes basic etched (with highest adhesive strength of 1041 kgf/mm) and blasting (153.6 kgf/mm). Fig. 4.42 (a) shows that the diamond film peeled off around the indented area with radial cracks extending from various points. Fig. 4.42(b) on the other hand showing no sign of spalling or delamination around the indented area and the radial cracks extended only from the corner of the Vickers indent. The SEM observation did not agree with the value of adhesive strength obtained from indentation load versus crack length curves shown in Fig. 4.40.

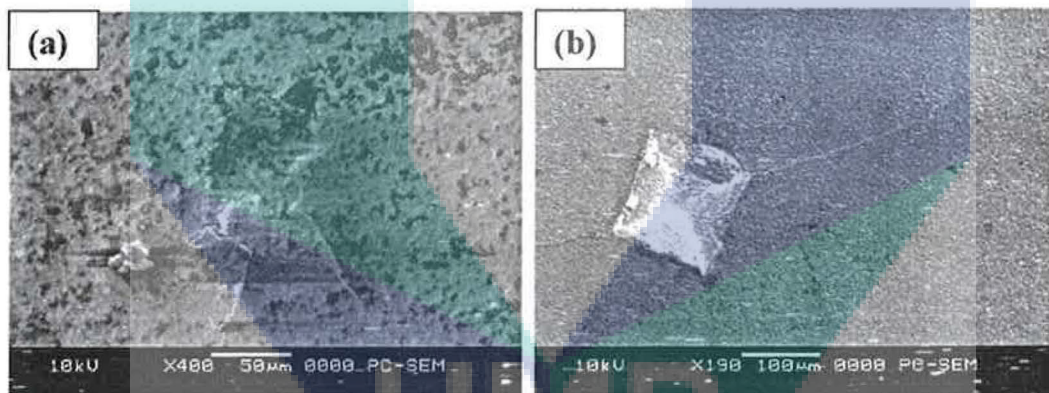


Figure 4.42 Crack response of diamond deposited on (a) basic etched and (b) pretreatment by blasting to Vickers indentation

Due to discrepancy between value of adhesive strength and behavior of indented diamond film, another approach was taken to quantify the adhesive strength of the diamond film which is by measuring delamination radius as a function of indentation load.

4.5.3.2 Adhesive strength determination based on delamination radius

Fig. 4.43 shows the optical micrograph of diamond film showing the typical response of diamond film to indentation load. Measurement tools in the image analyzer systems were used to determine the delamination radius of diamond film.

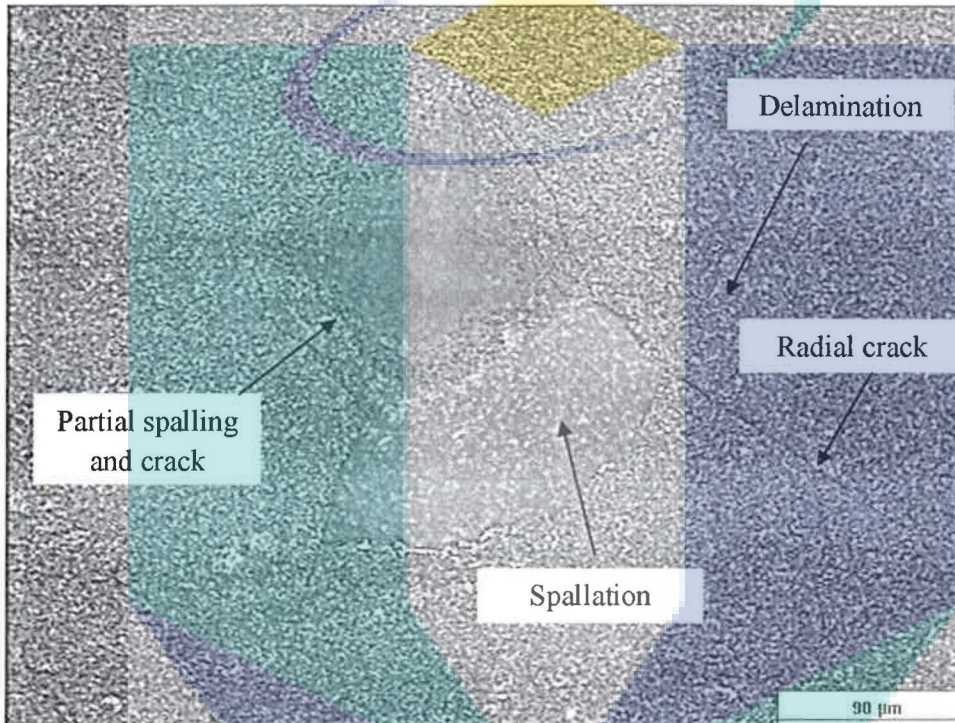
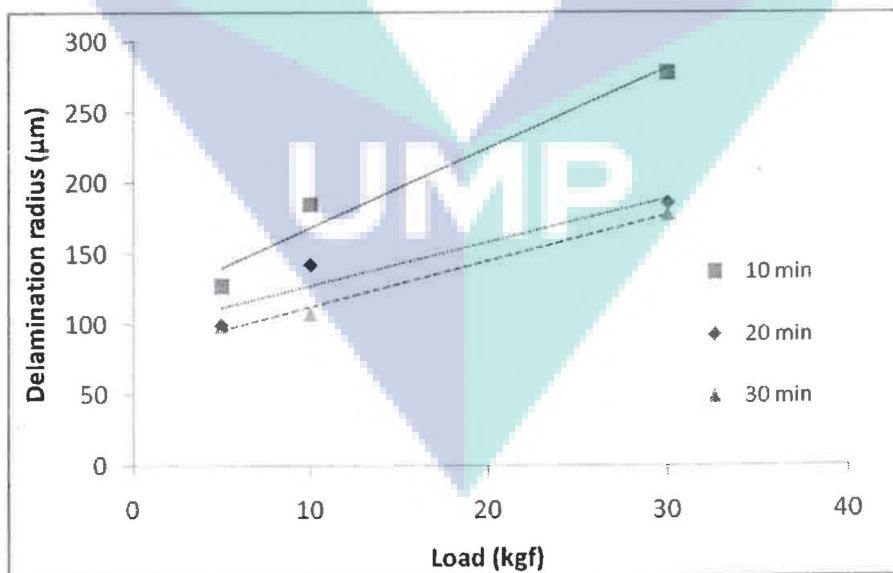


Figure 4.43 Typical crack response of diamond film due to Vickers indentation observed under optical microscopy.

Delamination of diamond film will cause the area to appear whitish due to loss of adhesion to the substrates. Small radius will be observed if the film have good adherence toward the substrates and vice versa. Table 4.5 shows the delamination radius of each sample at different loads.

Table 4.5 Delamination radius of various samples under various indentation load

Sample	5kgf	10kgf	30kgf
1	126.4	184.2	277.7
3	99.32	62.5	185.4
5	99.41	107.3	277.7
7	175.3	203.7	318.5
9	122.6	95.68	345.2
11	101.5	58.83	189.6
13	184	161.7	167.2
15	92.85	104.1	165.6
17	81.43	120.3	203.3
19	115.9	151.3	190.6
21	86.95	62.43	192.3
23	109.4	103	261.2

**Figure 4.44** Plot of delamination radius versus load for strong acid pretreated substrates

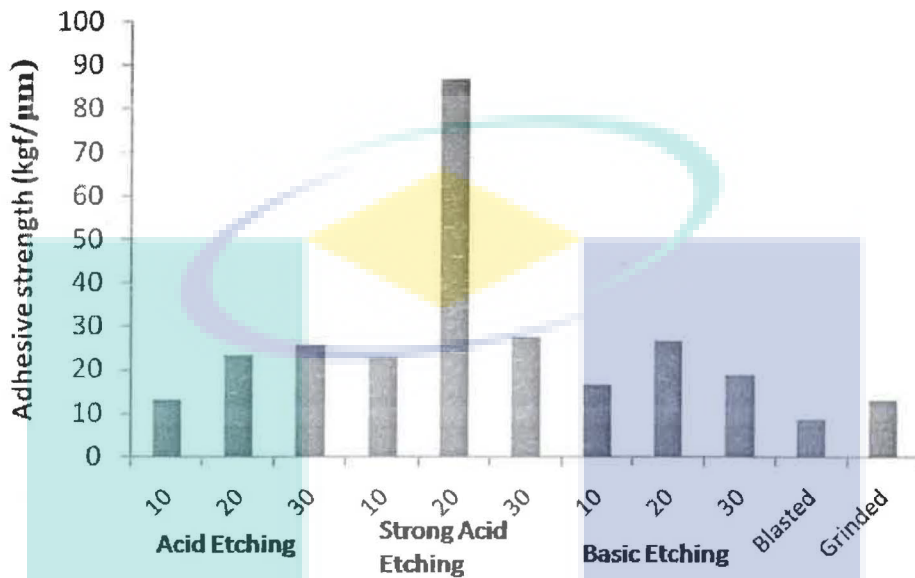


Figure 4.45 Adhesive strength of diamond films.

Plot of delamination radius versus indentation load were obtained for each sample to determine their adhesive strength by taking the inverse slope of the curve. Fig. 4.44 shows the typical curve of delamination radius versus indentation load for strong acid etched substrates at three different etching time. The adhesive strengths then were determined by taking the inverse slope of each line and the value are shown in Fig. 4.45.

By measuring the radius of delaminated area, its relationship with surface roughness and sp^2/sp^3 content were established.

4.5.4 Surface roughness with adhesion

Fig. 4.46 shows the relationship between surface roughness of diamond film and adhesive strength. With exception for few samples, it is shown that as the surface roughness of diamond film decreases, the radii of delaminated diamond film also decreases.

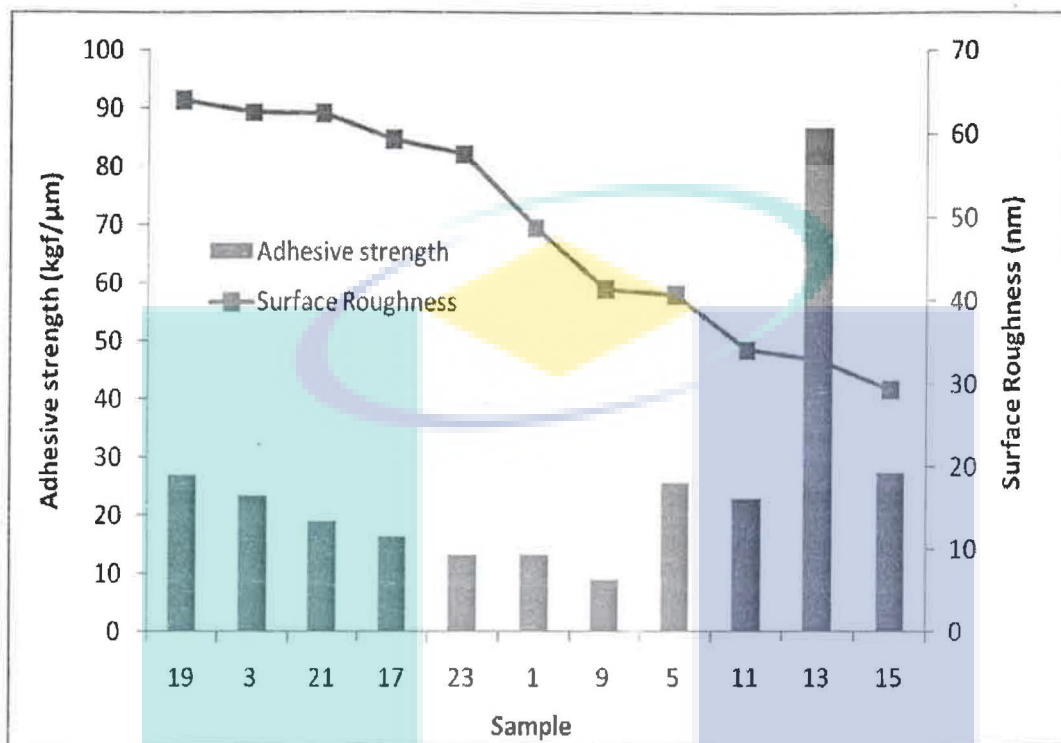


Figure 4.46 Relationship between surface roughness of diamond film and adhesive strength

Surface roughness of the diamond film is associated with grain size as discussed by Askari et. al. [13]. Reduction of grain size increases the hardness significantly by providing more resistance to deformation by Vickers indent tips. Thus, the delamination and adhesion wear become less prominent compared to those with higher surface roughness [33, 34]. Nanocrystalline diamond observed by SEM and Raman yields very smooth surface as discussed in Section 4.3.3. Furthermore, small fraction of amorphous carbon at the boundaries of diamond grains has lubricating effect to resist the adhesion wear caused by Vickers indent.

4.5.5 Adhesive strength relate with sp^2/sp^3 ratio

The effect of sp^2/sp^3 on the adhesive strength of the diamond films was investigated. The sp^2/sp^3 carbon fraction within the diamond film strongly determines the mechanical properties of these diamond films [28]. Higher concentrations of non-diamond phases at the nucleation side lead to higher propensity for film delamination [32].

However, in our case, no clear relationship between adhesive strength and sp^2/sp^3 ratio can be seen as illustrated in Fig 4.47. The changes in the sp^2/sp^3 are too small for noticeable changes to be observed.

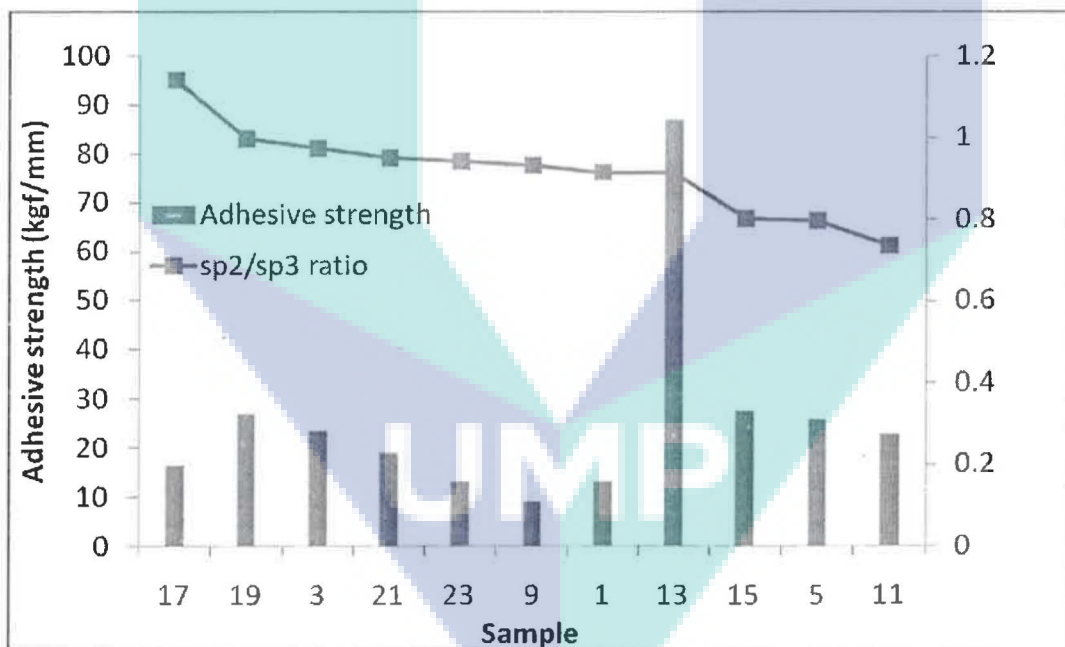


Figure 4.47 Relationship between adhesion strength and sp^2/sp^3 ratio of diamond film

CHAPTER 5

CONCLUSIONS AND RECOMMENDATIONS

5.1 Conclusions

Diamond coating has been deposited on Si_3N_4 using hot filament chemical vapour deposition method with fixed parameter. The effect of substrates pretreatment on formation of diamond film has been studied. Based on results and discussions, it can be concluded that:

1. Substrates that pretreated with sand blasting has yield diamond film with well-facetted morphology with high crystallinity and better adhesion. However, the surface roughness of the diamond film deposited on substrates pretreated with blasting are also higher.
2. Diamond films formed on chemical pretreated substrates has cauliflower morphology and low adhesive strength. However, the surface roughness of diamond film deposited on chemically pretreated substrates was found to be among the lowest compared to mechanically pretreated.
3. XRD analysis shows that there is no graphite formation in all substrates.

4. Raman analyses further confirm the diamonds are consisted of nanocrystalline diamond based on soft peak at 1140 cm^{-1} and broad peak at 1480cm^{-1} . The diamond peaks at 1330 cm^{-1} also observed in all sample. Furthermore, the shift in the diamond peak indicates that residual stress on the diamond is tensile stress attributed either to thermal stress or low film thickness.
5. The response of diamond film formed on mechanically pretreated substrates toward Vickers indentation test are much better compared to chemically pretreated substrates. No peeling or complete spallation are observes in mechanically pretreated substrates

5.2 Recommendations for future works

In the present work, the scopes of the research are constrained by fixed HF-CVD parameter and done only on one substrates material which is Si_3N_4 . Thus, following are recommendation for future works:

1. The effect of deposition parameter on various surfaces pretreatments should be done to investigate the quality of diamond formed.
2. The formation of nanocrystalline diamond should be further investigated regarding its relation toward surface pretreatment.

REFERENCES

1. May, P.W., *Diamond thin films: a 21st-century material*. Philosophical transactions of the royal society A, 2000. **358**: p. 473-495.
2. Ashfold, M.N.R., P.W. May, and C.A. Rego, *Thin Film Diamond by Chemical Vapour Deposition Methods*. Chemical Society Review, 1994. **23**: p. 21-30.
3. Kubelka, S., et al., *Influences of WC-Co hard metal substrate pre-treatments with boron and silicon on low pressure diamond deposition*. Diamond and Related Materials, 1994. **3**(11-12): p. 1360-1369.
4. Kalpakjian, S. and S. Schmid. *Manufacturing Engineering and Technology*. 2005 [cited; 5th Edition:]
5. Gaebler, J., et al. *Tool coatings-new developments for forming, cutting and abrasive machining*. . in *Annual Technical Conference Proceedings*. 2007: Society of Vacuum Coaters.
6. Liu, H. and D.S. Dandy, in *Diamond Chemical Vapor Deposition: Nucleation and early growth stage*. 1995, Noyes Publications: Park Ridge, N.J.
7. Ehrhardt, H., *New developments in the field of superhard coatings*. Surface and Coatings Technology, 1995. **74-75**: p. 29-35.
8. Callister, W.D., in *Materials Science and Engineering: An Introduction*. 2003, John Wiley & Sons, Inc: New York, NY.
9. Wild, C., et al., *Oriented CVD diamond films: twin formation, structure and morphology*. Diamond and Related Materials, 1994. **3**(4-6): p. 373-381.
10. Gielisse, P., in *Diamond and Diamond-Like Film Applications*. 1998, Technomic Publishing Company Inc.: Lancaster, Pennsylvania.
11. Pierson, H.O., in *Handbook of carbon, graphite, diamond, and fullerenes : properties, processing, and applications*. 1993, Noyes Publications: Park Ridge, N.J.
12. Davis, R.F., in *Diamond Films and Coatings: Development, Properties and Applications*. 1993, Noyes Publications: Park Ridge, NJ.

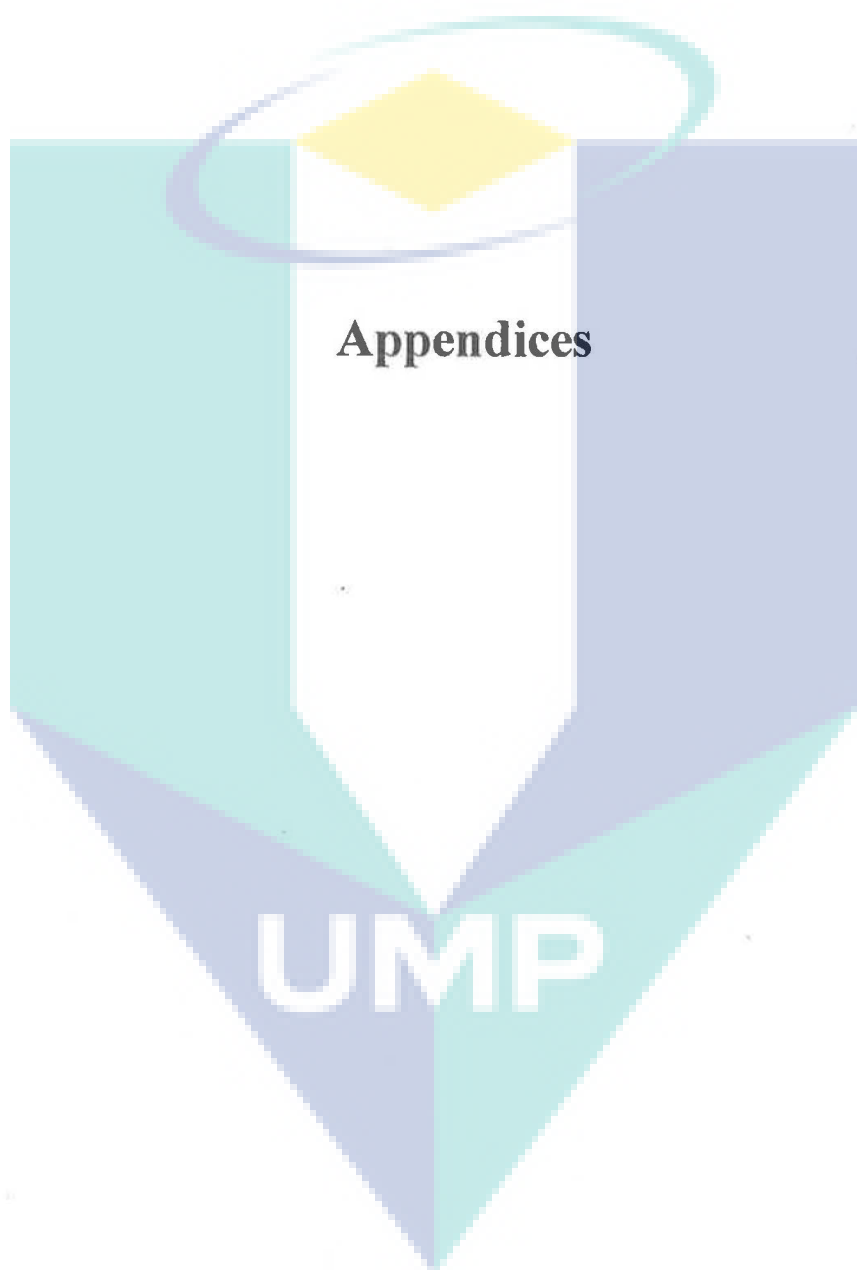
13. Pehrsson, P.E., F.G. Celii, and J.E. Butler, *Chemical Mechanisms of Diamond CVD*, in *Diamond Films and Coatings: Development, Properties and Applications*, R.F. Davis, Editor. 1993, Noyes Publications: Park Ridge, NJ.
14. Polini, R. and M. Barletta, *On the use of CrN/Cr and CrN interlayers in hot filament chemical vapour deposition (HF-CVD) of diamond films onto WC-Co substrates*. *Diamond and Related Materials*, 2008. **17**(3): p. 325-335.
15. Xu, Z., et al., *Effects of surface pretreatments on the deposition of adherent diamond coatings on cemented tungsten carbide substrates*. *Diamond and Related Materials*, 2007. **16**(3): p. 461-466.
16. Polini, R., *Chemically vapour deposited diamond coatings on cemented tungsten carbides: Substrate pretreatments, adhesion and cutting performance*. *Thin Solid Films*, 2006. **515**(1): p. 4-13.
17. Oles, E.J., A. Inspektor, and C.E. Bauer, *The new diamond-coated carbide cutting tools*. *Diamond and Related Materials*, 1996. **5**(6-8): p. 617-624.
18. Cappelli, E., et al., *Diamond nucleation and adhesion on sintered nitride ceramics*. *Diamond and Related Materials*, 2002. **11**(10): p. 1731-1746.
19. Shibuya, Y. and M. Takaya, *Effects of substrate pretreatments on diamond synthesis for Si₃N₄ based ceramics*. *Surface and Coatings Technology*, 1998. **106**(1): p. 66-71.
20. Everitt, N.M., et al., *Friction measurements on hot filament CVD diamond films deposited on etched tungsten carbide surfaces*. *Diamond and Related Materials*, 1995. **4**(5-6): p. 730-734.
21. Silva, V.A., E.J. Corat, and C.R.M. Silva, *Influence of CF₄ addition for HFCVD diamond growth on silicon nitride substrates*. *Diamond and Related Materials*, 2001. **10**(11): p. 2002-2009.
22. Rozbicki, R.T. and V.K. Sarin, *Nucleation and growth of combustion flame deposited diamond on silicon nitride*. *International Journal of Refractory Metals and Hard Materials*, 1998. **16**(4-6): p. 377-388.
23. Endler, I., et al., *Interlayers for diamond deposition on tool materials*. *Diamond and Related Materials*, 1996. **5**(3-5): p. 299-303.

24. Itoh, H., et al., *Adhesion improvement of diamond coating on silicon nitride substrate*. Surface and Coatings Technology, 1999. **112**(1-3): p. 199-203.
25. Peng, X.L., et al., *Characterization and adhesion strength of diamond films deposited on silicon nitride inserts by d.c. plasma jet chemical vapour deposition*. Diamond and Related Materials, 1995. **4**(11): p. 1260-1266.
26. Koba, R.J., *Technology of Vapor Phase Growth of Diamond Films*, in *Diamond Films and Coatings: Development, Properties and Applications*, R.F. Davis, Editor. 1993, Noyes Publications: Park Ridge, NJ.
27. Sarangi, S.K., A. Chattopadhyay, and A.K. Chattopadhyay, *Effect of pretreatment, seeding and interlayer on nucleation and growth of HFCVD diamond films on cemented carbide tools*. International Journal of Refractory Metals and Hard Materials, 2008. **26**(3): p. 220-231.
28. May, P.W., et al., *Diamond deposition in a hot-filament reactor using different hydrocarbon precursor gases*. Applied Surface Science, 1993. **68**.
29. Sanchez, G., et al., *Nucleation of diamond on silicon by biased HFCVD: a comparative study*. Diamond and Related Materials, 1998. **7**: p. 200-204.
30. Ahmed, W., et al., *CVD diamond: controlling structure and morphology*. Vacuum, 2000. **56**(3): p. 153-158.
31. Mattox, D.M., *Handbook of Physical Vapor Deposition (PVD) Processing: Film Formation, Adhesion, Surface Preparation and Contamination Control*. 1998: William Andrew Inc.
32. Belmonte, M., et al., *Surface pretreatment of silicon nitride for CVD diamond deposition*. Journal of American Ceramic Society, 2003. **86**(5): p. 749-754.
33. Yoon, J.-B., et al. *Fabrication of a single crystal silicon substrate for AM-LCD using vertical etching of (110) silicon*. in *Materials Research Society Symposium Proceeding*. 1995: Materials Research Society.
34. Panda, S., et al., *Silicon nitride etching methods*, U.P. Office, Editor. 2007, International Business Machines Corporation: US.
35. May, G.S. and C.J. Spanos, *Fundamentals of semiconductor manufacturing and process control*: John Wiley and Sons. 463.

36. Deng, J., et al., *Wear of ceramic nozzles by dry sand blasting*. Tribology International, 2006. **39**(3): p. 274-280.
37. Liang, X., et al., *Effect of pressure on nanocrystalline diamond films deposition by hot filament CVD technique from CH₄/H₂ gas mixture*. Surface and Coatings Technology, 2007. **202**(2): p. 261-267.
38. Buhlmann, S., et al., *Characterization of ballas diamond depositions*. Diamond and Related Materials 1999. **8**(194-201).
39. Haubner, R. and B. Lux, *Deposition of ballas diamond and nano-crystalline diamond*. International Journal of Refractory Metals & Hard Materials 2002. **20**(93-100).
40. Silva, F., et al., *Formation of <110> texture during nanocrystalline diamond growth: an X-ray diffraction study*. Diamond and Related Materials, 2005. **14**(3-7): p. 398-403.
41. Tang, C.J., et al., *Effect of nitrogen and oxygen addition on morphology and texture of diamond films (from polycrystalline to nanocrystalline)*. Diamond and Related Materials, 2008. **17**(1): p. 72-78.
42. Askari, S.J., G.C. Chen, and F.X. Lu, *Growth of polycrystalline and nanocrystalline diamond films on pure titanium by microwave plasma assisted CVD process*. Materials Research Bulletin, 2008. **43**(5): p. 1086-1092.
43. Askari, S.J., et al., *Adherent and low friction nano-crystalline diamond film grown on titanium using microwave CVD plasma*. Diamond and Related Materials, 2008. **17**(3): p. 294-299.
44. Chowdhury, S., E.d. Barra, and M.T. Laugier, *Study of mechanical properties of CVD diamond on SiC substrates*. Diamond and Related Materials, 2004. **13**: p. 1625– 1631.
45. Wiora, M., et al., *Grain size dependent mechanical properties of nanocrystalline diamond films grown by hot-filament CVD*. Diamond and Related Materials, 2009.
46. Lu, F.X., et al., *Novel pretreatment of hard metal substrate for better performance of diamond coated cutting tools*. Diamond and Related Materials, 2006. **15**(11-12): p. 2039-2045.

47. Zuiker, C., et al., *Physical and tribological properties of diamond films grown in argon-carbon plasmas*. *Thin Solid Films*, 1995. **270**(1-2): p. 154-159.
48. Sakamoto, Y. and M. Takaya, *Preparation of diamond-coated tools and their cutting performance*. *Journal of Materials Processing Technology*, 2002. **127**(2): p. 151-154.
49. Hao, T., et al., *Nano-crystalline diamond films synthesized at low temperature and low pressure by hot filament chemical vapor deposition*. *Surface and Coatings Technology*, 2006. **201**(3-4): p. 801-806.
50. Ristic, G.S., et al., *Effect of the substrate material on diamond CVD coating properties*. *Materials Chemistry and Physics*, 2003. **80**(2): p. 529-536.
51. Kulisch, W., et al., *Nanocrystalline diamond growth on different substrates*. *Thin Solid Films*, 2006. **515**(3): p. 1005-1010.
52. Almeida, F.A., et al., *Nano to micrometric HFCVD diamond adhesion strength to Si₃N₄*. *Vacuum*, 2007. **81**(11-12): p. 1443-1447.
53. Meng, X.M., et al., *Application of CVD nanocrystalline diamond films to cemented carbide drills*. *International Journal of Refractory Metals and Hard Materials*, 2008. **26**(5): p. 485-490.
54. Liu, F.-X., K.-L. Yao, and Z.-L. Liua, *Substrate tilting effect on structure of tetrahedral amorphous carbon films by Raman spectroscopy*. *Surface and Coatings Technology*, 2007. **201**(16-17): p. 7235-7240.
55. Liu, F.-X. and Z.-L. Wang, *Thickness dependence of the structure of diamond-like carbon films by Raman spectroscopy*. *Surface and Coatings Technology*, 2009. **203**(13): p. 1829-1832.
56. Huang, B.-R., et al., *Effects of pretreatment and post-annealing on the field emission property of diamond-like carbon grown on a titanium/silicon substrate*. *New Carbon Materials*, 2008. **23**(3): p. 209-215.
57. Ballutaud, D., et al., *Sp³/sp² character of the carbon and hydrogen configuration in micro- and nanocrystalline diamond*. *Diamond and Related Materials*, 2008. **17**(4-5): p. 451-456.
58. Mousinho, A.P., R.D. Mansano, and M.C. Salvadori, *Influence of substrate surface topography in the deposition of nanostructured diamond-like carbon*

- films by high density plasma chemical vapor deposition. Surface and Coatings Technology*, 2009. **203**(9): p. 1193-1198.
59. Lin, C.R., C.T. Kuo, and R.M. Chang, *Improvement in adhesion of diamond films on cemented WC substrate with Ti-Si interlayers. Diamond and Related Materials*, 1998. **7**(11-12): p. 1628-1632.
60. Buijnsters, J.G., et al., *Adhesion analysis of polycrystalline diamond films on molybdenum by means of scratch, indentation and sand abrasion testing. Thin Solid Films*, 2005. **474**(1-2): p. 186-196.
61. Erdemir, A., et al., *Tribological properties of nanocrystalline diamond films. Surface and Coatings Technology*, 1999. **120-121**: p. 565-572.
62. Wang, L., et al., *A comparative study on the tribological behavior of nanocrystalline nickel and cobalt coatings correlated with grain size and phase structure. Materials Chemistry and Physics*, 2006. **99**(1): p. 96-103.
63. Çakır, O., *Chemical etching of aluminium. Journal of Materials Processing Technology*, 2008. **199**(1-3): p. 337-340.
64. Madou, M.J., *Fundamentals of Microfabrication: The Science of Miniaturization*. Second Edition ed. 2002: CRC.
65. Haubner, R., A. Köpf, and B. Lux, *Diamond deposition on hardmetal substrates after pre-treatment with boron or sulfur compounds. Diamond and Related Materials*, 2002. **11**(3-6): p. 555-561.
66. Schade, A., S.M. Rosiwal, and R.F. Singer, *Influence of surface topography of HF-CVD diamond films on self-mated planar sliding contacts in dry environments. Surface and Coatings Technology*, 2007. **201**(14): p. 6197-6205.
67. Yang, S., et al., *Diamond films with preferred <110> texture by hot filament CVD at low pressure. Diamond and Related Materials*, 2008. **17**(12): p. 2075-2079.
68. Fabisiak, K., et al., *Structural characterization of CVD diamond films using Raman and ESR spectroscopy methods. Optical Materials*, 2006. **28**(1-2): p. 106-110.



Appendices

UMP

A1: Abstract accepted for International Conference on Advances in Mechanical Engineering 2009-(ICAME 2009), 24-25 June 2009 , Shah Alam, Malaysia.

Effect of surface pretreatments on polycrystalline diamond deposited on Si₃N₄ substrate using Hot Filament Chemical Vapor Deposition technique

Dayangku Noorfazidah Awang Sh'ri^a and E. Hamzah^b

^aFaculty of Mechanical Engineering,
Universiti Malaysia Pahang,
Lebuhraya Tun Abdul Razak, 26300,
Kuantan, Pahang.

^bFaculty of Mechanical Engineering,
Universiti Teknologi Malaysia,
81310, Skudai, Johor, Malaysia.

email: noorfazidah@ump.edu.my

Abstract: The deposition of diamond films on a silicon nitride (Si₃N₄) substrate is an attractive technique for industrial applications because of the excellent properties of diamond. Diamond possesses remarkable physical and mechanical properties such as chemical resistant, extreme hardness and highly wears resistant. Pretreatment of substrate is very important prior to diamond deposition to promote nucleation and adhesion between coating and substrate. Polycrystalline diamonds films have been deposited on silicon nitride substrate by Hot Filament Chemical Vapor Deposition (HF-CVD) technique using mixture of methane and hydrogen gases. The Si₃N₄ substrates have been subjected to various pretreatment methods prior to diamond deposition namely chemical etching and mechanical abrasion. The structure and morphology of diamond coating have been studied using X-ray Diffraction (XRD) and Scanning Electron Microscopy (SEM) while diamond film quality has been characterized using Raman spectroscopy. It was found that the sandblasting produced highest surface roughness. Diamond deposited on as-received, basic etched and grinded substrate shows the morphology of cauliflower while blasted and acidic etched substrates produce smooth, continuous diamond film. However, the XRD and Raman investigation did not show any deviation for any pretreatment. The quality of diamond film produced is not significantly affected by surface pretreatment, but more by the deposition parameter.

Keywords: Nanocrystalline diamond, Chemical Vapor Deposition, Pretreatment, Silicon Nitride

Abstract accepted for *Advances in Materials and Processing Technologies (AMPT) 2009 (AMPT 2009)*, 26 - 29 October 2009, Kuala Lumpur, Malaysia.

Effect of surface pretreatments and seeding on morphology and quality of polycrystalline diamond deposited on Si_3N_4 substrate

Dayangku Noorfazidah Awang Sh'ri^a and E. Hamzah^b

^aFaculty of Mechanical Engineering,
Universiti Malaysia Pahang,
Lebuhraya Tun Abdul Razak, 26300,
Kuantan, Pahang.

^bFaculty of Mechanical Engineering,
Universiti Teknologi Malaysia,
81310, Skudai, Johor, Malaysia.

email: noorfazidah@ump.edu.my

Abstract

The deposition of diamond films on a Si_3N_4 substrate is an attractive technique for industrial applications because of the excellent properties of diamond. Pretreatment of substrate is very important prior to diamond deposition to promote nucleation and adhesion between coating and substrate. Polycrystalline diamonds films have been deposited on silicon nitride substrate have been carried out by HF-CVD technique using mixture of methane and hydrogen gases. Different pretreatment of substrate including chemical etching consists of hot acid etching and basic etching and mechanical etching were used to study the quality of diamond formed on the substrate. The structure and morphology of diamond coating have been studied using X-ray Diffraction (XRD) and Scanning Electron Microscopy (SEM) while diamond film quality has been characterized using Raman spectroscopy. The adhesion properties of polycrystalline diamond film have been evaluated using blast wear test and indentation technique using Vicker's hardness.

Keywords: Polycrystalline diamond, Chemical Vapor Deposition, Pretreatment, Silicon Nitride